

國立交通大學

電信工程學系

博士論文

適用於直接序列碼分多重擷取系統多用戶偵測之部分平行式干擾消除：效能分析  
與新演算法



Partial Parallel Interference Cancellation for  
DS-CDMA Multiuser Detection: Performance  
Analysis and New Algorithms

研究生： 謝 雨 滔

指導教授： 吳 文 榕

中 華 民 國 93 年 7 月

Partial Parallel Interference Cancellation for DS-CDMA  
Multiuser Detection: Performance Analysis and New  
Algorithms

適用於直接序列碼分多重擷取系統多用戶偵測之  
部分平行式干擾消除：效能分析與新演算法

研究生：謝雨滔

Student: Yu-Tao Hsieh

指導教授：吳文榕 博士

Advisor: Dr. Wen-Rong Wu



A Dissertation  
Submitted to Department of Communication Engineering  
College of Electrical Engineering and Computer Science  
National Chiao Tung University  
in Partial Fulfillment of the Requirement  
for the Degree of  
Doctor of Philosophy  
In  
Communication Engineering  
July 2004  
Hsinchu, Taiwan, Republic of China

中華民國九十三年七月

# 適用於直接序列碼分多重擷取系統多用戶偵測之部分 平行式干擾消除：效能分析與新演算法

研究生：謝 雨 滔

指導教授：吳 文 榕 教授

國立交通大學電信工程學系博士班



平行式干擾消除法乃是針對直接序列碼分多重擷取系統一簡單而有效之多用戶偵測器。然而其效能表現可能因前幾階不可靠之干擾消除而降低，因此就有部分平行式干擾消除法的發展，此法乃利用部分消除因子來控制欲消除之干擾量，而提高系統效能。雖然部分消除因子佔有關鍵地位，然其完整的最佳解尚未有深入探討。本論文重點即在於針對不同形式之部分平行式干擾消除法，求得其最佳消除因子值，並進行效能分析。在論文的第一部份，吾人考慮一個二階式軟決策部分平行式干擾消除接收機，利用最低位元錯誤率的條件，吾人導證出完整的部分消除因子解，其中包括了週期碼、非週期碼系統，並適用於白高斯通道，與多重路徑通道。實驗結果顯示，經由理論求得之最佳部分消除因子值與實際值相當接近。此利用最佳部分消除因子值之二階式部分平行式干擾消除法不僅優於二階全平行式干擾消除法，亦優於三階全平行式干擾消除法。在論文的第二部分，吾人

分析二階適應性盲蔽型硬決策部分平行式干擾消除法。在此架構中，經調適過而被用作最佳消除因子之權重值，乃是由最小均方理論訓練而得。吾人推導出最佳權重值、權重值之平均誤差、及其均方差值。根據這些理論結果，吾人得到每個使用者之輸出信號均方差及位元錯誤率。步階值在最小均方理論的收斂行為中，扮演著關鍵角色，對部分平行式干擾消除法的系統效能也影響甚鉅。藉著所推導之輸出信號均方差，吾人可以求得最佳步階值。在論文的最後一部份，吾人針對適應性盲蔽型硬決策部分平行式干擾消除法，提出一改善方法，其主要概念在於減低最小均方理論中所訓練之權重值的數目，並且進行權重值之後續濾波處理，使得最終多餘的均方差能因此減低。吾人也推導改良理論之輸出均方差與位元錯誤率。實驗結果證實所提出之改良理論表現優於傳統部分平行式干擾消除法，而理論分析結果也相當準確。



# Partial Parallel Interference Cancellation for DS-CDMA Multiuser Detection: Performance Analysis and New Algorithms

Student: Yu-Tao Hsieh

Advisor: Dr. Wen-Rong Wu

Department of Communication Engineering

National Chiao Tung University

Hsinchu, Taiwan 30050



## **Abstract**

Parallel interference cancellation (PIC) is considered a simple yet effective multiuser detector for direct-sequence code-division multiple-access (DS-CDMA) systems. However, its performance may deteriorate due to unreliable interference cancellation in the early stages. Thus, a partial PIC detector in which partial cancellation factors (PCFs) are introduced to control the interference cancellation level has been developed as a remedy. Although PCFs are crucial, complete solutions for their optimal values are not available. In this dissertation we focus on the determination of optimal PCFs and performance analysis for various partial PICs. In the first part of the work, we consider a two-stage soft-decision partial PIC receiver. Using the minimum bit error rate (BER) criterion, we derive a complete set of optimal PCFs in the second stage. This includes optimal PCFs for periodic and aperiodic spreading codes in additive white Gaussian channels and multipath channels. Simulation results show that our theoretical

optimal PCFs agree closely with empirical ones. Our two-stage partial PIC using derived optimal PCFs outperforms not only a two-stage, but also a three-stage full PIC. In the second part of the work, we analyze the performance of a two-stage adaptive blind hard-decision partial PIC. In this scheme, the adapted weights serving as optimal PCFs are trained using the least mean square (LMS) algorithm. We derive the analytical results for optimal weights, weight error means, and weight error variances. Based on these results, we also derive the output mean square error (MSE) and BER for each user. The step size known to be a critical parameter in the LMS algorithm controls the LMS convergence behavior and partial PIC performance. Using the output MSE criterion, we can then optimize the step size. Simulation results indicates that our analytical results can well match with empirical ones. In the final part of the work, we propose an improved adaptive blind hard-decision partial PIC and analyze its performance. The main idea is to reduce the number of active weights in the LMS algorithm and to perform weight post filtering such that the resultant excess MSE can be reduced. We also derive the output MSE and BER for the proposed algorithm. Simulation results verify that the proposed algorithm outperforms the conventional partial PIC approach and analytical results are accurate.

## Acknowledgements

I would like to thank my advisor, Dr. Wen-Rong Wu, for his constant support, encouragement, and guidance, in my research work. His enthusiasm and persistence in discovering in new avenues of research impressed me deeply. I really appreciate his efforts in improving my paper organization and writing skills. I would also especially thank him for his helpful advice and experience not only on academic fields but also in my building my future career.

I am grateful to my colleges in WTSP Lab for building a comfortable environment. I also would like to thank my parents and my friends for their support and love.

Finally I would like to give a special thanks to my beloved wife, Amy, for being with me whatever has happened to me in my pursuit to the phd program. I would like to thank her for being always believed me that I can accomplish my dream, and being a forever supporter in every aspect of my life.



# Table of Contents

<b>Abstract</b>		<b>iii</b>
<b>Acknowledgements</b>		<b>v</b>
<b>List of Figures</b>		<b>ix</b>
<b>List of Tables</b>		<b>xiii</b>
<b>1 Introduction</b>		<b>1</b>
1.1 Background . . . . .		1
1.2 Multiuser Detection . . . . .		4
1.3 Objective and Overview . . . . .		8
1.4 Organization of the Dissertation . . . . .		10
<b>2 Multiuser Detection</b>		<b>11</b>
2.1 Optimal Multiuser Receiver . . . . .		12
2.2 Linear Suboptimal Receivers . . . . .		13
2.3 Interference Cancellation Methods . . . . .		17
2.3.1 Successive Interference Cancellation . . . . .		20
2.3.2 Parallel Interference Cancellation . . . . .		21
<b>3 Optimal Two-stage Partial SPIC Receivers</b>		<b>26</b>





3.1	Introduction . . . . .	26
3.2	System Model . . . . .	27
3.3	Optimal PCFs for AWGN Channels . . . . .	29
3.3.1	Periodic Code Scenario . . . . .	30
3.3.2	Aperiodic Code Scenario . . . . .	33
3.4	Optimal PCFs for Multipath Channels . . . . .	35
3.4.1	Periodic Code Scenario . . . . .	35
3.4.2	Aperiodic Code Scenario . . . . .	38
3.5	Simulation Results . . . . .	41
<b>4</b>	<b>Analysis of Adaptive Two-stage Partial HPIC Receivers</b>	<b>49</b>
4.1	System Model . . . . .	50
4.2	Exact Analysis for Single-user Scenario . . . . .	54
4.2.1	Optimal Weight Analysis . . . . .	54
4.2.2	Weight Error Mean Analysis . . . . .	57
4.2.3	Weight Error Variance Analysis . . . . .	59
4.3	Exact Analysis for Two-user Scenario . . . . .	63
4.3.1	Optimal Weight Analysis . . . . .	64
4.3.2	Weight Error Mean Analysis . . . . .	69
4.4	Approximate Analysis for $K$ -user Scenario . . . . .	73
4.4.1	Optimal Weight Analysis . . . . .	74
4.4.2	Weight Error Mean Analysis . . . . .	76
4.4.3	Weight Error Variance Analysis . . . . .	79
4.4.4	Output MSE and BER . . . . .	80
4.5	Simulation Results . . . . .	81
<b>5</b>	<b>Improved Adaptive Blind Partial HPIC Receivers</b>	<b>89</b>
5.1	Adaptive Blind Partial HPIC Receivers . . . . .	90

5.2	Proposed Algorithm . . . . .	94
5.2.1	Gradient Guided Search Algorithm . . . . .	98
5.3	Performance Analysis of the Proposed Algorithm . . . . .	99
5.4	Simulation Results . . . . .	103
<b>6</b>	<b>Conclusions</b>	<b>114</b>
	<b>Appendix</b>	<b>117</b>
<b>A</b>	<b>Periodic Code System Optimal PCFs for Asynchronous AWGN Channels</b>	<b>117</b>
<b>B</b>	<b>Expressions for Expected Terms in (3.50)-(3.51)</b>	<b>121</b>
<b>C</b>	<b>Optimal PCFs under Fading Channels</b>	<b>127</b>
<b>D</b>	<b>Supplemental Derivation for Analytical Results in Chapter 4</b>	<b>129</b>
D.1	Two-user Scenario . . . . .	129
D.2	$K$ -user Scenario . . . . .	130
	<b>Bibliography</b>	<b>132</b>



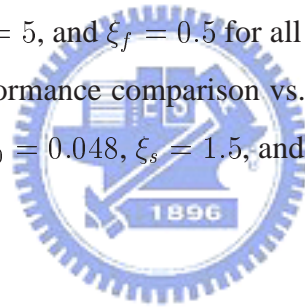
# List of Figures

2.1	BER performance comparison of multiuser receivers for the first user ( $E_b/N_0 = 7$ dB, and $\rho = 0.8$ ). . . . .	15
2.2	BER performance comparison of multiuser receivers ( $K = 10$ , and $\rho = 0.8$ ). . . . .	16
2.3	BER performance comparison of multiuser receivers (random codes, $N = 15$ , and $E_b/N_0 = 6$ dB.) . . . . .	17
2.4	Interference estimate functions. (a) Soft-decision function (b) Hard-decision function (c) Null-zone function (d) Hyperbolic tangent function (e) Unit-clipper function (f) Modified unit-clipper function. . . . .	18
2.5	Block diagram for an SIC receiver. . . . .	19
2.6	Block diagram for a general two-stage partial SPIC receiver. . . . .	20
2.7	Block diagram for a two-stage coupled partial HPIC receiver. . . . .	21
2.8	Block diagram for a two-stage decoupled partial SPIC receiver. . . . .	22
2.9	LMS algorithm for two-stage adaptive blind partial HPIC receivers. . . . .	23
2.10	BER performance comparison for different multiuser receivers ( $\rho = 0.1$ , $E_b/N_0 = 6$ dB, and power balanced). . . . .	24
3.1	General partial SPIC receiver structure. . . . .	29
3.2	Performance comparison for HPIC and SPIC ( $N = 31$ , $\rho = 1/\sqrt{N}$ , and $E_b/N_0 = 8$ dB); The optimal PCFs for the partial HPIC were obtained by trial and error and those for the SPIC were obtained from (3.27). . . . .	41

3.3	Performance comparison for the coupled and decoupled structures (three users with $E_b/N_0 = 8 - 2\Delta\eta$ , $8 - \Delta\eta$ , and 8 dB); The optimal PCFs for the coupled structure were obtained by trial and error, and those for the decoupled structure were obtained from (3.38). . . . .	42
3.4	BER of the partial SPIC detector versus $E_b/N_0$ (aperiodic AWGN channels, and power balanced). . . . .	43
3.5	Optimal PCF versus number of users (Gold codes, asynchronous AWGN channels, $E_b/N_0 = 8$ dB, and power balanced). . . . .	44
3.6	Optimal PCF versus number of users (aperiodic codes, multipath channels, $E_b/N_0 = 10$ dB, and power balanced). . . . .	45
3.7	BER versus number of users (Gold codes, asynchronous AWGN channels, $E_b/N_0 = 10$ dB, and power balanced). . . . .	46
3.8	BER versus number of users (aperiodic spreading codes, multipath channels, $E_b/N_0 = 10$ dB, and power balanced). . . . .	47
3.9	BER with channel estimation error (aperiodic spreading codes, multipath channels, $K=6$ , $E_b/N_0 = 10$ dB, and power balanced). . . . .	48
4.1	LMS algorithm for two-stage adaptive blind partial HPIC receivers. . . . .	50
4.2	Optimal weight comparison for two power-balanced users. . . . .	82
4.3	Optimal weight comparison for five power-balanced users. . . . .	83
4.4	Optimal weight comparison for 15 power-balanced users. . . . .	84
4.5	Weight mean comparison for two power-balanced users ( $\mu_0 = 0.02$ , and $E_b/N_0 = 6$ dB). . . . .	85
4.6	Weight mean comparison for five power-balanced users ( $\mu_0 = 0.02$ , and $E_b/N_0 = 6$ dB). . . . .	85
4.7	Weight mean comparison for 15 power-balanced users ( $\mu_0 = 0.02$ , and $E_b/N_0 = 6$ dB). . . . .	86

4.8	Weight error power comparison for two power-balanced users ( $\mu_0 = 0.02$ , and $E_b/N_0 = 6$ dB). . . . .	86
4.9	Weight error power comparison for five power-balanced users ( $\mu_0 = 0.02$ , and $E_b/N_0 = 6$ dB). . . . .	87
4.10	Weight error power comparison for 15 power-balanced users ( $\mu_0 = 0.02$ , and $E_b/N_0 = 6$ dB). . . . .	87
4.11	Optimal step-size comparison for different user numbers. . . . .	88
4.12	Second-stage BER comparison for power-balanced cases ( $\mu_0 = 0.02$ ). . . . .	88
5.1	Adaptive blind partial HPIC receivers. . . . .	92
5.2	Functions used in the proposed algorithm. (a) Weight selection function. (b) Weight post filtering function. . . . .	96
5.3	Flow chart for the proposed algorithm. . . . .	97
5.4	Probability density function for adapted weights from LMS algorithm. . . . .	102
5.5	Second stage parameter optimization for the proposed algorithm. (Weight selection is not performed). . . . .	103
5.6	Second stage parameter optimization for the proposed algorithm ( $\mu_0^{(2)} = 0.048$ ). . . . .	104
5.7	Second stage BER performance for the proposed algorithm ( $K = 20$ , $\mu_0^{(2)} = 0.048$ , and $E_b/N_0 = 7$ dB). . . . .	105
5.8	Second stage BER performance comparison vs. user numbers ( $\xi_s = 1.2$ , $\xi_f = 0.4$ , $\mu_0 = 0.048$ , and $E_b/N_0 = 7$ dB). . . . .	106
5.9	Third stage BER performance comparison vs. user numbers (the parameter setting is the same as that in Figure 5.8 for all stages). . . . .	107
5.10	Fourth stage BER performance comparison vs. user numbers (the parameter setting is the same as that in Figure 5.8 for all stages). . . . .	108
5.11	Fifth stage BER performance comparison vs. user numbers (the parameter setting is the same as that in Figure 5.8 for all stages). . . . .	109

5.12	Second stage BER performance comparison vs. $E_b/N_0$ ratios ( $K = 10$ , and the parameter setting is the same as that in Figure 5.8 for all stages). . . . .	110
5.13	Fifth stage BER performance comparison vs. $E_b/N_0$ ratios ( $K = 10$ , and the parameter setting is the same as that in Fig. 5.8). . . . .	110
5.14	Second stage BER performance comparison for the weakest user (power-imbalanced, $E_b/N_0 = 7$ dB, and the parameter setting is the same as that in Fig. 5.8). . . . .	111
5.15	Fifth stage BER performance comparison for the weakest user (power-imbalanced, $E_b/N_0 = 7$ dB and the parameter setting is the same as that in Fig. 5.8). . . . .	111
5.16	Fifth stage BER performance comparison for single-path rician fading channels ( $E_b/N_0 = 7$ dB, $\xi_s = 1.4$ , and $\xi_f = 0.3$ for all stages). . . . .	112
5.17	Fifth stage BER performance comparison for two-ray multipath fading channels ( $E_b/N_0 = 17$ dB, $\xi_s = 5$ , and $\xi_f = 0.5$ for all stages). . . . .	112
5.18	Fifth stage BER performance comparison vs. channel estimation errors ( $K = 20$ , $E_b/N_0 = 7$ dB, $\mu_0 = 0.048$ , $\xi_s = 1.5$ , and $\xi_f = 0.5$ for all stages). . . . .	113



# List of Tables

2.1	Required information for different multiuser receivers. . . . .	25
4.1	Sets of $\gamma$ for all decision and bit patterns . . . . .	68
4.2	Complete list of conditional optimal weights . . . . .	69



# Chapter 1

## Introduction

### § 1.1 Background

Since G. Marconi first used radio for wireless communication in 1897, many new methods have been developed. In the 1960s and 1970s, Bell Laboratories developed the cellular concept in wireless communication systems. At the same time, the semiconductor industry has also experienced enormous progress such that design and manufacture of low-cost radio frequency devices appeared feasible. These result in the today's exponential growth in cellular radio and personal communication systems throughout the world. As known, the most critical resource in wireless communication is the spectrum. In order to support as many users as possible on a limited spectrum, multiple access techniques have been developed. The progressive multiple access schemes also witness the development of the advanced techniques, which raises to deal with the increasing demands for both voice and data service, accompanied by the performance guarantee under diverse environments and stringent device specification.

The first-generation (1G) mobile cellular system was developed in early 1980's and deployed in mid 1980's. The 1G system used the frequency division multiple access (FDMA) as the multiple access scheme. The well known standards include the advanced mobile phones system (AMPS) in the United States, the total access communications system (TACS) in Eu-



rope, and the NTT system in Japan. Due to the use of the cell structure, frequencies can then be reused and handover among cells is required between cells. In the 1G era, the service content consists the voice data only. The rapidly increasing demand for higher system capacity has soon pushed the development of an improved system, the second generation (2G) system. The 2G system claimed to support at least three-folded capacity than the 1G system. Most of 2G systems adopted time division multiple access (TDMA) as the multiple access scheme. The scheme uses non-overlapping time-slots to transmit data of different users. Since more users can use the same frequency band, its efficiency is higher than the pure FDMA systems. Since then the cellular system becomes digital, and the advanced signal processing techniques, such as the voice compression, error control coding, and encryption, were incorporated. The representative standards are the IS-136 in the United States and the GSM in Europe. Specifically, the GSM system enjoys a great success. At the end of 2003, the GSM system has a total subscribers over one billion in more than 170 networks over the world. In addition to the aforementioned capacity advantage, the 2G communication system also provides low-rate data services. It uses voice activity detectors and insert data in the unused slots. This enables the packet-based data services, such as e-mail and internet browsing. Typical standards include generation packet radio service (GPRS) and enhanced data rate for GSM evolution (EDGE). Yet, there is another 2G system that uses a totally different multiple access scheme, the code division multiple access (CDMA) [1]. In conventional multiple access methods, the transmission is partitioned into dedicated channels in frequency and/or time domain such that the interference among users can be avoided. In the CDMA system, however, orthogonal codes are used as the user signatures. These codes, when transmitted, occupy the same frequency band and same time period. The CDMA belongs to the spread spectrum communication technique and its required bandwidth is wider than the TDMA system. Conventional CDMA systems were used in military application since it has the advantages of high tolerance for jamming or unintentional interference, as well as low detectability [2]. The major advantage of commercial CDMA is to provide higher capacity (than TDMA and FDMA). The first commercial CDMA system was developed by

Qualcomm and referred to as the IS-95 in United States.

Although the 2G system can support data service, its data-rate is low. As a result, the third-generation (3G) standard, which is supposed to supply a transmission rate of 2M bits per second, were developed. It turns out that most standard bodies chose CDMA as the multiple access scheme. This includes cdma2000, WCDMA, and TD-SCDMA [3]. As mentioned, in CDMA all users share the same frequency bands and time slots, and thus the main factor limiting the system capacity is the interference from other users. Hence suppression of cochannel interference becomes a major challenge for CDMA systems. The major distinction between CDMA and other multiple access schemes is the virtual code space in which users can be identified when sharing the same time slots and frequency bands. There are two major classes of spreading codes utilized in the CDMA system based on the correlation property between codes. The first class is the orthogonal codes, which are Walsh codes in general. The other class belongs to the pseudonoise(PN) code. When Walsh codes are used, there will be no interference between users. However, there are several reasons for which the PN codes are preferred in real-world applications. Firstly, the number of Walsh codes is limited (the number of active users is limited). Secondly, the orthogonal property only holds in synchronous transmission and additive white Gaussian noise (AWGN) channel. In the uplink transmission or multipath environments, code orthogonality can not be hold. The PN sequence has the property that the normalized auto-correlations equal  $-1/N$  for all time lags, where  $N$  is the processing gain. This makes the receiver more robust to the coherent interference in multipath environments. Although the CDMA receiver inherently has the interference suppression property, however, as the user number increases, interference (due to non-orthogonal codes) becomes stronger and stronger. The performance is then degraded accordingly. The interference from other users is generally referred to as multiple access interference (MAI). In order to combat the MAI, some signal processing techniques have been proposed and these include

- Source and channel coding / interleaving
- Spatial-temporal signal processing

- Multiuser detection

This dissertation focus on the third one, the multiuser detection (MUD) algorithms.

## § 1.2 Multiuser Detection

The significant progress of the MUD development was due to the work of S. Verdu. He proposed a multiuser receiver utilizing the maximum-likelihood criterion [4] and showed a great performance enhancement. However, He also showed that the computational complexity grows exponentially with the user number. The high computational complexity adversely affects its real-world applications. Thus, a variety of low-complexity suboptimum receivers were then proposed [5]-[7],[8].

The first category of suboptimal receivers is the linear receiver. It performs MUD through a linear transformation of the matched filter outputs. The rationale behind this approach is similar to that of equalization in TDMA systems [9]. The decorrelating detector (or decorrelator), being a linear receiver, uses the correlation matrix inverse as the transformation matrix [10]. It can completely eliminate the MAI and achieve the near-far resistance close to the optimal receiver. Another feature of the decorrelator is that the algorithm does not require the receive signal powers (for each user) nor the noise variance. However, it may enhance noise and thus the performance is degraded when signal to noise ratio (SNR) is low . The linear minimum mean square error (LMMSE) detector, an improvement to the decorrelator, gives a compromise between interference suppression and noise enhancement [11],[12]. Leveraging the linear property, the linear receivers lends the performance analysis feasible [10],[13], [14]. Although the linear approaches are much more simpler than the optimal one, they may require matrix inversion operations. The computational complexity is on the order of  $O(K^3)$  where  $K$  is the user number. In [15] and [16], iterative algorithms, which do not require matrix inversion, were proposed to obtain the decorrelator and linear MMSE receivers. These iterative methods were shown to have a close relationship with the soft-decision interference cancellation methods that

will be described later. The other strategy reducing the complexity of these detectors is the use of adaptive algorithms, which includes the least mean square (LMS) algorithm [17],[18], [19] [20], the recursive least square (RLS) algorithm [21], and the Kalman filtering algorithm [22].

In addition to the aforementioned linear detectors, another category of interest is the subtractive type multistage interference cancellation method. Cancellation of this type involves only vector operations making it a good candidate for real-world implementation. For a particular desired user, the subtractive-type canceller estimates interference from other users, regenerates it, and cancels it from the received signal. This canceller is usually implemented with a multistage structure. The temporary data decision for a stage is obtained from its previous stage. The successive interference cancellation (SIC) cancels interference from other users one by one [23],[24],[25], while the parallel interference cancellation (PIC) cancels it all at one time [26], [27], [28]. A hybrid of PIC and SIC is also possible [29]. To have best performance, signal power ranking is necessary in SIC. The strongest user usually has lowest probability of decision errors and cancellation of its interference gives the most significant result. For these reasons, SIC works well where users have unbalanced powers. However, SIC requires additional complexity for power ranking and the longer processing delay. By contrast, PIC cancels the interference disregard to the interference power distribution and is more suitable for power-balanced systems.

As mentioned, the subtractive-type of MUD estimates the interference from other users and then subtract it from the received signal. Each interference estimate involves bit estimation and spread signal regeneration. According to how the transmit bits are estimated, an interference cancellation algorithm can be classified as linear or nonlinear [30], [31], [32], [33]. For each stage, the simplest bit estimate is the soft-decision operated on the previous stage output (for each user) [34], [30], [35]. This bit estimate gives a linear receiver. It has been shown that the soft-decision PIC (SPIC) can converge to the decorrelator when the number of stage is infinite [32]. In practice, a two-stage SPIC may approximate the decorrelator well [37]. Due to the linear property, we can use the Gaussian approximation [38] or an improved Gaussian

approximation [34] to carry out SPIC performance analysis. The analysis was extended to include the scenario when the timing and phase errors were present [39]. Although simple, some undesirable properties were reported that the SPIC may perform worse than the matched filter when the correlation between user signals exceeds a certain threshold [40]. The analysis for SIC can also be found in [25].

The other commonly used bit estimate is the hard-decision. In this approach, channel information is generally required. The hard-decision PIC (HPIC) was investigated in [26], [41], [42] while the hard-decision SIC was investigated in [64]. The HPIC operated in a multipath fading channel was considered in [43],[44]. Theoretical analysis for this type of interference cancellation appears more complicated due to the non-linear decision operation. A two-stage HPIC was analyzed in [45]. Other performance criteria such as the signal-to-interference-noise-ratio (SINR) or the capacity were discussed in [46]. The decision function is not limited to be soft or hard. In [47], the hyperbolic tangent function was used as the decision function. This function can reflect the reliability of interference estimate more faithfully. Note that the hard-decision and soft-decision functions are special cases of the hyperbolic tangent function. The null-zone decision function was also studied for PIC [48], [49] and SIC [50]. Other decision functions can be found in [31], [51].

One problem in the PIC approach is that the interference estimates may not be reliable in early stages. In other words, interference cancellation does not necessarily reduce interference. To alleviate this problem, partial PIC was then developed. Partial cancellation factors (PCFs) ranging from 0 to 1, were introduced to control the signal cancellation level. The partial HPIC approach was first proposed in [30]. Since the interference estimate reliability is different, the PCF is usually different for each stage. It has been shown that the performance of the linear MMSE receiver can be achieved using partial SPIC through proper choice of PCFs [52],[53]. The PCF optimization for multistage SPIC has also been considered in [54]. It was shown that partial SPIC can converge to the decorrelator with very few stages. It was also shown that the partial SPIC can be seen as a realization of the steepest descent MMSE optimization method

where the PCF acts as the step size in each stage. The bias reduction in the partial SPIC was further analyzed in [55] and [56].

Let the number of user be  $K$ . Thus, a specific user has  $K - 1$  interfering users. To have best cancellation result, we then require  $K - 1$  PCFs. However, we have total  $K$  users to consider. Thus, a general partial PIC require  $K(K - 1)$  PCFs. As we can see, the computational complexity of the general partial PIC is high. In order to reduce the computational complexity, two simplified structures were developed; we refer to them as the coupled and the decoupled structure. In these two structures, only  $K$  PCFs are involved. The difference of these two structures lies in the position where the PCF is inserted. In the coupled structure, PCFs are inserted (multiplied) after each regenerated user signal. For a specific user, the interference estimate is just the summation of  $K - 1$  weighted regenerated signal. Thus, the estimate involve  $K - 1$  PCFs. For the decoupled structure, the  $K - 1$  regenerated signals are first summed and then a PCF is inserted (multiplied). Thus, for a specific user, the interference estimate only involve one PCF. In partial HPIC, the coupled structure is usually employed and only the approximated optimal PCFs are available for a two-stage processing [57]. The derived PCFs is obtained by minimizing the MSE between signal outputs and desired data. The approximate optimal PCFs for partial HPIC with timing error can be found in [58] while the optimal PCFs supports the multicode transmission was reported in [59]. The PCFs for coded systems with HPIC were investigated in [60]. The coupled partial SPIC has been considered in [61] and the closed-form results applied to a power balanced control scenario were derived. Besides the theoretical solutions, the LMS adaptive algorithm was also used to search optimal PCFs for partial HPIC [62],[63]. Due to its special architecture, this approach does not need training sequence. We call it a adaptive blind partial HPIC algorithm. It was found that this partial HPIC outperforms non-adaptive ones. The LMS algorithm was also utilized to track the channel information in hard-decision SIC [64].

The MUD algorithms are by no means limited to those described above. However, other algorithms either require higher computational complexity, or consider special operation condi-

tions (no user information for example). The objective of this work is to study low-complexity MUD algorithms that are suitable for real-world implementation. As mentioned, the interference cancellation method only involves vector operations making its computational complexity lower than others'. We will then focus on this type of MUD. For other MUD related works, please see [65].

### § 1.3 Objective and Overview

As mentioned, the PIC performance may deteriorate due to unreliable interference cancellation in the early stages. Thus, the partial PIC detector in which partial cancellation factors (PCFs) are introduced to control the interference cancellation level has been developed as a remedy. It is apparent that these PCFs are crucial. However, complete solutions for their optimal values are not available. Also, performance analysis is only available for limited scenarios. In this dissertation we focus on the determination of optimal weights and performance analysis for various partial PICs. There are three main parts in this work. In the first part of the work, we consider a two-stage decoupled soft-decision partial PIC receiver. The reason to consider this architecture has manifold. Firstly, it is known that the value of PCFs will approach to one when the number of stage is greater than two [55]. Thus, there is no need to consider a higher stage structure. Secondly, theoretical analysis is much more simpler for a two-stage structure. The analysis is also simpler for the decoupled SPIC. The performance of the partial SPIC is similar to that of other structures (for example, the coupled partial HPIC). Using the minimum bit error rate (BER) criterion, we derive a complete set of optimal PCFs for the second stage. This includes optimal PCFs for periodic and aperiodic spreading codes in additive white Gaussian channels and multipath channels. Simulation results show that our theoretical optimal PCFs agree closely with empirical ones. Our two-stage partial PIC using derived optimal PCFs outperforms not only a two-stage, but also a three-stage full PIC.

In the second part of the work, we analyze the performance of a two-stage adaptive blind

partial HPIC receiver. This is known to be a difficult problem and the corresponding result is not reported in literature. In this scheme, the adapted weights serving as optimal PCFs are trained using the least mean square (LMS) algorithm. The analysis difficulty arises from the nonlinear operation involved in the decision process and its interaction with the LMS algorithm. Although there exist many theoretical results for the LMS algorithm, most of them consider the steady-state performance and are valid only for the small step size scenario. This cannot be applied in the problem considered here. This is because the sample size available is small and a large step size must be used. Also the weights will not converge at the end of each bit interval and the LMS algorithm is still in its transient-state. Note that the input to the LMS algorithm depends on the decision in the previous stage and this complicates the problem furthermore. We derive the analytical results for optimal weights, weight error means, and weight error variances. Based on these results, we also derive the output mean square error (MSE) and BER for each user. The step size known to be a critical parameter in the LMS algorithm controls the LMS convergence behavior and partial PIC performance. Using the output MSE criterion, we are able to obtain an optimal step size. Simulation results indicates that our analytical results can well match with empirical ones.

In the final part of the work, we propose an improved adaptive blind multistage hard-decision partial PIC and analyze its performance. It is well known that the LMS is a stochastic gradient descent algorithm and its excess MSE is proportional to the number of filter taps and the step size value. The main idea here is to reduce the number of active weights in the LMS algorithm and reduce the adapted weight variance such that the resultant excess MSE can be reduced. To implement this idea, we include a decision making mechanism before adaptation and a weight post filtering function after adaptation. We also derive the output MSE and BER for the proposed algorithm. Simulation results verify that the proposed algorithm outperforms the conventional partial PIC approach and analytical results are accurate.



## § 1.4 Organization of the Dissertation

The organization of this dissertation is described as follows. In Chapter 2 we survey significant contributions in multiuser detection. The optimal and several suboptimal multiuser receivers are described.

Chapter 3 presents a two-stage partial SPIC multiuser receiver with a decoupled structure. We derive the optimal partial cancellation factors (PCFs) based on the minimum BER criterion. We consider periodic and periodic code scenarios, the AWGN as well as multipath channels.

Chapter 4 focuses on the analysis of a two-stage adaptive partial HPIC receivers. In this regard, the LMS algorithm is used to obtain optimal PCFs. We derive the optimal weights and analyze the weight error mean and weight error variance for one and two-user cases. We then extend the results to the general  $K$ -user case. Due to the difficulty of the problem, we are only able to obtain approximate results. However, simulations show that our results are accurate. We also use our theoretical results to optimize the step size used in the LMS algorithm.

In Chapter 5, we propose an improved adaptive blind multistage HPIC receiver. We show that the convergence rate of the LMS algorithm can be accelerated and the performance can be enhanced. Based on the convergence analysis given in Chapter 4, we also analyze its performance and derive theoretical MSE and BER.

Chapter 6 gives the conclusion remarks and outlines some topics for further research.

## Chapter 2

# Multuser Detection

At the time of introduction of CDMA, it was argued that interference from other users (after despreading) has the statistical property just as the noise. Thus in the receiving end each user can use a matched filter to demodulate its own signal independently. It is simple to see that the interference level is proportional to the number of users and their signal strength. This is referred to as the single-user detection scheme. The performance of the matched filter will be greatly affected when the near-far effect arises. In this case, the weak user signals may be overwhelmed by strong user signals. In this regard, using power control to balance the receiving powers among users seems the most efficient way. However, the challenges for power control is the requirement of fast and accurate power adjustment to maintain the received levels within a fraction of one dB error from the possible dynamic range up to 90 dB. In addition, different services may have different transmission rates and powers making power control difficult. Multuser detection (MUD) was developed to alleviate this problem. In MUD, all users are demodulated simultaneously. Signal from other users are not treated as interference any more. Application of the MUD algorithm greatly improves the system performance and at the same time eliminates the precise power control requirement. In this chapter, several MUD techniques are briefly reviewed. In Section 1, the optimal receiver are described. Section 2 presents the linear suboptimal receivers, which include the decorrelator and the LMMSE receiver. In Section

3, we described the interference cancellation methods that include SIC, PIC, and partial PIC.

## § 2.1 Optimal Multiuser Receiver

Consider a synchronous CDMA system for the AWGN channel with  $K$  users. The received signal at a certain bit interval can be represented by

$$\begin{aligned} r(t) &= \sum_{k=1}^K s_k(t) + v(t) \\ &= \sum_{k=1}^K a_k b_k x_k(t) + v(t), \quad t \in \{0, T\} \end{aligned} \quad (2.1)$$

where  $s_k(t)$  is the received signal for the  $k$ th user,  $a_k$  and  $b_k$  are the channel and data bit for the  $k$ th user,  $x_k(t)$  is the normalized spreading waveform, and  $T$  is the bit interval length. The AWGN is denoted by  $v(t)$ . The mean and the variance of  $v(t)$  is zero and  $\sigma^2$ , respectively. The maximum likelihood (ML) solution for the input bits maximizes the likelihood function shown below.

$$\max_{\mathbf{b}} \exp \left\{ -\frac{1}{2\sigma^2} \int_0^T \left[ r(t) - \sum_k a_k b_k x_k(t) \right]^2 dt \right\} \quad (2.2)$$

where  $\mathbf{b} = [b_1, b_2, \dots, b_K]^T$ . The log-likelihood function, which is equivalent the likelihood function, is used more frequently. The log-likelihood function is shown to be

$$\begin{aligned} \mathcal{L}(\mathbf{b}) &= 2 \int_0^T \sum_k [a_k b_k x_k(t)] r(t) dt - \int_0^T \left[ \sum_k a_k b_k x_k(t) \right]^2 dt \\ &= 2\mathbf{b}^T \mathbf{A} \mathbf{y} - \mathbf{b}^T \mathbf{A} \mathbf{R} \mathbf{A} \mathbf{b} \end{aligned} \quad (2.3)$$

where  $\mathbf{A} = \text{diag}[a_1, a_2, \dots, a_K]$ ,  $\mathbf{R}$  is the correlation matrix with the  $ij$  entry  $\rho_{jk}$  given by

$$\rho_{jk} = \int_0^T x_j(t) x_k(t) dt \quad (2.4)$$

and  $\mathbf{y} = [y_1, y_2, \dots, y_K]^T$  is the matched filter output vector with its element given by

$$y_k = \int_0^T r(t) x_k(t) dt. \quad (2.5)$$

The the matched filter output vector can be written as

$$\mathbf{y} = \mathbf{R}\mathbf{A}\mathbf{b} + \boldsymbol{\gamma} \quad (2.6)$$

where  $\boldsymbol{\gamma} = [\gamma_1, \gamma_2, \dots, \gamma_K]^T$ ,  $\gamma_k = \sum_n x_k(n)v(n)$ , is a noise related vector. It is well known that the optimal solution  $\mathbf{b}$  maximizing  $\mathcal{L}(\mathbf{b})$  requires an exhausted bit search. This combinatorial problem is shown to be NP hard and the required computation complexity is on the order of  $O(2^K)$ . Although the ML criterion and the minimum BER criterion are different, their solutions are close especially for high SNR ratios. When the asynchronous transmission is considered, it has been shown that the complexity of the optimal receiver, implemented by a matched filter bank followed by the Viterbi algorithm, remains  $O(2^K)$ . The ML receiver requires the information of the signal amplitudes, signature waveforms, and signal delays for all users. When the criterion of minimum BER is utilized, the optimum detection, implemented with the backward-forward dynamic programming, still requires the complexity of  $O(2^K)$ . In this case, the variance of background noise is also necessary. These requirements along with the high computational complexity makes the optimal receiver infeasible for real-world implementation.

## § 2.2 Linear Suboptimal Receivers

The optimal MUD has been regarded as powerful yet complicated. The suboptimal MUD was developed to reduce the complexity while still provide performance gain. In this section, we describe the suboptimal linear multiuser receivers. The linear receiver performs a linear transformation on the received signal vector  $\mathbf{y}$ . The first linear multiuser receiver is called the decorrelating detector or simply the decorrelator, whose name stems from the fact that the detector simply inverts the correlation matrix in (2.6). Let

$$\mathbf{M}_D = \mathbf{R}^{-1}. \quad (2.7)$$

Then, the receiver output is given by

$$\begin{aligned}\mathbf{z}_D &= \mathbf{M}_D \mathbf{y} \\ &= \mathbf{A} \mathbf{b} + \mathbf{R}^{-1} \boldsymbol{\gamma}.\end{aligned}\quad (2.8)$$

As shown, the interference from the MAI is eliminated completely. However, noise becomes colored and its level may be enhanced. When the noise level dominates the MAI, the performance of the decorrelator is degraded. The decorrelator is also the joint ML solution for the simultaneous estimate of channel gains and transmission bits. The solution can be found by the minimization of a least-squares criterion.

$$\{\hat{\mathbf{A}}, \hat{\mathbf{b}}\}_D = \min_{\mathbf{b}} \min_{a_k \geq 0, \forall k} \int_0^T \left[ r(t) - \sum_k a_k b_k x_k(t) \right]^2 dt. \quad (2.9)$$

In contrast to the optimal MUD, the decorrelator does not require user signal amplitudes. In addition, it was shown that the near-far resistance is equal to the that of the optimal receiver. The fluctuation of the interference powers do not have any influence on the performance of the decorrelator.

Another commonly cited suboptimal linear receiver is the LMMSE receiver whose transformation matrix is defined by

$$\mathbf{M}_L = \min_{\mathbf{M}} E[|\mathbf{b} - \mathbf{M} \mathbf{y}|^2]. \quad (2.10)$$

After some matrix manipulation, we can obtain the transformation matrix for the LMMSE multiuser receiver as

$$\mathbf{M}_L = [\mathbf{R} + \sigma^2 \mathbf{A}^{-2}]^{-1}. \quad (2.11)$$

Comparing the decorrelator with LMMSE receivers, we can observe that the LMMSE receiver becomes the decorrelator as  $\sigma^2$  approaches zero. On the other hand, the LMMSE receiver will degenerate into the matched filter when noise  $\sigma^2$  approaches infinity. This means that LMMSE multiuser receiver performs a compromise between noise enhancement and interference cancellation. When the LMMSE receiver is used, the signal amplitudes as well as the noise variance have to be known, in addition to the signal spreading codes and received signal delays.

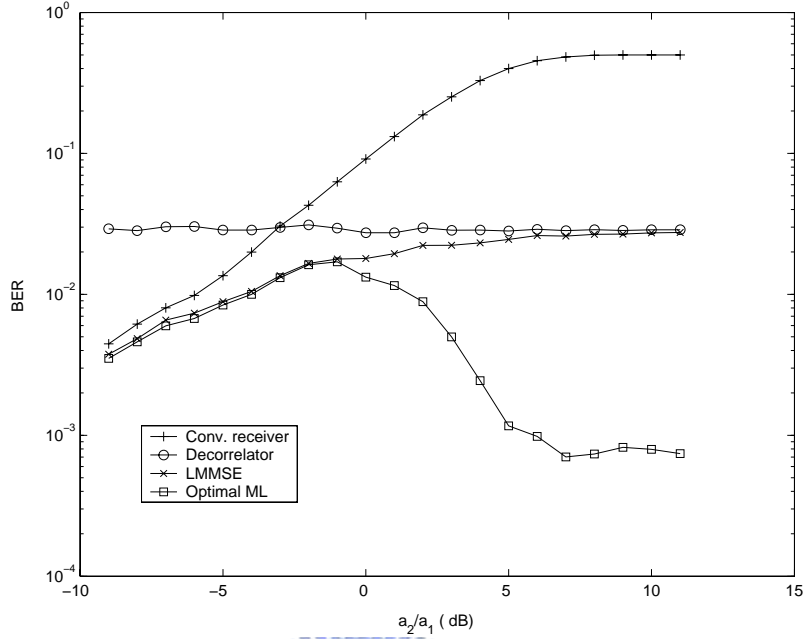


Figure 2.1: BER performance comparison of multiuser receivers for the first user ( $E_b/N_0 = 7$  dB, and  $\rho = 0.8$ ).

It can be observed that the matrix inversion is required in linear receivers. In order to reduce the computational burden, adaptive implementation was proposed. Let  $\varsigma_k = a_k b_k$ ,  $\varsigma = [\varsigma_1, \varsigma_2, \dots, \varsigma_K]^T$ . Rewrite (2.9) as

$$\hat{\varsigma} = \min_{\varsigma} \sum_{n=0}^{N-1} \left[ r(n) - \sum_k \varsigma_k x_k(n) \right]^2 dt. \quad (2.12)$$

where  $r(n)$  and  $x_k(n)$  are the chip-sampled sequences of  $r(t)$  and  $x_k(t)$ , respectively, and  $N$  is the processing gain. The estimate of  $\hat{\varsigma}$  gives the channel gains and bits, which are those in (2.8). The adaptive implementation of the decorrelator does not involve the complicated matrix inversion operation. Similarly, the LMMSE receiver can have an adaptive implementation. Let  $\mathbf{r} = [r(0), r(1), \dots, r(N-1)]^T$ . It can be easily shown that the LMMSE receiver output is

$$z_L = \mathbf{D}_L \mathbf{r} \quad (2.13)$$

where  $\mathbf{D}_L = [\mathbf{d}_1, \mathbf{d}_2, \dots, \mathbf{d}_K]^T$  is an  $K \times N$  matrix. Thus, we can use the MMSE criterion to

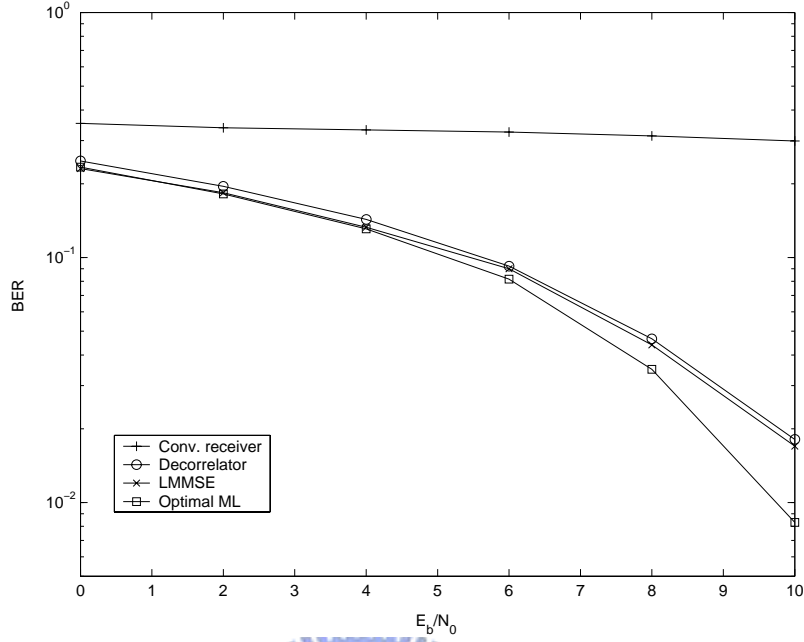


Figure 2.2: BER performance comparison of multiuser receivers ( $K = 10$ , and  $\rho = 0.8$ ).

derive  $\mathbf{d}_k$ . Thus,

$$\hat{\mathbf{d}}_k = \min_{\mathbf{d}_k} E \left[ b_k - \sum_{n=0}^{N-1} d_k(n)r(n) \right]^2 dt \quad (2.14)$$

Note that some transmission bits are required for training. The MUD performance measure includes the BER, the asymptotic multiuser efficiency, and the near-far resistance [7]. We have carried out some simulations to evaluate the performance of the receivers described above. Figure 2.1 shows the result for BER vs. interference power. Here, the user number is two, the code correlation is  $\rho = 0.8$ , and  $E_b/N_0 = 7$  dB ( $N_0 = 2\sigma^2$ ). Note that the  $x$ -axis of the figure is the power ratio of the two users. The conventional receiver suffers from the interference from the second user, and its performance degrades rapidly when the normalized interference power increases up to 5 dB. The ML receiver has the best near-far resistance among the four detectors. The decorrelator exhibits a constant near-far resistance in all interference power ratios. The LMMSE receiver is degenerated to the conventional receiver when the interference is weak while to the decorrelator when the interference is strong; it performs very similarly to the ML

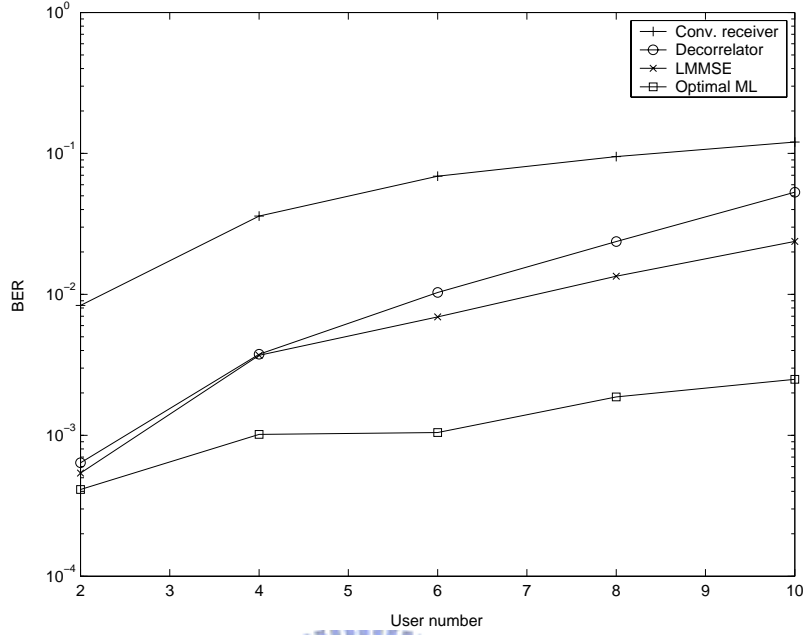


Figure 2.3: BER performance comparison of multiuser receivers (random codes,  $N = 15$ , and  $E_b/N_0 = 6$  dB.)

receiver in weak interference. Figure 2.3 shows the BER vs.  $E_b/N_0$  for ten equicorrelated users ( $\rho = 0.8$ ). The single-user receiver suffers from MAI and perform poorly in most cases. The linear receivers perform similarly to the ML receiver when the number of users is small.

## § 2.3 Interference Cancellation Methods

The interference cancellation scheme first estimates interference from other users and then cancels it from the received signal. Let  $\hat{r}_k(t)$  be the interference cancelled signal for User  $k$ . We then have

$$\begin{aligned}
 \hat{r}_k(t) &= r(t) - \sum_j \hat{s}_j(t) \\
 &= r(t) - \sum_j g_j x_j(t)
 \end{aligned} \tag{2.15}$$



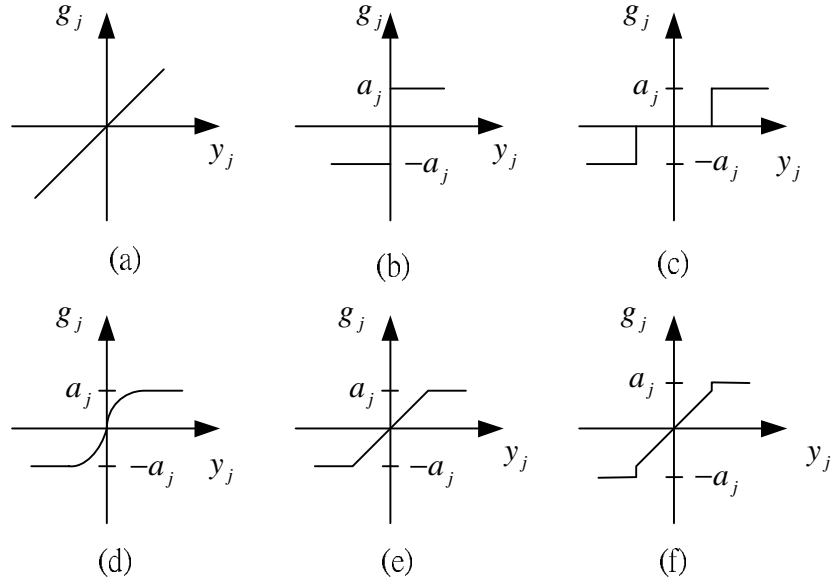


Figure 2.4: Interference estimate functions. (a) Soft-decision function (b) Hard-decision function (c) Null-zone function (d) Hyperbolic tangent function (e) Unit-clipper function (f) Modified unit-clipper function.

where  $g_j$  represents the interference estimate of  $a_j b_j$ . The number of interference cancelled in (2.15) depends on the algorithm used. For description simplicity, we assume a two-stage cancellation scheme such that  $g_j = F(y_j)$ , where  $F(\cdot)$  is a decision function. Commonly used decision functions are summarized in Fig. 2.4. Note that channel gains are assumed to be known. The second stage output is obtained by

$$z_k = \int_0^T \hat{r}_k(t) x_k(t) dt. \quad (2.16)$$

The decision functions in Fig. 2.4 are further described below.

(a) Soft-decision function:  $g_j = y_j$

(b) Hard-decision function:  $g_j = a_j \text{sgn}[y_j]$

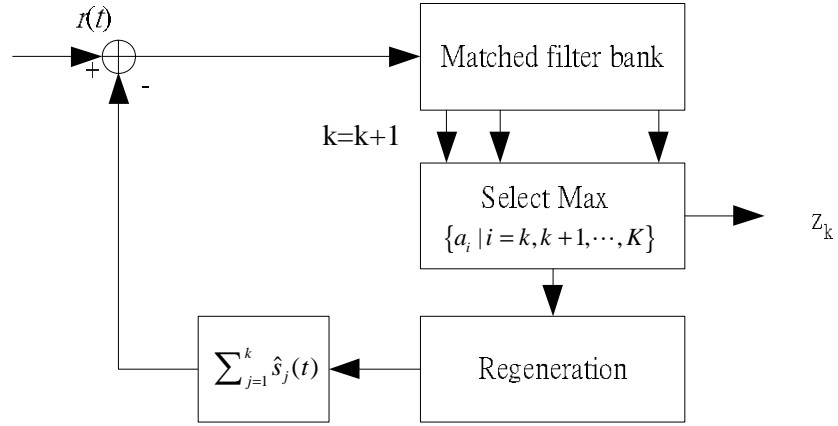


Figure 2.5: Block diagram for an SIC receiver.

(c) Null-zone function: 
$$g_j = \begin{cases} a_j & y_j \geq \xi \\ 0 & -\xi < y_j < \xi \\ -a_j & y_j \leq -\xi \end{cases}$$

(d) Hyperbolic tangent function: 
$$g_j = a_j \tanh(a_j y_j / \sigma_j^2)$$
  
 where  $\sigma_j^2$  represents the power of interference and noise for the  $j$ th user.

(e) Unit-clipper function: 
$$g_j = \begin{cases} a_j & y_j \geq a_j \\ y_j & -a_j < y_j < a_j \\ -a_j & y_j \leq -a_j \end{cases}$$

(f) Modified unit-clipper function: 
$$g_j = \begin{cases} a_j & y_j \geq \xi \\ y_j & -\xi < y_j < \xi \\ -a_j & y_j \leq -\xi \end{cases}, \text{ where } \xi < a_j$$

In the following, we describe the basic types of interference cancellation schemes, namely, SIC and PIC.

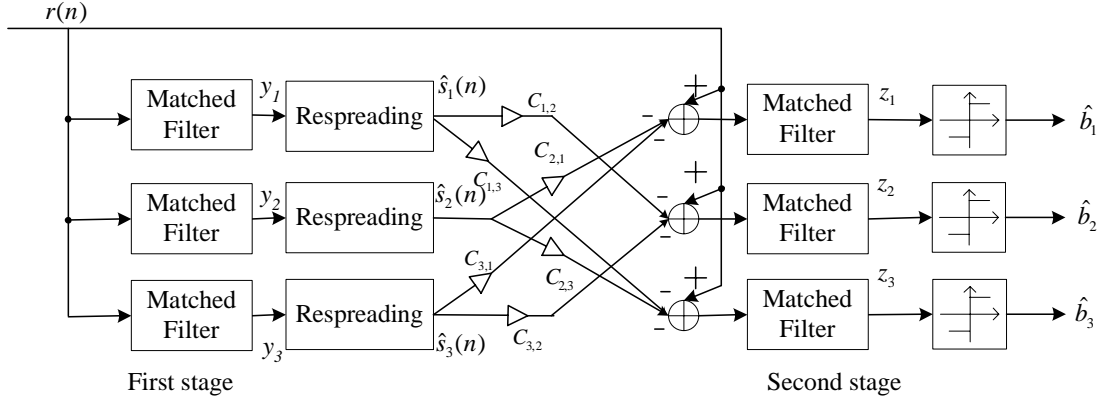


Figure 2.6: Block diagram for a general two-stage partial SPIC receiver.

### § 2.3.1 Successive Interference Cancellation

The SIC cancels one user interference from the received signal at a time. Since only one interference needs to be estimated and subtracted in each stage, the strongest user signal is then the best candidate. Its structure is depicted in Figure 2.5. Assume that the received signal powers are ranked as  $a_1 \geq a_2 \dots \geq a_K$ , and the interference cancelled signal for user  $k$  at the  $i$ th stage is obtained as

$$\hat{r}_k^{(i)}(t) = \hat{r}_k^{(i-1)}(t) - g_i x_i(t), \quad k = 1, 2, \dots, K, k \neq i \quad (2.17)$$

where  $\hat{r}_k^{(0)}(t) = r(t)$ , for all  $k$  is the initial receive signal. The SIC output at the  $i$ th stage is then

$$z_k = \int_0^T \hat{r}_k^{(i)}(t) x_k(t) dt. \quad (2.18)$$

Although the SIC is simple to apply, there are some drawbacks listed below.

- Since the user is detected successively, the subsequent users will experience less interference. To make all users have similar performance, transmission power for each user will be different. A proper power profile may not be easy to obtain. In addition, the power ordering operation requires additional computational complexity.
- The interference resulted from the erroneous cancellation will propagate to all the users at following stages. This introduces the error propagation effect.

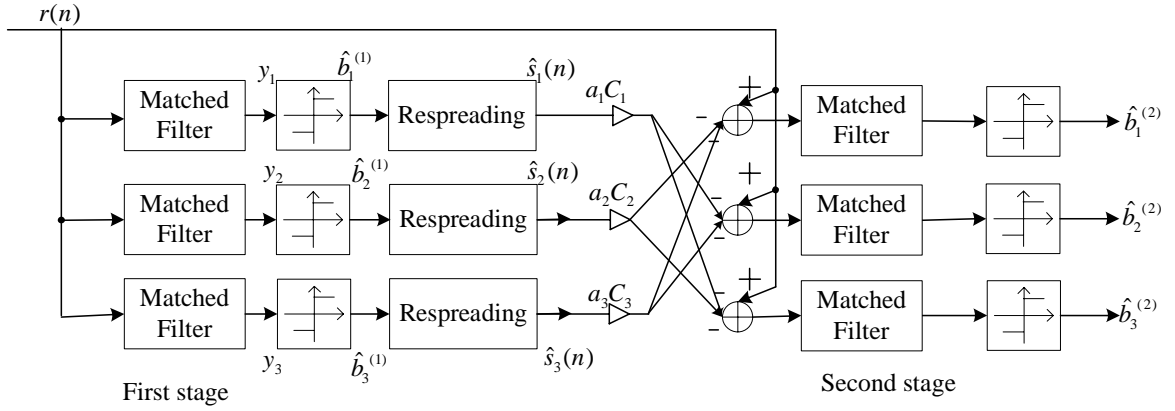


Figure 2.7: Block diagram for a two-stage coupled partial HPIC receiver.

- A SIC scheme needs at least  $K$  stages for a  $K$ -user environment. This will greatly increase the detection delay especially when the user number is large.

### § 2.3.2 Parallel Interference Cancellation

The PIC cancels interference from all other users at the same time. In contrast to SIC, the PIC has lower detection delay and does not have the power assignment problem. It has been shown that the PIC has superior performance over the SIC in an power balanced scenario. Conventional PIC receivers permit a full cancellation of the MAI. One problem associated with this full PIC is that the MAI estimate may not be reliable in the earlier canceling stages. This makes the PIC less effective when the number of users is large. As a remedy, the partial PIC detector has been proposed in which partial cancellation factors (PCFs) are introduced to control the interference cancellation level. As shown in 2.6, a complete partial PIC requires  $K(K - 1)$  PCFs for one stage where  $K$  is the number of users; the computational complexity is high. Simplified partial PICs have been proposed, in which only  $K$  PCFs are needed. Two structures are commonly used for simplified partial PICs; we call them the coupled and decoupled structures. In the coupled structure, each user output is influenced by all  $K$  PCFs [62] as seen in Figure 2.7, while in the decoupled structure each user output is only influenced by a specific PCF as shown

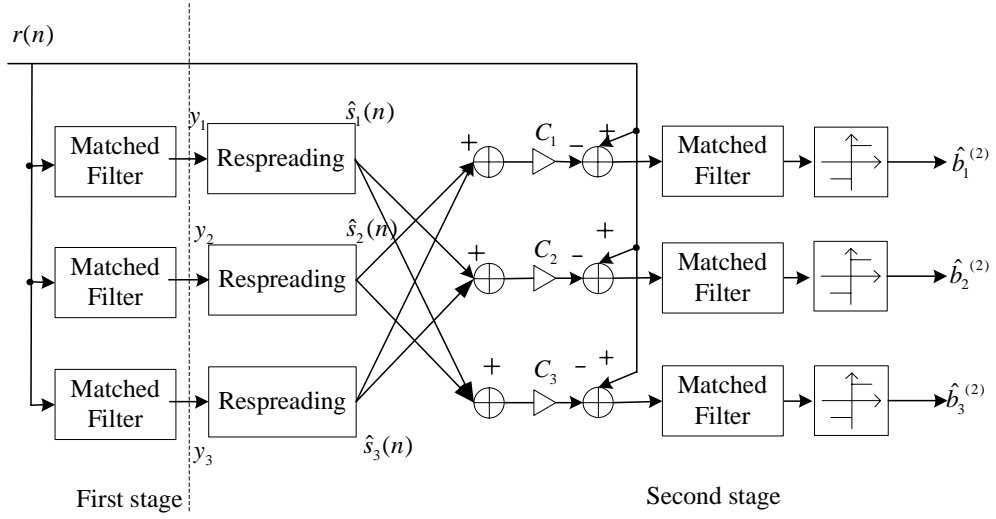


Figure 2.8: Block diagram for a two-stage decoupled partial SPIC receiver.

in Figure 2.8. The partial HPICs mentioned in Chapter 1 all use the coupled structure. A MSE criterion, as shown below, has been proposed to optimize PCFs [57].

$$\begin{aligned}
C_k &= \min_{C_k} E\{[a_k b_k - C_k \hat{b}_k]^2\} \\
&= \min_{C_k} \left\{ a_k^2 + C_k^2 - 2a_k C_k E\{b_k \hat{b}_k\} \right\} \\
&= \min_{C_k} \left\{ a_k^2 + C_k^2 - 2a_k C_k (1 - 2P_{e,k}) \right\} \\
&= a_k (1 - 2P_{e,k})
\end{aligned} \tag{2.19}$$

where  $P_{e,k}$  is the error probability for the  $k$ th user. As we can see, each PCF can be determined independently. From (2.19), we can observe that when the data bits are all correctly detected, the optimal PCFs will approach unity. On the other hand, when the data bits are all erroneously detected, ( $P_{e,k} \approx 1/2$ ), the optimal PCFs will approach zero. This is intuitively appealing. Although simple, the optimal PCFs in (2.19) are not accurate for short codes. Thus, its real-world application is limited.

The optimal PCF obtained by theoretical calculation may not be efficient when the channel is time-varying. There exist an adaptive partial HPIC that can overcome this problem [62]. This adaptive HPIC is blind in the sense that no training sequence is required. Due to its simplicity

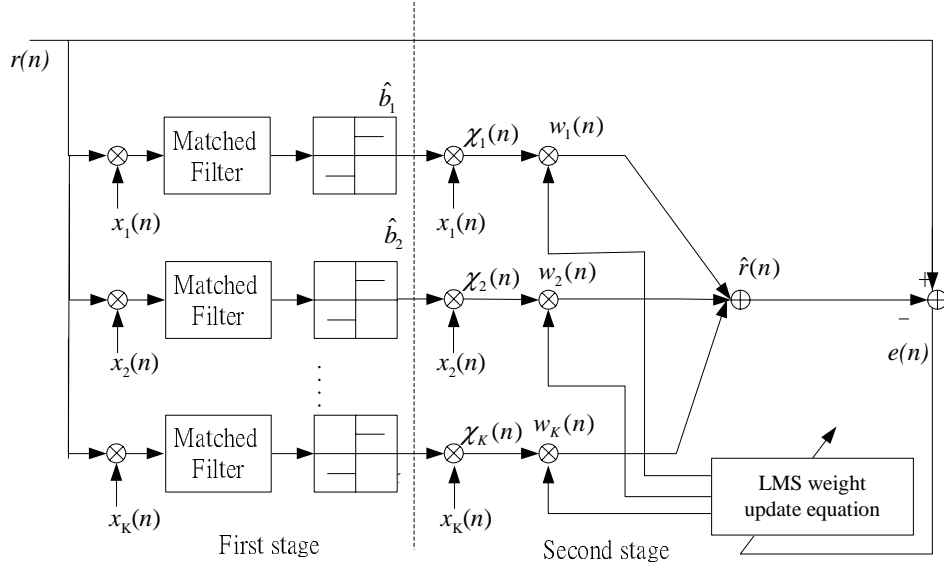


Figure 2.9: LMS algorithm for two-stage adaptive blind partial HPIC receivers.

and robustness, the LMS algorithm was used as the adaptive algorithm. A typical block diagram for a two-stage HPIC is shown in Fig. 2.9. The weights are trained using the LMS algorithm which minimizes a MMSE criterion defined as (for the  $i$ th stage)

$$\mathbf{w}_{opt}^{(i)} = \min_{\mathbf{w}^{(i)}} J^{(i)}(n) \quad (2.20)$$

where  $\mathbf{w}_{opt}^{(i)}$  is the optimal weight vector at the  $i$ th stage, and

$$J^{(i)}(n) = E \left\{ \left[ r(n) - \sum_{k=1}^K w_k^{(i)}(n) \hat{b}_k^{(i-1)} x_k(n) \right]^2 \right\}. \quad (2.21)$$

The weight after trained,  $w_j^{(i)}(N)$ , acts as each user' PCF. Note that this is a system identification problem. The LMS update equation for the  $i$ th stage (with  $i - 1$  stages of interference cancellation) is formulated as

$$\begin{aligned} \hat{r}^{(i)}(n) &= \boldsymbol{\chi}^{(i)}(n)^T \mathbf{w}^{(i)}(n) \\ e^{(i)}(n) &= r(n) - \hat{r}^{(i)}(n) \\ \mathbf{w}^{(i)}(n+1) &= \mathbf{w}^{(i)}(n) + \mu e^{(i)}(n) \boldsymbol{\chi}^{(i)}(n) \end{aligned} \quad (2.22)$$

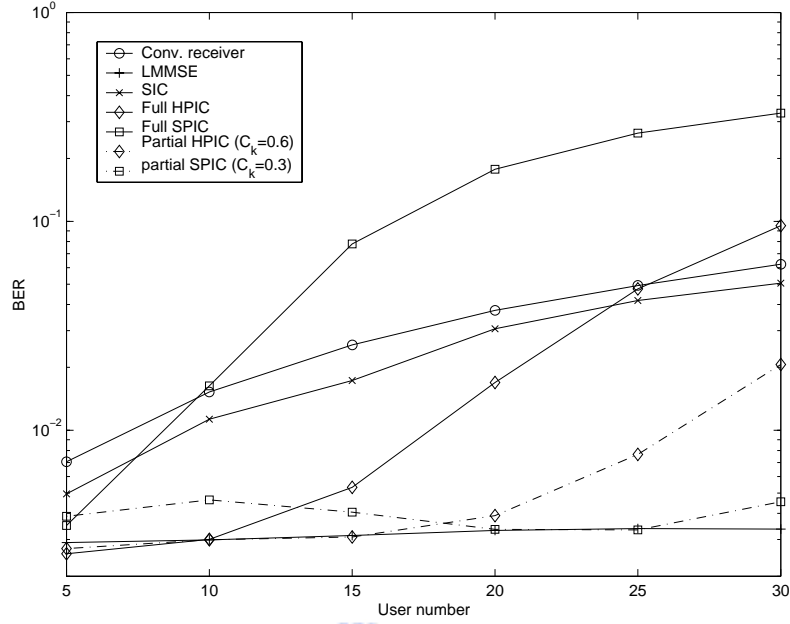


Figure 2.10: BER performance comparison for different multiuser receivers ( $\rho = 0.1$ ,  $E_b/N_0 = 6$  dB, and power balanced).

where  $\mathbf{x}^{(i)} = [\hat{b}_1^{(i-1)} x_1(n), \hat{b}_2^{(i-1)} x_2(n), \dots, \hat{b}_K^{(i-1)} x_K(n)]^T$  is the input vector. The interference estimate for the  $k$ th user in the  $i$ -stage is given by

$$\hat{r}_k^{(i)}(n) = \sum_{j \neq k} w_j^{(i)}(N) \hat{b}_j^{(i-1)} x_j(n). \quad (2.23)$$

Then the  $i$ -stage output from the adaptive blind partial HPIC can be obtained

$$y_k^{(i)} = \sum_{n=0}^{N-1} \hat{r}_k^{(i)}(n) x_k(n). \quad (2.24)$$

Note that the adaptive blind partial HPIC is different from the work in [17], since this scheme does not require the training sequence. The optimal weights are optimized in one bit interval; its adaptation is on the chip-level.

As to the partial SPIC, both the coupled and decoupled structures have been studied. In this dissertation, we focus on the decoupled structure which is shown in Figure 2.8. The reason to consider this structure is that the PCF optimization is simpler and its performance is comparable

Table 2.1: Required information for different multiuser receivers.

	SU	ML	MBER	DEC	LMMSE	AMMSE	IC
Desired user's signature	✓	✓	✓	✓	✓		✓
Desired user's timing	✓	✓	✓	✓	✓	✓	✓
User amplitude		✓	✓		✓		✓
noise variance			✓		✓		
Others' signature		✓	✓	✓	✓		✓
Others' timing		✓	✓	✓	✓		✓
Training data						✓	

- SU : Single-user receiver
- ML : Maximum-likelihood receiver
- MBER : Minimum BER receiver
- DEC : Decorrelator
- LMMSE : Linear mean square error receiver
- AMMSE : Adaptive LMMSE
- IC : Interference cancellation receiver

to other structures. We have carried out simulations to compare performance of various two-stage PIC with LMMSE receivers. The result is shown in Figure 2.10 ( $\rho = 0.1$ ,  $E_b/N_0 = 6$  dB, and power balance is assumed). The LMMSE performs the best among all multiuser receivers. The SIC has only minor advantage over the single-user receiver. This is because in the power balanced scenario, the power ranking does not have advantages. The full HPIC performs better than SIC. Note that the full SPIC perform poorly when the user number increases. Partial PICs with optimal PCFs perform much better and the partial SPIC performs similarly to the LMMSE receiver. In Table 2.1 we summarize requirement information for various MUD methods.



# Chapter 3

## Optimal Two-stage Partial SPIC Receivers

### § 3.1 Introduction

In this chapter, we focus on a two-stage partial SPIC receiver with a decoupled structure. Our motivation for using two-stage processing is that it requires low computational complexity and is particularly suitable for real-world implementation. As indicated in [55] that in higher stage processing, the PCFs will approach unity for stages greater than two. In other words, the PCFs in the second stage will dominate system performance. We first consider the additive white Gaussian noise (AWGN) channel and derive optimal PCFs for systems employing periodic codes. The criterion for optimization is the bit error rate (BER). We then extend the result to systems with aperiodic spreading codes. Finally, we consider optimal PCFs with multipath channels. Simulations show that the performance of our theoretical optimal PCFs is close to that of empirical ones. In addition, the optimal two-stage partial SPIC outperforms not only the two-stage full SPIC, but also the three-stage full SPIC. The remainder of this chapter is organized as follows. In Section 2, we describe the two-stage full and partial SPIC receiver structures. In Section 3 and Section 4, we derive optimal PCFs with periodic and aperiodic codes, both in AWGN and multipath channels. Simulation results are presented and discussed in Section 5.

## § 3.2 System Model

Consider a synchronous CDMA system accommodating  $K$  users. Let  $r(t)$  denote the received signal (for a certain bit interval),  $s_k(t)$  the  $k$ th user's transmitted signal, and  $n(t)$  additive white Gaussian noise. The equivalent baseband received signal can be described as

$$\begin{aligned} r(t) &= \sum_{k=1}^K s_k(t) + n(t) \\ &= \sum_{k=1}^K a_k b_k x_k(t) + n(t), \quad t \in [0, T] \end{aligned} \quad (3.1)$$

where  $a_k$  and  $b_k$  are the  $k$ th user's amplitude and data bit,  $x_k(t)$  denotes its signature waveform, and  $T$  is the bit period. The signature waveform can be expressed as

$$x_k(t) = \sum_{i=0}^{N-1} x_{k,i} \Pi_{T_c}(t - iT_c) \quad (3.2)$$

where  $x_{k,i} \in \{1/\sqrt{N}, -1/\sqrt{N}\}$  is the binary spreading chip sequence for User  $k$ ,  $N$  is the processing gain,  $\Pi_{T_c}$  is a rectangular pulse waveform with support  $T_c$  and unit magnitude. Note that  $T_c$  is the chip period.

The first stage of a PIC receiver is the conventional matched filter bank. The output can be represented as

$$\begin{aligned} y_k &= \int_0^T r(t) x_k(t) dt \\ &= a_k b_k + \sum_{j \neq k} a_j b_j \rho_{jk} + \gamma_k \end{aligned} \quad (3.3)$$

where  $\rho_{jk}$  is a correlation coefficient and  $\gamma_k$  is the noise term after despreading. They are defined as

$$\rho_{jk} \triangleq \int_0^T x_j(t) x_k(t) dt, \quad (3.4)$$

and

$$\gamma_k \triangleq \int_0^T n(t) x_k(t) dt. \quad (3.5)$$

It can be seen that the output metric in (3.3) consists of three parts: the desired signal, MAI, and  $\gamma_k$ . The conventional detector makes a decision based on  $y_k$ . Thus, MAI is treated as another noise source. When the number of users is large, MAI will seriously degrade the system performance. A PIC, being a multiuser detection scheme, was proposed to alleviate this problem. Let  $\hat{r}_k(t)$  be an interference-subtracted signal (for User  $k$ ) given by

$$\hat{r}_k(t) = r(t) - \sum_{j \neq k} \hat{s}_j(t) \quad (3.6)$$

where  $\hat{s}_j(t)$  is a regenerated signal for User  $j$ . For SPIC, this signal is obtained by

$$\hat{s}_j(t) = y_j x_j(t). \quad (3.7)$$

Thus, the output signal in the second stage is then

$$z_k = \int_0^T \hat{r}_k(t) x_k(t) dt. \quad (3.8)$$

Finally, the symbol data is detected as  $\hat{b}_k = \text{sgn}(z_k)$ . In principle, the interference cancellation procedure in (3.6)-(3.8) can be repeated with multiple stages to obtain better performance. It is apparent from (3.3) and (3.7) that the regenerated signal is noisy. Thus, fully cancelling the regenerated interference may not yield best results. One solution to this problem is to partially cancel the interference. This idea is implemented by modifying (3.6) as

$$\hat{r}_k(t) = r(t) - \sum_{j \neq k} C_{jk} \hat{s}_j(t). \quad (3.9)$$

The constants  $C_{jk}$ 's are called the partial cancellation factors (PCFs) for User  $k$  and their amplitudes should reflect the fidelity of the interference estimate. The structure of a partial SPIC receiver with three users is shown in Figure 3.1.

Generally,  $K \times (K - 1)$  PCFs are needed for a two-stage partial PIC. It is apparent that the computational complexity of the partial PIC is high when the number of users is large [on the order of  $O(K^2)$ ]. Two simplified structures, whose complexities are on the order of  $O(K)$ , were investigated in the literature. The first one corresponds to the case in which  $C_{jk} = C_j$  [in (3.9)].

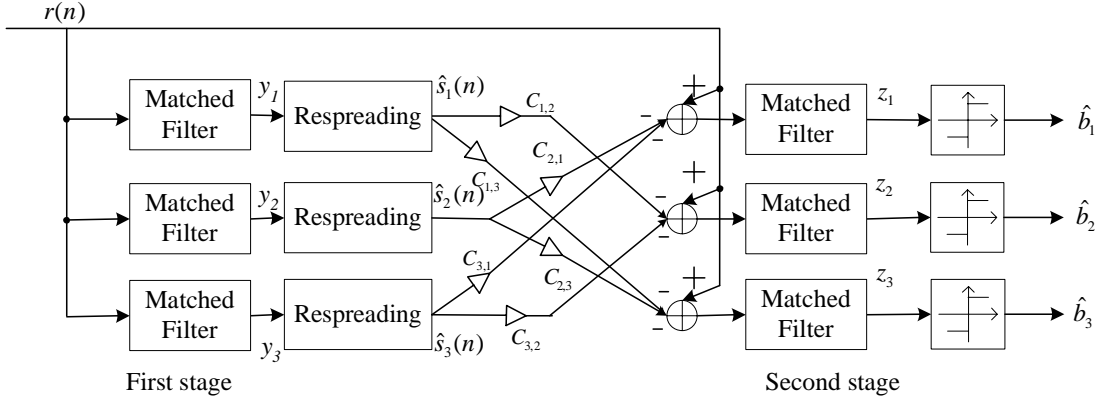


Figure 3.1: General partial SPIC receiver structure.

In this case, all regenerated signals are first weighted and then summed. Thus, each regenerated interference signal in (3.9) has an individual PCF and the signal to be estimated is a function of all PCFs. We call this structure the coupled structure. The other structure is one in which  $C_{jk} = C_k$ . In this case, all regenerated signals are summed first and then weighted. Thus, there is one PCF for the signal to be estimated. We thus call this structure the decoupled structure. A thorough discussion of both structures is not available in the literature. Optimal PCFs have only been derived for the coupled structure under power balanced scenarios [61]. In what follows, we focus on a two-stage partial SPIC receiver with a decoupled structure. Primary simulation results (in Section 5) show that both PIC structures with optimal PCFs perform similarly.

### § 3.3 Optimal PCFs for AWGN Channels

In this section, we derive the optimal PCFs for a two-stage partial SPIC under an AWGN channel. For ease of description, we only give the results associated with synchronous transmission. Periodic and aperiodic spreading codes are both considered.

### § 3.3.1 Periodic Code Scenario

Assuming perfect chip synchronization, we first sample the received continuous-time signal in (3.1) with period  $T_c$ . Let  $\mathbf{r} = [r(0), r(T_c), \dots, r((N-1)T_c)]^T$  be the received signal sample vector,  $\mathbf{x}_k \triangleq [x_{k,0}, x_{k,1}, \dots, x_{k,N-1}]^T$  be the  $k$ th user's spreading sequence vector, and  $\mathbf{v} \triangleq [v(0), v(T_c), \dots, v((N-1)T_c)]^T$  be the noise sample vector. From (3.1), we have

$$\mathbf{r} = \sum_k a_k b_k \mathbf{x}_k + \mathbf{v}. \quad (3.10)$$

Thus, we can obtain the matched filter output as

$$\begin{aligned} y_k &= \mathbf{r}^T \mathbf{x}_k \\ &= a_k b_k + \sum_{j \neq k} a_j b_j \mathbf{x}_j^T \mathbf{x}_k + \mathbf{x}_k^T \mathbf{v}. \end{aligned} \quad (3.11)$$

Note that  $\mathbf{x}_j^T \mathbf{x}_k$  is a discrete version of the correlation term  $\rho_{jk}$  shown in (3.4). Similarly,  $\mathbf{x}_k^T \mathbf{v}$  is a discrete version of the noise-related term  $\gamma_k$  in (3.5). For notational simplicity, we still use  $\rho_{jk}$  to represent  $\mathbf{x}_j^T \mathbf{x}_k$  and  $\gamma_k$  to represent  $\mathbf{x}_k^T \mathbf{v}$ . Thus, (3.11) can be re-written as

$$y_k = a_k b_k + \sum_{j \neq k} a_j b_j \rho_{jk} + \gamma_k. \quad (3.12)$$

For the second stage of a partial SPIC (with the decoupled structure), the regenerated signal for User  $k$  is

$$\hat{\mathbf{r}}_k = \mathbf{r} - C_k \sum_{j \neq k} \hat{\mathbf{s}}_j \quad (3.13)$$

where  $\hat{s}_j = y_j \mathbf{x}_j$ . The second stage output is then

$$\begin{aligned}
z_k &= \hat{\mathbf{r}}_k^T \mathbf{x}_k \\
&= y_k - C_k \sum_{j \neq k} y_j \rho_{jk} \\
&= a_k b_k + \sum_{j \neq k} a_j b_j \rho_{jk} + \gamma_k - C_k \sum_{j \neq k} \left( a_j b_j + \sum_{m \neq j} a_m b_m \rho_{mj} + \gamma_j \right) \rho_{jk} \\
&= a_k b_k \left( 1 - C_k \sum_{j \neq k} \rho_{jk}^2 \right) + \left( \gamma_k - C_k \sum_{j \neq k} \gamma_j \rho_{jk} \right) \\
&\quad + \sum_{j \neq k} a_j b_j \left( \rho_{jk} - C_k \rho_{jk} - C_k \sum_{m \neq j, k} \rho_{jm} \rho_{mk} \right). \tag{3.14}
\end{aligned}$$

The bit error probability for User  $k$ , denoted as  $P(z_k)$ , can be written as

$$\begin{aligned}
P(z_k) &= \frac{1}{2} P(z_k | b_k = 1) + \frac{1}{2} P(z_k | b_k = -1) \\
&= P(z_k | b_k = 1). \tag{3.15}
\end{aligned}$$

In (3.15), we assume that the occurrence probabilities for  $b_k = 1$  and  $b_k = -1$  are equal, and the error probabilities for  $b_k = 1$  and  $b_k = -1$  are also equal. As we can see, there are three terms in (3.14). The first term corresponds to the desired user bit. If we let  $b_k = 1$ , it is a deterministic value. The second term corresponds to noise interference which is Gaussian distributed. The third term corresponds to the interference from other users and each interference is Binomial distributed. Note that correlation coefficients in (3.14) are small and CDMA systems are usually operated in low signal-to-noise ratio (SNR) environments. The variance of the third term is then much smaller than that of the second term. Thus, we can assume that  $z_k$  conditioned on  $b_k = 1$  is Gaussian distributed. The error probability is then

$$P(z_k) = Q \left\{ \sqrt{\frac{\mathcal{M}_k}{\mathcal{V}_k}} \right\} \tag{3.16}$$

where  $Q\{\cdot\}$  is the Q-function and

$$\mathcal{M}_k = \left( E\{z_k | b_k = 1\} \right)^2 \tag{3.17}$$

$$\mathcal{V}_k = E\{z_k^2\} - \mathcal{M}_k. \tag{3.18}$$

Note that the expectations in (3.17) and (3.18) are operated on interfering user bits and noise. Let  $E\{\mathbf{v}\mathbf{v}^T\} = \sigma^2\mathbf{I}_N$  and  $\eta_j \triangleq a_j^2/\sigma^2$ . Evaluating (3.17), we obtain

$$\mathcal{M}_k = a_k^2 (1 - C_k \Lambda_k)^2 \quad (3.19)$$

where

$$\Lambda_k \triangleq \sum_{j \neq k} \rho_{jk}^2. \quad (3.20)$$

Similarly, we obtain the variance as

$$\mathcal{V}_k = \sigma^2 (\Omega_{1,k} C_k^2 - 2\Omega_{2,k} C_k + \Omega_{3,k}) \quad (3.21)$$

where the coefficients of  $\mathcal{V}_k$  are represented by

$$\Omega_{1,k} = \sum_{j \neq k} \eta_j \left( \rho_{jk} + \sum_{m \neq j,k} \rho_{jm} \rho_{mk} \right)^2 + \sum_{j \neq k} \left( \rho_{jk}^2 + \sum_{m \neq j,k} \rho_{jm} \rho_{mk} \rho_{jk} \right), \quad (3.22)$$

$$\Omega_{2,k} = \sum_{j \neq k} \eta_j \left( \rho_{jk}^2 + \sum_{m \neq j,k} \rho_{jm} \rho_{mk} \rho_{jk} \right) + \sum_{j \neq k} \rho_{jk}^2, \quad (3.23)$$

$$\Omega_{3,k} = \sum_{j \neq k} \eta_j \rho_{jk}^2 + 1. \quad (3.24)$$

The optimal PCF for User  $k$  can be found as

$$\begin{aligned} C_{k,opt} &= \arg \max_{C_k} \left\{ \frac{\mathcal{M}_k}{\mathcal{V}_k} \right\} \\ &= \left\{ C_{k,opt} : \mathcal{V}_k \frac{d\mathcal{M}_k}{dC_k} - \mathcal{M}_k \frac{d\mathcal{V}_k}{dC_k} = 0 \right\}. \end{aligned} \quad (3.25)$$

Substituting (3.19) and (3.21) into (3.25) and simplifying the result, we have the following equation.

$$(1 - C_{k,opt} \Lambda_k) \left[ C_{k,opt} (\Omega_{1,k} - \Lambda_{1,k} \Omega_{2,k}) + \Lambda_k \Omega_{3,k} - \Omega_{2,k} \right] = 0. \quad (3.26)$$

We have two possible solutions now. The first solution for the first parenthesis is trivial since it makes the squared mean value  $\mathcal{M}_k$  in (3.19) zero. The optimum PCF is then

$$C_{k,opt} = \frac{\Omega_{2,k} - \Omega_{3,k} \Lambda_k}{\Omega_{1,k} - \Omega_{2,k} \Lambda_k}. \quad (3.27)$$

We also derived optimal PCFs for an asynchronous CDMA system. The results are summarized in Appendix A. In what follows we discuss some special cases to give a better understanding of the optimal PCF characteristics. Let the correlations between any two user spreading codes be equal ( $\rho_{jk} = \rho$  for  $j \neq k$ ) and the power control be perfect ( $a_k = a$  and  $\eta_k = \eta$ ). The optimal PCF can then be expressed as

$$C_{k,opt} = \frac{\eta}{1 + \eta[1 + \rho(K - 2)]}. \quad (3.28)$$

As we can see from (3.28), the optimal PCF is smaller when  $\rho$  or  $K$  is larger, because when the correlations between user codes are higher and the number of users is larger, the MAI is larger and the regenerated signal is unreliable. As a result, the PCF should be smaller. Also, when the user power is larger or the noise is smaller ( $\eta$  is larger), the optimal PCF is larger. If we assume that the noise is much smaller than the signal power ( $\eta \gg 1$ ), the optimal PCF can be further simplified to

$$C_{k,opt} = \frac{1}{1 + \rho(K - 2)}. \quad (3.29)$$

Now the optimal PCF is independent of the transmission signal power. The bit error performance would also be saturated in this interference-limited region. From (3.28), we can also see that when the noise is large ( $\eta \ll 1$ ), the optimal PCF tends to be small ( $C_k \rightarrow 0$ ). Note that the effect of the processing gain  $N$  is reflected in the receiving SNR. If  $N$  is larger, the receiving SNR will become smaller.

### § 3.3.2 Aperiodic Code Scenario

In commercial CDMA systems, the users' spreading codes are often modulated with another code having a very long period. As far as the received signal is concerned, the spreading code



is not periodic. In other words, there will be many possible spreading codes for each user. If we use the result derived above, we then have to calculate the optimum PCFs for each possible code and the computational complexity will become very high. Since the period of the modulating code is usually very long, we can treat the code chips as independent random variables and approximate the correlation coefficient,  $\rho_{jk}$ , as a Gaussian random variable. As a result, the expectations in (3.17) and (3.18) can be further operated on  $\rho_{jk}$ . This greatly simplifies the optimal PCF evaluation. We now rewrite (3.16) as

$$P(z_k) = \mathcal{Q} \left\{ \sqrt{\frac{E_{\mathcal{L}}\{\mathcal{M}_k^{(l)}\}}{E_{\mathcal{L}}\{\mathcal{V}_k^{(l)}\}}} \right\} \quad (3.30)$$

where  $E_{\mathcal{L}}\{\cdot\}$  denotes the expectation operator over the spreading code set  $\mathcal{L}$  and  $\mathcal{M}_k^{(l)}$  and  $\mathcal{V}_k^{(l)}$  are the expected squared mean and variance of  $z_k$ , respectively, given the  $l$ th possible code in  $\mathcal{L}$ . Letting  $I_k = \sum_{j \neq k} \eta_j$ , considering  $\rho_{jk}$  as a Gaussian random variable, and evaluating (3.17) and (3.18), we have

$$E_{\mathcal{L}}\{\mathcal{M}_k^{(l)}\} = a_k^2 \left( 1 - C_k E_{\mathcal{L}}\{\Lambda_k^{(l)}\} \right)^2 \quad (3.31)$$

where

$$E_{\mathcal{L}}\{\Lambda_k^{(l)}\} = \frac{K-1}{N}, \quad (3.32)$$

and

$$E_{\mathcal{L}}\{\mathcal{V}_k^{(l)}\} = \sigma^2 \left( E_{\mathcal{L}}\{\Omega_{1,k}^{(l)}\} C_k^2 - 2E_{\mathcal{L}}\{\Omega_{2,k}^{(l)}\} C_k + E_{\mathcal{L}}\{\Omega_{3,k}^{(l)}\} \right) \quad (3.33)$$

where

$$E_{\mathcal{L}}\{\Omega_{1,k}^{(l)}\} = I_k \left( \frac{1}{N} + \frac{3(K-2)}{N^2} + \frac{(K-2)(K-3)}{N^3} \right) + \frac{K-1}{N} + \frac{(K-1)(K-2)}{N^2}, \quad (3.34)$$

$$E_{\mathcal{L}}\{\Omega_{2,k}^{(l)}\} = I_k \left( \frac{1}{N} + \frac{K-2}{N^2} \right) + \frac{K-1}{N}, \quad (3.35)$$

$$E_{\mathcal{L}} \left\{ \Omega_{3,k}^{(l)} \right\} = \frac{I_k}{N} + 1. \quad (3.36)$$

In the above expressions, the notation  $X^{(l)}$  denotes the  $X$  value given the  $l$ -th possible spreading code in  $\mathcal{L}$ . Equation (3.25) can be re-expressed as

$$\begin{aligned} C_{k,opt} &= \arg \max_{C_k} \left\{ \frac{E_{\mathcal{L}} \{ \mathcal{M}_k^{(l)} \}}{E_{\mathcal{L}} \{ \mathcal{V}_k^{(l)} \}} \right\} \\ &= \left\{ C_{k,opt} : E_{\mathcal{L}} \{ \mathcal{V}_k^{(l)} \} \frac{dE_{\mathcal{L}} \{ \mathcal{M}_k^{(l)} \}}{dC_k} - E_{\mathcal{L}} \{ \mathcal{M}_k^{(l)} \} \frac{dE_{\mathcal{L}} \{ \mathcal{V}_k^{(l)} \}}{dC_k} = 0 \right\}. \end{aligned} \quad (3.37)$$

Substituting (3.31)-(3.36) into (3.37) and simplifying the result, we finally obtain

$$C_{k,opt} = \frac{E_{\mathcal{L}} \{ \Omega_{2,k}^{(l)} \} - E_{\mathcal{L}} \{ \Omega_{3,k}^{(l)} \} E_{\mathcal{L}} \{ \Lambda_k^{(l)} \}}{E_{\mathcal{L}} \{ \Omega_{1,k}^{(l)} \} - E_{\mathcal{L}} \{ \Omega_{2,k}^{(l)} \} E_{\mathcal{L}} \{ \Lambda_k^{(l)} \}}. \quad (3.38)$$

As we can see, (3.38) only involves (3.32) and (3.34)-(3.36) and these expressions are easy to work with. We further consider the case in which noise is small ( $I_k \gg K$ ). Equation (3.38) can be simplified to

$$C_{k,opt} = \frac{1896N}{N + 2K - 4}. \quad (3.39)$$

This result is remarkably simple. We only require  $N$  and  $K$  to calculate optimal PCFs; this will be useful in real-world applications.

## § 3.4 Optimal PCFs for Multipath Channels

### § 3.4.1 Periodic Code Scenario

Let the transfer function for User  $k$ 's channel be

$$\mathcal{W}_k(z) = \sum_{i=1}^L h_{k,i} z^{-\tau_{k,i}}. \quad (3.40)$$

As we can see from (3.40), the number of paths is  $L$  and the gain and delay for the  $i$ th channel path are  $h_{k,i}$  and  $\tau_{k,i}$ , respectively. We use two vectors to represent these parameters:  $\mathbf{t}_k =$

$[\tau_{k,1}, \tau_{k,2}, \dots, \tau_{k,L}]^T$  and  $\mathbf{h}_k = [h_{k,1}, h_{k,2}, \dots, h_{k,L}]^T$ . Let  $\tau_{k,1} \leq \tau_{k,2} \leq \dots \leq \tau_{k,L}$  and the channel power is normalized ( $\sum h_{k,i}^2 = 1$ ). Without loss of generality, we may assume that  $\tau_{k,1} = 0$  for each user and  $L$  is the maximum possible number of paths. When a user's path number, say  $L'$ , is less than  $L$ , we can let all the elements in  $\tau_{k,i}$  and  $h_{k,i}$  be zero for  $L' + 1 \leq i \leq L$ . We may also assume that the maximum delay is much smaller than the processing gain  $N$  [67]. Before our formulation, we first define a  $(2N - 1) \times L$  composite signature matrix  $\mathbf{S}_k$  as

$$\mathbf{S}_k \triangleq [\tilde{\mathbf{x}}_{k,1}, \tilde{\mathbf{x}}_{k,2}, \dots, \tilde{\mathbf{x}}_{k,L}] \quad (3.41)$$

where  $\tilde{\mathbf{x}}_{k,i}$  is a vector containing  $i$ th delayed spreading code for User  $k$ . It is defined as

$$\tilde{\mathbf{x}}_{k,i} \triangleq [0 \dots 0, \mathbf{x}_k^T, 0, \dots, 0]^T. \quad (3.42)$$

Since a multipath channel is involved, the current received bit signal will be interfered by previous bit signals. As mentioned above, the maximum path delay is much smaller than the processing gain. The interference will not be severe and for simplicity we may ignore this effect. Let  $\mathbf{f}_k = \mathbf{S}_k \mathbf{h}_k$ . As that in (3.10), we can obtain the received signal vector as

$$\mathbf{r} = \sum_k a_k b_k \mathbf{f}_k + \mathbf{v}. \quad (3.43)$$

To have better results, we use a maximum ratio rake combining scheme in the receiver. Let  $q_{jk} = \mathbf{f}_j^T \mathbf{f}_k$ ,  $q_k = q_{kk}$ , and  $u_k = \mathbf{v}^T \mathbf{f}_k$ . The output of the receiver is then

$$\begin{aligned} y_k &= \mathbf{r}^T \mathbf{f}_k \\ &= a_k b_k \mathbf{f}_k^T \mathbf{f}_k + \sum_{j \neq k} a_j b_j \mathbf{f}_j^T \mathbf{f}_k + \mathbf{v}^T \mathbf{f}_k \\ &= a_k b_k q_k + \sum_{j \neq k} a_j b_j q_{jk} + u_k. \end{aligned} \quad (3.44)$$

This result is similar to that in (3.12) except that  $\rho_{jk}$  is replaced by  $\varrho_{jk}$  and  $\gamma_k$  is replaced by  $u_k$ .

For the second stage of a partial SPIC, the regenerated signal is

$$\begin{aligned}\hat{\mathbf{r}}_k &= \mathbf{r} - C_k \sum_{j \neq k} \hat{\mathbf{s}}_j \\ &= \mathbf{r} - C_k \sum_{j \neq k} y_j \mathbf{f}_j.\end{aligned}\quad (3.45)$$

We then have the output signal for the second stage as

$$\begin{aligned}z_k &= \hat{\mathbf{r}}_k^T \mathbf{f}_k \\ &= a_k b_k \left( \varrho_k - C_k \sum_{j \neq k} \varrho_{j,k}^2 \right) + u_k - C_k \sum_{j \neq k} v_j \varrho_{jk} \\ &\quad + \sum_{j \neq k} a_j b_j \left( \varrho_{jk} - C_k \varrho_{jk} - C_k \sum_{m \neq j,k} \varrho_{jm} \varrho_{mk} \right).\end{aligned}\quad (3.46)$$

As previously, we assume that  $z_k$  is Gaussian distributed, the interfering bits and noise are random, and parameters  $N$ ,  $K$ ,  $\mathbf{t}_k$ ,  $\mathbf{h}_k$ ,  $\eta_k$ , and  $\varrho_{jk}$  are known beforehand. Thus, the output error probability is expressed as in (3.16) where the squared mean for  $z_k$ , similar to that of (3.19), is obtained from (3.17) and (3.46) as

$$\mathcal{M}_k = a_k^2 (\varrho_k - C_k \Gamma_k)^2 \quad (3.47)$$

where

$$\Gamma_k \triangleq \sum_{j \neq k} \varrho_{jk}^2, \quad (3.48)$$

and the variance is obtained from (3.18) and (3.46) as

$$\mathcal{V}_k = \sigma^2 (\Xi_{1,k} C_k^2 - 2\Xi_{2,k} C_k + \Xi_{3,k}) \quad (3.49)$$

where

$$\Xi_{1,k} = \sum_{j \neq k} \eta_j \left( \varrho_{jk} \varrho_j + \sum_{m \neq j,k} \varrho_{jm} \varrho_{mk} \right)^2 + \sum_{j \neq k} \left( \varrho_{jk}^2 \varrho_j + \sum_{m \neq j,k} \varrho_{jm} \varrho_{mk} \varrho_{jk} \right), \quad (3.50)$$

$$\Xi_{2,k} = \sum_{j \neq k} \eta_j \left( \varrho_{jk}^2 \varrho_j + \sum_{m \neq j,k} \varrho_{jm} \varrho_{mk} \varrho_{jk} \right) + \sum_{j \neq k} \varrho_{jk}^2, \quad (3.51)$$

$$\Xi_{3,k} = \sum_{j \neq k} \eta_j \varrho_{jk}^2 + \varrho_k. \quad (3.52)$$

The optimal PCF derivation for the multipath channels is similar to that in (3.25). Substituting (3.47) and (3.49) into (3.25), we then obtain

$$C_{k,opt} = \frac{\varrho_k \Xi_{2,k} - \Xi_{3,k} \Gamma_k}{\varrho_k \Xi_{1,k} - \Xi_{2,k} \Gamma_k}. \quad (3.53)$$

### § 3.4.2 Aperiodic Code Scenario

If aperiodic codes are utilized,  $\varrho_{jk}$ 's can be seen as Gaussian random variables. Using the method in Section III, we can obtain the corresponding optimal PCFs. From (3.47), we have the expected squared mean as

$$\begin{aligned} E_{\mathcal{L}} \{ \mathcal{M}_k^{(l)} \} &= a_k^2 \left( E_{\mathcal{L}} \{ \varrho_k^{(l)} \} - C_k E_{\mathcal{L}} \{ \Gamma_k^{(l)} \} \right)^2 \\ &= a_k^2 \left( 1 - C_k E_{\mathcal{L}} \{ \Gamma_k^{(l)} \} \right)^2 \end{aligned} \quad (3.54)$$

and the variance as

$$E_{\mathcal{L}} \{ \mathcal{V}_k^{(l)} \} = \sigma^2 \left( E_{\mathcal{L}} \{ \Xi_{1,k}^{(l)} \} C_k^2 - 2 E_{\mathcal{L}} \{ \Xi_{2,k}^{(l)} \} C_k + E_{\mathcal{L}} \{ \Xi_{3,k}^{(l)} \} \right). \quad (3.55)$$

Comparing (3.54)-(3.55) with (3.31)-(3.33), we see that the optimal PCF here is similar to that in (3.37). We then have the optimal PCF as

$$C_{k,opt} = \frac{E_{\mathcal{L}} \{ \Xi_{2,k}^{(l)} \} - E_{\mathcal{L}} \{ \Xi_{3,k}^{(l)} \} E_{\mathcal{L}} \{ \Gamma_k^{(l)} \}}{E_{\mathcal{L}} \{ \Xi_{1,k}^{(l)} \} - E_{\mathcal{L}} \{ \Xi_{2,k}^{(l)} \} E_{\mathcal{L}} \{ \Gamma_k^{(l)} \}}. \quad (3.56)$$

Unlike that in AWGN channel, the result for the aperiodic code scenario is more difficult to obtain because there are more correlation terms in (3.48) and (3.50)-(3.52) to work with. Before

evaluating expectation terms in (3.56), we define some functions as follows:

$$h_{jk}(p, q) = h_{j,p}h_{k,q}, \quad (3.57)$$

$$\tau_{jk}(p, q) = \tau_{j,p} - \tau_{k,q}, \quad (3.58)$$

$$\zeta_{jk}(p, q) = \tilde{\mathbf{x}}_{j,p}^T \tilde{\mathbf{x}}_{k,q}. \quad (3.59)$$

Thus, (3.57)-(3.59) define some relative figures between the  $p$ th channel path of the  $j$ th user and the  $q$ th channel path of the  $k$ th user. The notation  $h_{jk}(p, q)$  denotes the path gain product,  $\tau_{jk}(p, q)$  the relative path delay, and  $\zeta_{jk}(p, q)$  the code correlation with the relative delay  $\tau_{jk}(p, q)$ . Expanding (3.50)-(3.52), we have seven expectation terms to evaluate. For purpose of illustration, we show how to evaluate the first term,  $E_{\mathcal{L}}\{\varrho_{jk}^2\}$ , here. By definition, we have  $\varrho_{jk}$  as

$$\begin{aligned} \varrho_{jk} &= \mathbf{f}_j^T \mathbf{f}_k \\ &= \left( \sum_{p=1}^L \tilde{\mathbf{x}}_{j,p} h_{j,p} \right)^T \left( \sum_{q=1}^L \tilde{\mathbf{x}}_{k,q} h_{k,q} \right) \\ &= \sum_{p=1}^L \sum_{q=1}^L h_{j,p} h_{k,q} \tilde{\mathbf{x}}_{j,p}^T \tilde{\mathbf{x}}_{k,q} \\ &= \sum_{p=1}^L \sum_{q=1}^L h_{jk}(p, q) \zeta_{jk}(p, q). \end{aligned} \quad (3.60)$$

The expectation of  $\varrho_{jk}$  over all possible codes is then obtained as

$$\begin{aligned} E_{\mathcal{L}} \{ \varrho_{jk}^2 \} &= E \left\{ \sum_{p_1=1}^L \sum_{q_1=1}^L \sum_{p_2=1}^L \sum_{q_2=1}^L h_{jk}(p_1, q_1) \zeta_{jk}(p_1, q_1) h_{jk}(p_2, q_2) \zeta_{jk}(p_2, q_2) \right\} \\ &= \sum_{p_1=1}^L \sum_{q_1=1}^L \sum_{p_2=1}^L \sum_{q_2=1}^L h_{jk}(p_1, q_1) h_{jk}(p_2, q_2) E \left\{ \zeta_{jk}(p_1, q_1) \zeta_{jk}(p_2, q_2) \right\}. \end{aligned} \quad (3.61)$$

Let

$$\mathcal{F}_{jk}(p_1, q_1, p_2, q_2) = N^2 E \left\{ \zeta_{jk}(p_1, q_1) \zeta_{jk}(p_2, q_2) \right\}. \quad (3.62)$$

The coefficient  $N^2$  in (3.62) is only a normalization constant. Since the spreading codes are seen as random, only when  $\tau_{jk}(p_1, q_1)$  is equal to  $\tau_{jk}(p_2, q_2)$  will  $\mathcal{F}_{jk}(\cdot)$  be non-zero. Consider a specific set of  $\{p_1, q_1, p_2, q_2\}$  such that  $\tau_{jk}(p_1, q_1) = \tau_{jk}(p_2, q_2) = \tau$  and  $\tau \geq 0$ . We then have

$$\begin{aligned}\mathcal{F}_{jk}(p_1, q_1, p_2, q_2) &= N^2 \sum_{w=0}^{N-\tau-1} E\{x_{j,w+\tau}^2 x_{k,w}^2\} \\ &= N - \tau.\end{aligned}\quad (3.63)$$

For  $\tau < 0$ , we have the same result except that the sign of  $\tau$  in (3.63) is plus. We then conclude that the function  $\mathcal{F}_{jk}(\cdot)$  in (3.62) is

$$\mathcal{F}_{jk}(p_1, q_1, p_2, q_2) = \begin{cases} N - |\tau|, & \text{if } \tau_{jk}(p_1, q_1) = \tau_{jk}(p_2, q_2) = \tau \\ 0, & \text{otherwise.} \end{cases}\quad (3.64)$$

Using (3.62), (3.64), and (3.61), we can evaluate  $E_{\mathcal{L}}\{\varrho_{jk}^2\}$  in (3.50)-(3.52). The general formulations for the other six expectation terms are summarized in Appendix B.

We now provide a simple example to show the multipath effect on the optimal PCFs. Let  $\mathbf{t}_k = [0, D]^T$  and  $\mathbf{h}_k = [\alpha, \beta]^T$  for all  $k$ 's ( $\alpha^2 + \beta^2 = 1$ ). Also, let  $\mathcal{G}_a \triangleq (N - D)\alpha^2\beta^2$ , and  $\mathcal{G}_b \triangleq (N - 2D)\alpha^4\beta^4$ . Then

$$E_{\mathcal{L}}\{\Gamma_k^{(l)}\} = E_{\mathcal{L}}\{\Lambda_k^{(l)}\} + \frac{2\mathcal{G}_a(K-1)}{N^2},\quad (3.65)$$

$$\begin{aligned}E_{\mathcal{L}}\{\Xi_{1,k}^{(l)}\} &= E_{\mathcal{L}}\{\Omega_{1,k}^{(l)}\} + 2\mathcal{G}_a \left\{ \frac{I_k}{N^4} \left[ N^2 + 10N + 4\mathcal{G}_a + 2(K-2)(4N + 3K + \mathcal{G}_a + 1) \right] \right. \\ &\quad \left. + \frac{K-1}{N^3}(N + 3K - 2) \right\} + 4\mathcal{G}_b \left\{ \frac{I_k \cdot K}{N^4} + 6K - 12 \right\} \\ &\quad + \frac{I_k}{N^4}(6N - 10D)\alpha^4\beta^4,\end{aligned}\quad (3.66)$$

$$E_{\mathcal{L}}\{\Xi_{2,k}^{(l)}\} = E_{\mathcal{L}}\{\Omega_{2,k}^{(l)}\} + 2\mathcal{G}_a \left[ \frac{I_k}{N^3}(N + 3K - 2) + \frac{K-1}{N^2} \right],\quad (3.67)$$

$$E_{\mathcal{L}}\{\Xi_{3,k}^{(l)}\} = E_{\mathcal{L}}\{\Omega_{3,k}^{(l)}\} + 2\mathcal{G}_a \frac{I_k}{N^2}.\quad (3.68)$$

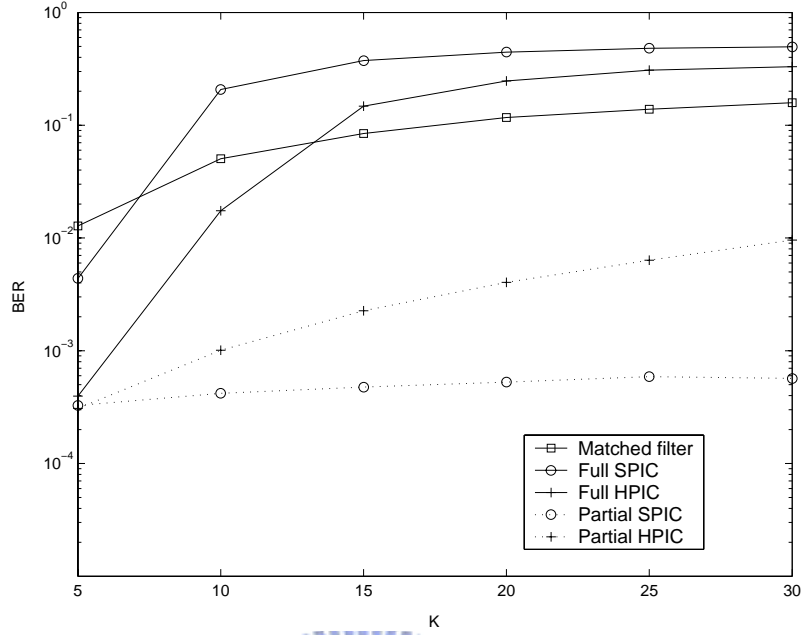


Figure 3.2: Performance comparison for HPIC and SPIC ( $N = 31$ ,  $\rho = 1/\sqrt{N}$ , and  $E_b/N_0 = 8$  dB); The optimal PCFs for the partial HPIC were obtained by trial and error and those for the SPIC were obtained from (3.27).

Note that the first terms in (3.65)-(3.68) are those in (3.32) and (3.34)-(3.36) which correspond to the optimal PCFs in an AWGN channel. Other terms are due to the multipath channel effect. It is evident to see that if  $\beta = 0$ ,  $\mathcal{G}_a = \mathcal{G}_b = 0$  and the metrics above are then degenerated to (3.32) and (3.34)-(3.36).

In prior sections optimal PCFs for different scenarios are derived under the assumption of static channels. The received user amplitudes are regarded known and to be varying slowly. The extension to fading channels is straightforward. The derivation is summarized in Appendix C.

## § 3.5 Simulation Results

### A. Performance comparison for various partial PIC structures



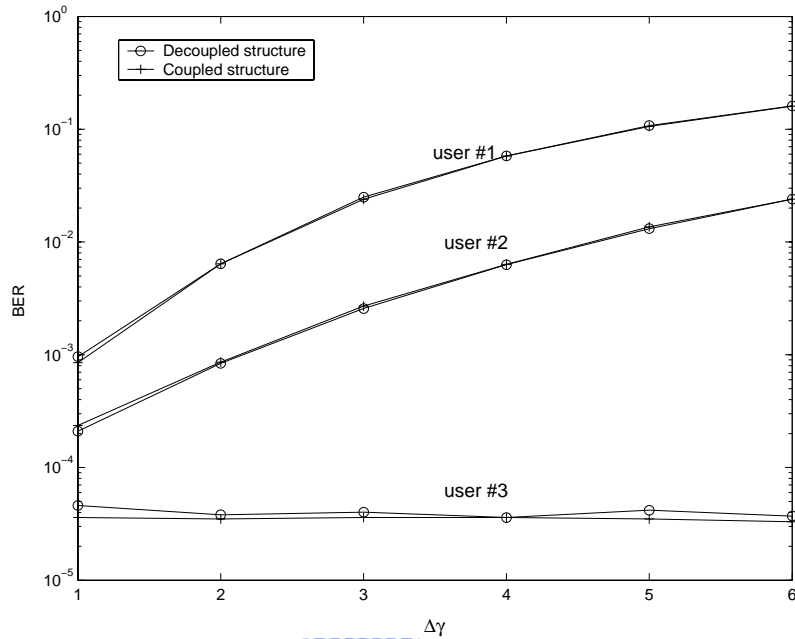


Figure 3.3: Performance comparison for the coupled and decoupled structures (three users with  $E_b/N_0 = 8 - 2\Delta\eta$ ,  $8 - \Delta\eta$ , and 8 dB); The optimal PCFs for the coupled structure were obtained by trial and error, and those for the decoupled structure were obtained from (3.38).

In this section we provide simulation results to verify the validity of our derived PCFs. Before we do that, we give some comparison results to justify the PIC structure we considered. First, we compare the performance of a partial SPIC and that of a partial HPIC. We used equicorrelated codes of length  $N = 31$  ( $\rho = 1/\sqrt{N}$ ) as spreading codes. Let  $E_b/N_0$  be 8 dB ( $\sigma^2 = N_0/2$ ), and assume a perfect power control scenario. It is straightforward to see that in the perfect power control case, optimal PCFs are equal for the coupled and decoupled structures. Figure 3.2 shows the bit error rate (BER) performance versus the number of users. Here, optimal PCFs for the partial HPIC were determined empirically (trial and error with a resolution of 0.01). Surprisingly, we found that the optimal partial SPIC outperformed the optimal partial HPIC. This result differs from the result given in [56] where the full SPIC was found to be inferior to the full HPIC.

In the second set of simulations, we compared the performance of the coupled and decou-

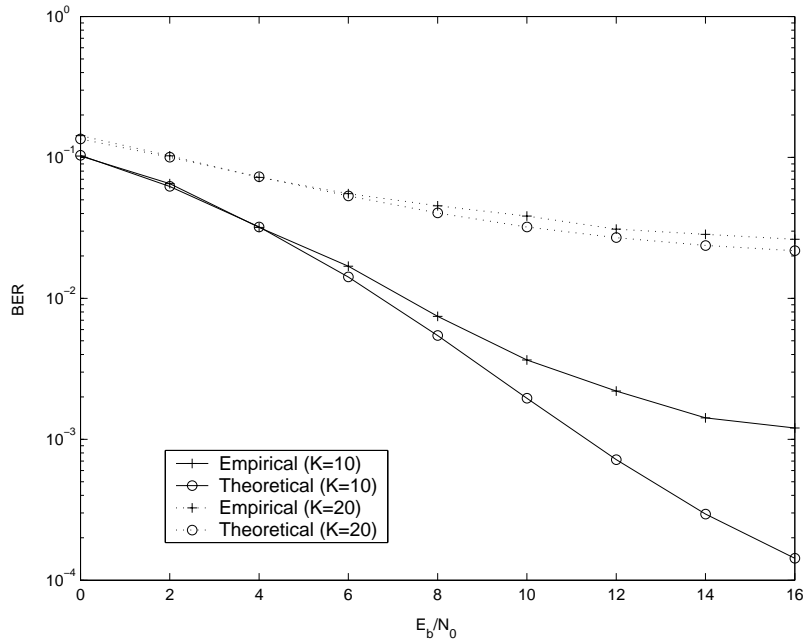


Figure 3.4: BER of the partial SPIC detector versus  $E_b/N_0$  (aperiodic AWGN channels, and power balanced).

pled structures (using a partial SPIC). As mentioned above, optimal PCFs are equal for both structures under perfect power control. Thus, we compared their performance in an imperfect power control scenario. The optimal PCFs for the coupled structure were determined empirically. Let the number of users be three and the spreading code be aperiodic (of length 31). We assumed that the third user had a fixed  $E_b/N_0$  of 8 dB, and the other two users had variable  $E_b/N_0$  values of  $8 - \Delta\eta$  and  $8 - 2\Delta\eta$  dB, respectively. Figure 3.3 shows the BER performance versus  $\Delta\eta$  for these two structures. As we can see, both structures performed similarly.

### B. Validity of derived PCFs

In this paragraph, we report simulation results demonstrating the accuracy of our theoretical solutions. A two-stage decoupled partial SPIC was considered. For the simulations conducted, we used Gold codes for periodic code systems and random codes for aperiodic code systems. Figure 3.4 gives the empirical and theoretical BERs for the optimal partial SPIC detector (with the aperiodic code scenario). This figure shows the validity of the Gaussian assumption used in

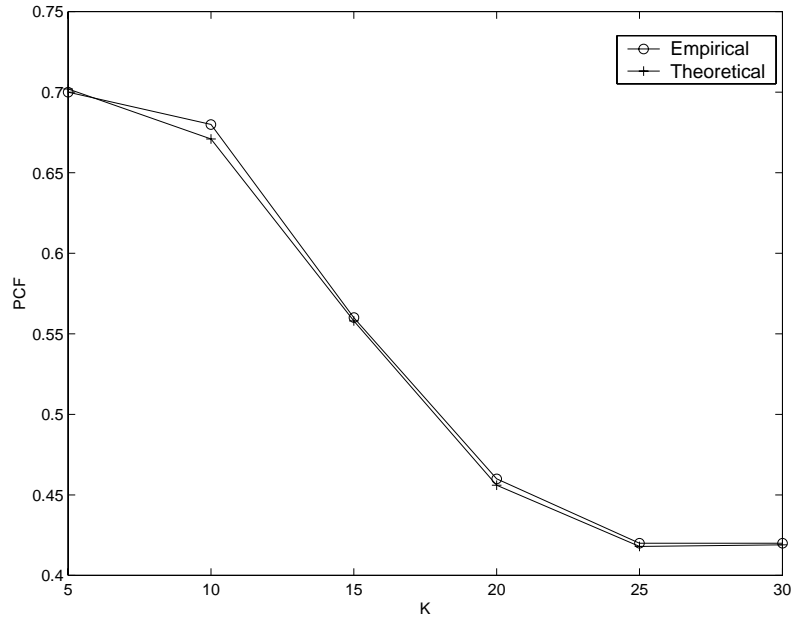


Figure 3.5: Optimal PCF versus number of users (Gold codes, asynchronous AWGN channels,  $E_b/N_0 = 8$  dB, and power balanced).

our derivation. As we can see, when the number of users was smaller and  $E_b/N_0$  was higher, the Gaussian approximation was less valid. Figure 3.5 shows the optimal PCFs in (3.27) and the empirical optimal PCFs versus the number of users. The channel here was an asynchronous AWGN channel, the spreading codes were periodic, and  $E_b/N_0$  was 8 dB for each user. In the figure, it can be seen that the theoretical optimal PCFs were very close to the empirical ones in all cases. We then considered optimal PCFs for a multipath channel. The multipath channel assumed was a two-ray channel with the transfer function  $W_k(z) = 0.762 + 0.648z^{-2}$  (for all users). Theoretical optimal PCFs derived in (3.56) were compared with empirical PCFs and the results are shown in Fig. 3.6. We can observe that the theoretical results also matched with the empirical ones satisfactorily. Note that when the number of users was smaller, the theoretical values were less accurate. This was because when the user number is small, the Gaussian approximation in (3.30) is less valid. This was also consistent with the result observed in Fig. 3.4.

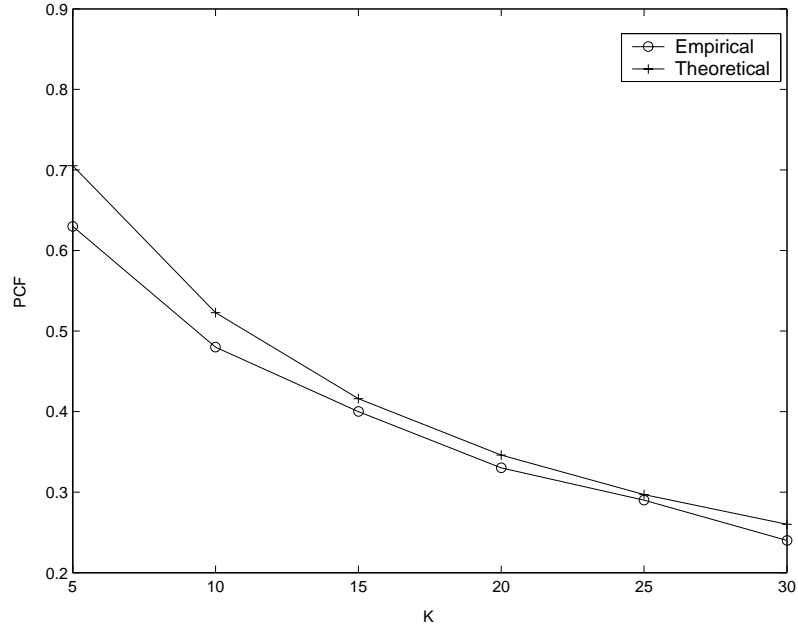


Figure 3.6: Optimal PCF versus number of users (aperiodic codes, multipath channels,  $E_b/N_0 = 10$  dB, and power balanced).

### C. BER performance comparison

In what follows, we report the BER performance for various SPIC detectors. Figure 3.7 gives the performance comparison for an optimal two-stage partial SPIC, a conventional matched-filter receiver, a two-stage full SPIC, and a three-stage full SPIC. The spreading codes were periodic and the channel was an asynchronous AWGN channel. Also,  $E_b/N_0$  was 10 dB and perfect power control was assumed. From the figure, we can see that the optimal two-stage partial SPIC outperformed others in all cases. The two-stage and three-stage SPIC receivers performed even worse than the conventional matched-filter receiver when the number of users was large. The optimal two-stage partial SPIC always performed better than the matched-filter receiver. Finally, Figure 3.8 shows the performance comparison for the detectors considered above in the multipath channel. The simulation setup was identical to that in the previous cases except that the spreading code was aperiodic. The PCFs for the optimal two-stage partial SPIC

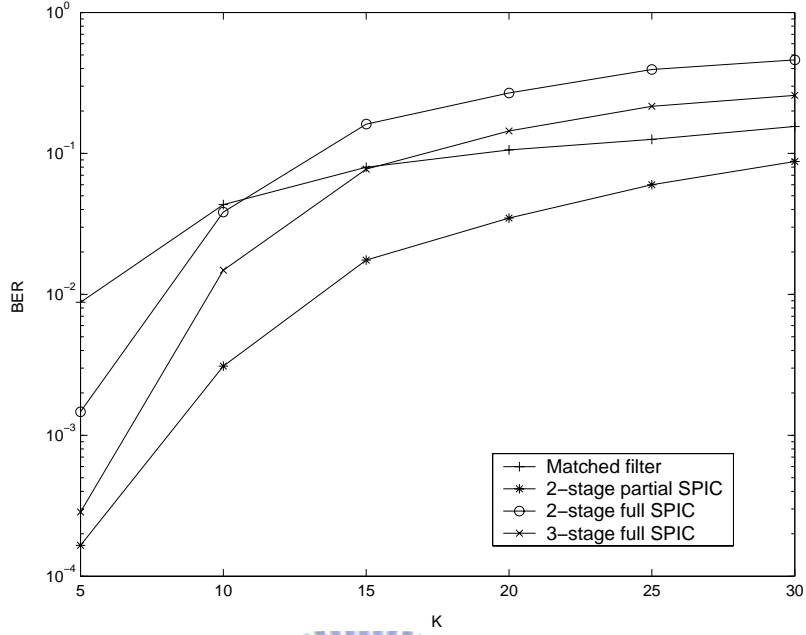


Figure 3.7: BER versus number of users (Gold codes, asynchronous AWGN channels,  $E_b/N_0 = 10$  dB, and power balanced).

were calculated using (3.56). As in the AWGN channel, the optimal two-stage partial SPIC outperformed other types of detectors.

#### D. Effect of imperfect parameter estimation

In the optimal PCF formulation, we assumed that the required parameters are perfectly known. In practice, this may not be always possible. Some parameters will have to be estimated for time-varying channels which may introduce errors. The main parameters we need to know are the channel responses and the noise variance. Once the channel responses are known,  $a_k$ 's,  $\rho_{jk}$ 's and  $\eta_k$ 's can be calculated accordingly. We modeled the channel estimation error as follows. Let  $g_{k,i} = a_k h_{k,i}$  be the  $i$ -th path channel of User  $k$ , and  $g'_{k,i} = g_{k,i} + \Delta g_{k,i}$ , where  $g'_{k,i}$  was the estimated channel response,  $g_{k,i}$  was the actual response, and  $\Delta g_{k,i}$  was a Gaussian random variable denoting the estimation error. We first let the noise variance be exactly known and varied the channel estimation error. The performance impact is shown in Fig. 3.9. The result corresponds to the case in which the user number was six, the spreading code was aperiodic, the

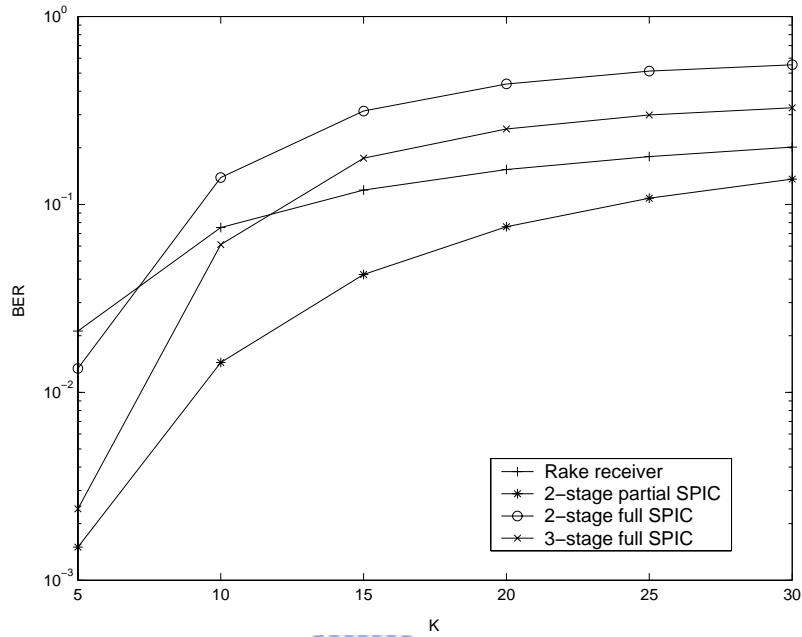


Figure 3.8: BER versus number of users (aperiodic spreading codes, multipath channels,  $E_b/N_0 = 10$  dB, and power balanced).

channel was the multipath channel, and  $E_b/N_0$  was 10 dB. In the figure,  $\sigma_g$  denotes the standard deviation of  $\Delta g_{k,i}$  (same for all  $k$ 's and  $i$ 's). Since the matched-filter and the full SPIC receivers do not rely on channel information, the channel estimation error had no influence on their performance. (The BER variations in Fig. 3.9 were due to the random data used in different runs). As we can see, the partial SPIC performance was not affected until  $\sigma_g = 0.3$ . Note that the magnitude of the main path was 0.762. Thus, the estimation error was quite large in this case. The second case we considered was noise variance estimation error. The simulation setup was identical to the previous one. We let the channel responses be known and varied noise variance from  $0.1 \times \sigma_n^2$  to  $10 \times \sigma_n^2$ , where  $\sigma_n^2$  was the actual noise variance. We found that the optimal SPIC performance was almost unaffected. Thus, we conclude that the optimal partial SPIC has good immunity to parameter estimation errors.

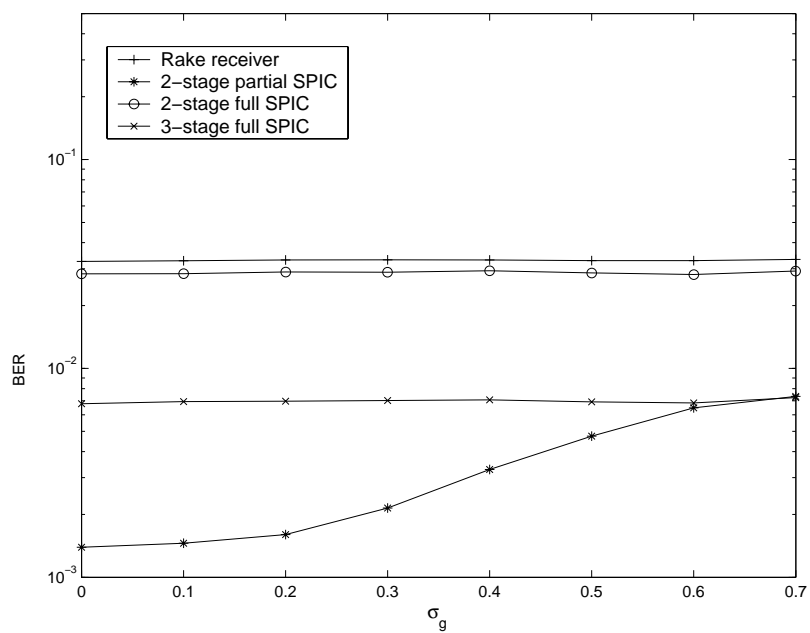
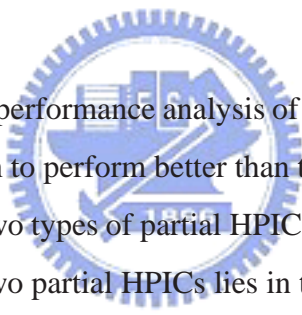


Figure 3.9: BER with channel estimation error (aperiodic spreading codes, multipath channels,  $K=6$ ,  $E_b/N_0 = 10$  dB, and power balanced).

# Chapter 4

## Analysis of Adaptive Two-stage Partial HPIC Receivers



This chapter is dedicated to the performance analysis of a two-stage adaptive blind partial HPIC receiver. This receiver is known to perform better than the non-adaptive partial HPIC. As mentioned in Chapter 2 that these two types of partial HPICs may give different optimal PCFs. The major difference between the two partial HPICs lies in the different optimization objectives. In the non-adaptive type partial HPIC, the optimal PCFs are determined based on the minimization of the ensemble error average for all transmission bits. In other words, optimal PCFs apply to all received bit signals. On the contrary, the PCF for the adaptive blind partial HPIC is obtained by minimizing the ensemble error average within a single bit interval (given the bit decision in first stage). Although the adaptive blind HPIC was studied extensively, its performance has not been analyzed before. We intend to fill this gap in this chapter. We first give the LMS framework for the blind partial HPIC in Section 1. In Section 2, a complete derivation for the LMS convergence statistics in a single-user scenario is given, which includes the optimal weight, the weight error means, and weight error variances. In Section 3, the result is extended to a two-user case. We derive the optimal weights and the weight error means. Finally, using some approximation techniques, we derive the corresponding analytical results for a general  $K$ -user



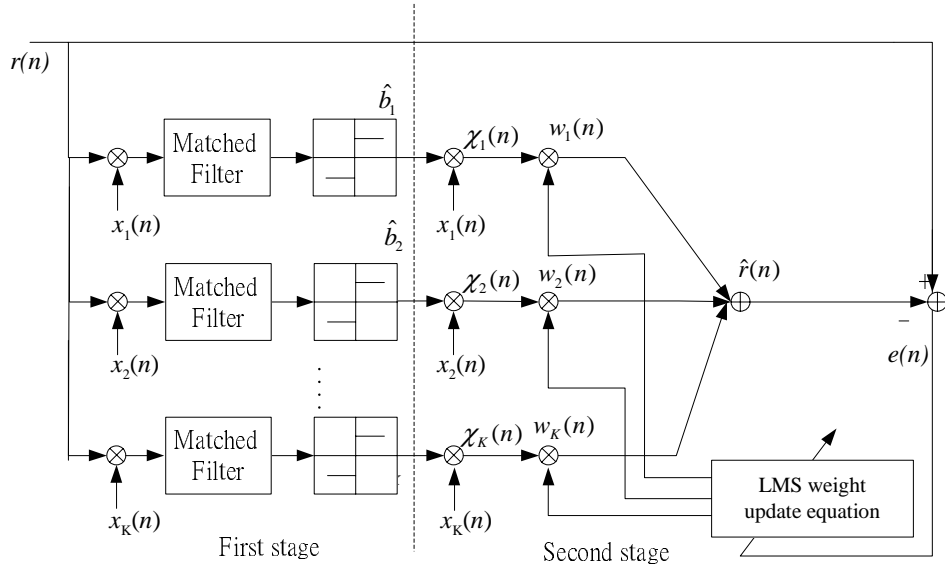


Figure 4.1: LMS algorithm for two-stage adaptive blind partial HPIC receivers.

scenario in Section 4. The simulation results and discussions are presented in Section 5.

## § 4.1 System Model

Consider a synchronous  $K$ -user CDMA system in the AWGN channel. Let the spreading sequence of the  $k$ th user denoted by  $x_k(n)$  with processing gain  $N$  and amplitude  $\pm 1/\sqrt{N}$ . Then the chip-sampled received signal in a certain bit interval can be represented as

$$r(n) = \sum_{k=1}^K a_k b_k x_k(n) + v(n), \quad n = 0, \dots, N - 1 \quad (4.1)$$

where  $a_k$  and  $b_k$  are the channel gain and data bit of the  $k$ th user, and  $v(n)$  is the AWGN with variance  $\sigma^2$ . The first stage of the partial HPIC is the matched filter output given by

$$\begin{aligned}
y_k^{(1)} &= \sum_{n=0}^{N-1} x_k(n)r(n) \\
&= a_k b_k + \sum_{j \neq k} a_j b_j \rho_{jk} + \sum_{n=0}^{N-1} x_k(n)v(n) \\
&= a_k b_k + \sum_{j \neq k} a_j b_j \rho_{jk} + \sum_{n=0}^{N-1} \nu_k(n)
\end{aligned} \tag{4.2}$$

where the time-averaged cross-correlation function between the  $i$ -th and the  $j$ th user is defined as

$$\rho_{jk} = \sum_{n=0}^{N-1} x_j(n)x_k(n)$$

and the noise sample after multiplying the spreading code is expressed by  $\nu_k(n) = x_k(n)v(n)$ . We further denote the noise term after despreading as  $\sum_n \nu_k(n) = \gamma_k$ . The adaptive blind partial HPIC uses an adaptive filter to estimate the channel gains and then cancel the interference produced by other users. The adaptive algorithm used is the well-known LMS algorithm, as depicted in Figure 4.1. The LMS algorithm minimizes the MSE between the received signal and the regenerated signal in a bit interval. The optimal weight vector can be obtained by

$$\mathbf{w}_{opt}^{(i)} = \min_{\mathbf{w}^{(i)}} J^{(i)}(n) \tag{4.3}$$

where the error signal is represented by

$$\begin{aligned}
J^{(i)}(n) &= E \{ [r(n) - \hat{r}(n)]^2 \} \\
&= E \left\{ \left[ r(n) - \sum_{k=1}^K w_k^{(i)}(n) \hat{b}_k^{(i-1)} x_k(n) \right]^2 \right\}.
\end{aligned} \tag{4.4}$$

In above equations, the superscript  $(i)$  denotes the corresponding variable is operated at the  $i$ th stage. Note that only one bit period is available for weight adaptation. We first express the

spreading sequence vector as

$$\mathbf{x}(n) = [x_1(n), x_2(n), \dots, x_K(n)]^T. \quad (4.5)$$

The LMS update equation for the  $i$ th HPIC stage (with  $i - 1$  stages of interference cancellation) is then formulated as

$$\begin{aligned} \hat{r}^{(i)}(n) &= \boldsymbol{\chi}^{(i)}(n)^T \mathbf{w}^{(i)}(n) \\ e^{(i)}(n) &= r(n) - \hat{r}^{(i)}(n) \\ \mathbf{w}^{(i)}(n+1) &= \mathbf{w}^{(i)}(n) + \mu e^{(i)}(n) \boldsymbol{\chi}^{(i)}(n) \end{aligned} \quad (4.6)$$

where the input signals are described as  $\boldsymbol{\chi}^{(i)}(n) = \hat{\mathbf{B}}^{(i-1)} \mathbf{x}(n)$  with the bit decision matrix

$$\hat{\mathbf{B}}^{(i)} \triangleq \text{diag}\{\hat{b}_1^{(i)}, \hat{b}_2^{(i)}, \dots, \hat{b}_K^{(i)}\}. \quad (4.7)$$

After the weights are trained, they are used to cancel the interference from other users such that the input to the  $k$ th user' slicer in the  $i$ -stage is

$$\hat{r}_k^{(i)}(n) = r(n) - \sum_{j \neq k} w_j^{(i)}(N) \hat{b}_j^{(i-1)} x_j(n). \quad (4.8)$$

Then the  $i$ th stage output from the partial HPIC (for User  $k$ ) can be formed by

$$y_k^{(i)} = \sum_{n=0}^{N-1} \hat{r}_k^{(i)}(n) x_k(n) \quad (4.9)$$

and the bit decision output for the  $k$ th user in the  $i$ th stage is denoted by  $\hat{b}_k^{(i)} = \text{sgn}[y_k^{(i)}(n)]$ . We will address a two-stage partial HPIC structure and omit the superscript for the stage number  $i$  such that  $\hat{r}^{(2)}(n) = \hat{r}(n)$ ,  $w_k^{(2)}(n) = w_k(n)$ , and  $\hat{b}_k^{(1)} = \hat{b}_k$  in the sequel.

It can be seen from (4.4) that in the perfect condition,  $\hat{r}(n) = r(n)$ . In that case the ideal convergent weights are

$$w_k(N) = \begin{cases} a_k, & \hat{b}_k = b_k \\ -a_k, & \hat{b}_k \neq b_k. \end{cases} \quad (4.10)$$

Thus, the convergence weights depend on whether the bit decision results in the previous stage are correct or erroneous. The adaptive algorithm allows each user can weight to attain the desired value symbol by symbol. This is the reason why the adaptive approach performs better than non-adaptive methods.

As mentioned, the adaptation period is constrained in one symbol period. This is because the optimal weight for User  $k$  may be  $+a_k$  or  $-a_k$  depending on the bit decision for each symbol. Although the LMS algorithm is simple, its convergence may slow and the weight may not converge to the desired value in such a short period. In addition, the resultant weight heavily depends on the parameters used in the LMS algorithm so is the cancellation performance. These parameters include the step size and weight initials. In the conventional approach, these parameters are determined heuristically. The weight initials are usually set as the channel gains, i.e.,  $w_k(0) = a_k$ . This is reasonable since the bit error probability is usually low, most of the weights will start their adaptation at the optimal values; only few weights are away from their desired values by  $2a_k$ . A larger step size will accelerate the convergence speed for the weights with erroneous decision, but also inevitably introduces a larger variance. There is little research regarding the convergence analysis for the adaptive blind partial HPIC receiver and this is the motivation of our research.

The LMS algorithm has been analyzed and developed for over four decades. However, most results cannot be used here. This is because the step size used in this application is large and this will violate many assumptions assumed. The other reason is that we most concern the transient behavior (due to small sample size) while most works only concern steady-state behavior. We then develop a novel method to overcome this problem. We will start the analysis with a single-user scenario. In this case, there is no MAI; however, the result can serve as a base for the two-user and general  $K$ -user scenario.

## § 4.2 Exact Analysis for Single-user Scenario

### § 4.2.1 Optimal Weight Analysis

Consider the CDMA system with only one active user, i.e.,  $K = 1$ . Since only one user is present, we will omit the subscript  $k$  for notational simplicity. Thus,  $x(n) = x_1(n)$ ,  $a = a_1$ ,  $b = b_1$ ,  $y^{(1)}(n) = y_1^{(1)}(n)$ ,  $\nu(n) = \nu_1(n)$ ,  $\gamma = \gamma_1$ , and  $\chi(n) = \hat{b}_1 x_1(n)$ . Note that by definition,  $\nu(n) = x(n)v(n)$  and

$$\gamma = \sum_{n=0}^{N-1} \nu(n). \quad (4.11)$$

The matched filter output signal in a certain bit interval in (4.2) can be rewritten as

$$\begin{aligned} y^{(1)} &= \sum_{n=0}^{N-1} x(n)r(n) \\ &= \sum_{n=0}^{N-1} x(n)(abx(n) + v(n)) \\ &= ab + \sum_{n=0}^{N-1} x(n)v(n) \\ &= ab + \sum_{n=0}^{N-1} \nu(n) \\ &= ab + \gamma \end{aligned} \quad (4.12)$$

where the noise samples  $\nu(n)$ ,  $n = 0, 1, \dots, N - 1$  are i.i.d. random variables with zero mean and variance  $\sigma_\nu^2 = \sigma^2/N$ . Note that in the following derivation, we refer to the first stage decision, the first stage correct decision, and the first stage erroneous decision as the decision, the correct decision, and erroneous decision, respectively. From (4.12), it is simple to see that the decision  $\hat{b}$ , which equals  $\text{sgn}[y^{(1)}]$ , depends on the noise term  $\gamma$ . It is simple to derive the condition for correct or erroneous decision. Denote the set for which decision is correct as  $\mathbb{V}^c$ ,

and that for which decision is erroneous as  $\mathbb{V}^e$ . Then,

$$\begin{aligned}\mathbb{V}^c &\triangleq \{\gamma|b = \hat{b}\} \\ &= \begin{cases} \gamma > -a & \text{for } b = 1 \\ \gamma < a & \text{for } b = -1 \end{cases}\end{aligned}\quad (4.13)$$

and

$$\begin{aligned}\mathbb{V}^e &\triangleq \{\gamma|b \neq \hat{b}\} \\ &= \begin{cases} \gamma < -a & \text{for } b = 1 \\ \gamma > a & \text{for } b = -1. \end{cases}\end{aligned}\quad (4.14)$$

We will first derive the optimal weight conditioned on  $\gamma$  and then take the expectation on the conditional optimal weight to obtain the final result. Since the input to the LMS filter depends on  $\hat{b}$ , the optimal weight will be different for  $\hat{b} = b$  and  $\hat{b} \neq b$ . To facilitate the derivation, we first define some notations. Let a random variable  $z$  conditioned on  $\gamma$  be denoted as  $\tilde{z}$ , i.e.,  $\tilde{z} = \{z|\gamma\}$ . Also let the conditional random variable with  $\gamma \in \mathbb{V}^c$  be denoted as  $\tilde{z}^c$ , i.e.,  $\tilde{z}^c = \{z|\gamma \in \mathbb{V}^c\}$ . Similarly,  $\tilde{z}^e = \{z|\gamma \in \mathbb{V}^e\}$ . Also let  $\tilde{z}_M^c = E_{v,x}\{\tilde{z}^c\}$ ,  $\tilde{z}_M^e = E_{v,x}\{\tilde{z}^e\}$ ,  $z_M^c = E_\gamma\{\tilde{z}_M^c\}$ , and  $z_M^e = E_\gamma\{\tilde{z}_M^e\}$  where the subscript  $M$  denotes the corresponding variable is a mean value,  $E_{v,x}\{\cdot\}$  denotes the expectation operated on  $v(n)$  and  $x(n)$ , and  $E_\gamma\{\cdot\}$  denotes the expectation operated on  $\gamma$ . Let  $E\{\cdot\}$  denote the expectation operated on all random variables, and we have  $E\{z^c\} = E_\gamma\{E_{v,x}\{\tilde{z}^c\}\} = z_M^c$ , and  $E\{z^e\} = E_\gamma\{E_{v,x}\{\tilde{z}^e\}\} = z_M^e$ . Using the similar rule, we define the optimal weight conditioned on  $\gamma \in \mathbb{V}^c$  as  $\tilde{w}_{opt}^c$ , and that on  $\gamma \in \mathbb{V}^e$  as  $\tilde{w}_{opt}^e$ . Also, let the optimal weight for correct decision be  $w_{opt}^c$  and that for erroneous decision be  $w_{opt}^e$ . We then have  $w_{opt}^c = E_\gamma\{\tilde{w}_{opt}^c\}$  and  $w_{opt}^e = E_\gamma\{\tilde{w}_{opt}^e\}$ . The conditional optimal weight is given by

$$\tilde{w}_{opt}^c = (\tilde{\mathbf{Q}}^c)^{-1}\tilde{\mathbf{p}}^c \quad (4.15)$$

where  $\tilde{\mathbf{Q}}^c = E_{v,x}\{\tilde{\chi}^c(n)^2\}$  and  $\tilde{\mathbf{p}}^c = E_{v,x}\{\tilde{\chi}^c(n)\tilde{r}^c(n)\}$ . Note that  $\tilde{\mathbf{Q}}^c = 1/N$ . We then have

$$\begin{aligned}\tilde{w}_{opt}^c &= NE_{v,x}\{\tilde{\chi}^c(n)\tilde{r}^c(n)\} \\ &= N\hat{b}E_{v,x}\{x^c(n)\tilde{r}^c(n)\} \\ &= N\hat{b}\left(\frac{a \cdot b}{N} + \tilde{\nu}_M^c(n)\right)\end{aligned}\quad (4.16)$$

$$= a + N\hat{b}\tilde{\nu}_M^c(n).\quad (4.17)$$

The conditional mean for  $\tilde{\nu}^c(n)$  can be obtained by taking the conditional expectation on both sides of (4.11).

$$\tilde{\gamma}^c = \sum_{n=0}^{N-1} \tilde{\nu}_M^c(n)\quad (4.18)$$

$$= N\tilde{\nu}_M^c(n).\quad (4.19)$$

Thus, (4.16) can be rewritten as

$$\tilde{w}_{opt}^c = a + \hat{b}\tilde{\gamma}^c\quad (4.20)$$

Assuming  $b = 1$ , we can obtain the optimal weight for correct decision as (the result is identical for  $b = -1$ )

$$\begin{aligned}w_{opt}^c &= E_\gamma\{\tilde{w}_{opt}^c\} \\ &= a + E_\gamma\{\tilde{\gamma}^c\}.\end{aligned}\quad (4.21)$$

Note that  $\gamma$  is a Gaussian random variable with zero mean and variance  $\sigma_\gamma^2 = N\sigma_\nu^2 = \sigma^2$ . Let  $f(\cdot)$  denote a probability density function. Thus, the second term in the righthand side of (4.21) can be expressed as

$$\begin{aligned}E_\gamma\{\tilde{\gamma}^c\} &= \int \gamma f(\gamma|\mathbb{V}^c)d\gamma \\ &= \frac{\int_{\mathbb{V}^c} \gamma f(\gamma)d\gamma}{\int_{\mathbb{V}^c} f(\gamma)d\gamma}.\end{aligned}\quad (4.22)$$

Similarly, from (4.16), we can obtain the conditional optimal weight for the erroneous decision as

$$\tilde{w}_{opt}^e = -a + \hat{b}\tilde{\gamma}^e.\quad (4.23)$$

The optimal weight is then

$$\begin{aligned} w_{opt}^e &= E_\gamma \{ \tilde{w}_{opt}^e \} \\ &= -a - E_\gamma \{ \tilde{\gamma}^e \} \end{aligned} \quad (4.24)$$

where  $E_\gamma \{ \tilde{\gamma}^e \}$  can be evaluated as that in (4.22).

## § 4.2.2 Weight Error Mean Analysis

The LMS update equation for the single-user scenario can be formulated as

$$\begin{aligned} \hat{r}(n) &= \chi(n)w(n) \\ e(n) &= r(n) - \hat{r}(n) \\ w(n+1) &= w(n) + \mu e(n)\chi(n). \end{aligned} \quad (4.25)$$

Define two weight errors as

$$\tilde{\epsilon}^c(n) = \tilde{w}^c(n) - w_{opt}^c \quad (4.26)$$

$$\tilde{\epsilon}^e(n) = \tilde{w}^e(n) - w_{opt}^e. \quad (4.27)$$

Our objective is to find close-form expressions for the mean values of  $\tilde{\epsilon}^c(n)$  and  $\tilde{\epsilon}^e(n)$ . Using the notations defined above, we have  $\epsilon_M^c(n) = E\{\tilde{\epsilon}^c(n)\}$  and  $\epsilon_M^e(n) = E\{\tilde{\epsilon}^e(n)\}$ . We first consider the scenario of correct decision and rewrite (4.26) as

$$\begin{aligned} \tilde{\epsilon}^c(n) &= \tilde{w}^c(n) - w_{opt}^c \\ &= \tilde{w}^c(n) - \tilde{w}_{opt}^c + \tilde{w}_{opt}^c - w_{opt}^c. \end{aligned} \quad (4.28)$$

We then define

$$\tilde{\tilde{\epsilon}}^c(n) = \tilde{w}^c(n) - \tilde{w}_{opt}^c \quad (4.29)$$

$$\tilde{\delta}^c = \tilde{w}_{opt}^c - w_{opt}^c. \quad (4.30)$$

From (4.28), we can have

$$\tilde{\epsilon}^c(n) = \tilde{\tilde{\epsilon}}^c(n) + \tilde{\delta}^c. \quad (4.31)$$



It is simple to see that  $E\{\tilde{\delta}^c\} = 0$ . Thus,  $\epsilon_M^c(n) = E\{\tilde{\epsilon}^c(n)\} = E\{\tilde{\epsilon}^c(n)\} = E_\gamma\{\tilde{\epsilon}_M^c(n)\}$ .

Expanding  $\tilde{\epsilon}^c(n)$ , we have

$$\begin{aligned}
\tilde{\epsilon}^c(n) &= \tilde{w}^c(n) - \tilde{w}_{opt}^c \\
&= \tilde{w}^c(n-1) + \mu\tilde{\chi}^c(n)\tilde{\epsilon}^c(n-1) - \tilde{w}_{opt}^c \\
&= (1 - \mu/N)\tilde{\epsilon}^c(n-1) + \mu(\tilde{\chi}^c(n-1)\tilde{r}^c(n-1) - \tilde{w}_{opt}^c/N) \\
&= (1 - \mu/N)\tilde{\epsilon}^c(n-1) + \mu[\tilde{\chi}^c(n-1)(ab \cdot \tilde{x}^c(n-1) + \tilde{v}^c(n-1)) - \tilde{w}_{opt}^c/N] \\
&= (1 - \mu/N)\tilde{\epsilon}^c(n-1) + \mu\hat{b}(\tilde{v}^c(n-1) - \gamma/N). \tag{4.32}
\end{aligned}$$

Iterating (4.32), we can obtain

$$\begin{aligned}
\tilde{\epsilon}^c(n) &= (1 - \mu/N)^n \tilde{\epsilon}^c(0) + \mu\hat{b} \left\{ \sum_{i=0}^{n-1} (1 - \mu)^{n-i} \tilde{v}^c(i) - \frac{1}{N} \sum_{i=0}^{n-1} (1 - \mu)^{n-i} \gamma \right\} \\
&= \alpha^n \tilde{\epsilon}^c(0) + \mu\hat{b} \sum_{i=0}^{n-1} \alpha^{n-i} \tilde{v}^c(i) - \mu\hat{b} \frac{\gamma}{N} \left( \frac{1 - \alpha^n}{1 - \alpha} \right) \tag{4.33}
\end{aligned}$$

where  $\alpha = 1 - \mu/N$  and  $\tilde{\epsilon}^c(0) = \tilde{w}^c(0) - \tilde{w}_{opt}^c$ . Note that  $w(0)$  is an deterministic initial value and  $\tilde{w}^c(0) = w(0)$ . Taking expectation on both sides of (4.33) with respect to  $v(n)$  and  $x(n)$ , we have

$$\begin{aligned}
\tilde{\epsilon}_M^c(n) &= \alpha^n \tilde{\epsilon}^c(0) + \mu\hat{b} \left\{ \sum_{i=0}^{n-1} (1 - \mu)^{n-i} \tilde{v}_M^c(i) - \frac{1}{N} \sum_{i=0}^{n-1} (1 - \mu)^{n-i} \gamma \right\} \\
&= \alpha^n \tilde{\epsilon}^c(0) + \mu\hat{b} \sum_{i=0}^{n-1} \alpha^{n-i} \tilde{v}_M^c(i) - \frac{\mu\hat{b}\gamma}{N} \left( \frac{1 - \alpha^n}{1 - \alpha} \right). \tag{4.34}
\end{aligned}$$

Using the result from (4.19), we have

$$\tilde{\epsilon}_M^c(n) = \alpha^n \tilde{\epsilon}^c(0). \tag{4.35}$$

From above, we know that  $\epsilon_M^c(n) = E_\gamma\{\tilde{\epsilon}_M^c(n)\}$ . Thus,

$$\begin{aligned}
\epsilon_M^c(n) &= \alpha^n E_\gamma\{\tilde{\epsilon}^c(0)\} \\
&= \alpha^n \epsilon^c(0) \tag{4.36}
\end{aligned}$$

where  $\tilde{w}^c(0) = w(0)$  and  $\epsilon^c(0) = w(0) - w_{opt}^c$ . The same result can be obtained for the weight error mean of erroneous decision.

$$\epsilon_M^e(n) = \alpha^n \epsilon^e(0) \quad (4.37)$$

where  $\epsilon^e(0) = w(0) - w_{opt}^e$ .

### § 4.2.3 Weight Error Variance Analysis

In this section, we will find close-form expressions for  $E\{[\tilde{\epsilon}^c(n)]^2\}$  and that of  $E\{[\tilde{\epsilon}^e(n)]^2\}$ . Let  $\epsilon_V^c(n) = E\{[\tilde{\epsilon}^c(n) - \epsilon_M^c(n)]^2\}$  and  $\epsilon_V^e(n) = E\{[\tilde{\epsilon}^e(n) - \epsilon_M^e(n)]^2\}$ . We then have

$$E\{[\tilde{\epsilon}^c(n)]^2\} = \epsilon_V^c(n) + [\epsilon_M^c(n)]^2 \quad (4.38)$$

$$E\{[\tilde{\epsilon}^e(n)]^2\} = \epsilon_V^e(n) + [\epsilon_M^e(n)]^2. \quad (4.39)$$

Thus, the central problem in this section is to find  $\epsilon_V^c(n)$  and  $\epsilon_V^e(n)$ . We define  $\tilde{\epsilon}_V^c(n) = E_{v,x}\{[\tilde{\epsilon}^c(n) - \epsilon_M^c(n)]^2\}$  and  $\tilde{\epsilon}_V^e(n) = E_{v,x}\{[\tilde{\epsilon}^e(n) - \epsilon_M^e(n)]^2\}$ . From the conditional random variable property, we have  $\epsilon_V^c(n) = E_\gamma\{\tilde{\epsilon}_V^c(n)\}$  and  $\epsilon_V^e(n) = E_\gamma\{\tilde{\epsilon}_V^e(n)\}$ . As previously, we first consider the scenario of correct decision. From (4.31) and (4.33), we have

$$\begin{aligned} \tilde{\epsilon}_V^c(n) &= E_{v,x}\{[\tilde{\epsilon}^c(n) - \epsilon_M^c(n)]^2\} \\ &= E_{v,x}\{[\tilde{\epsilon}^c(n) + \tilde{\delta}^c - \alpha^n \epsilon^c(0)]^2\} \\ &= E_{v,x}\left\{\left[\alpha^n (\tilde{\epsilon}^c(0) - \epsilon^c(0)) + \tilde{\delta}^c + \mu \hat{b} \left(\sum_{i=0}^n \alpha^{n-i} \tilde{\nu}^c(i) - \frac{\gamma}{N} \sum_{i=0}^n \frac{1 - \alpha^n}{1 - \alpha}\right)\right]^2\right\} \\ &= E_{v,x}\left\{\left[\alpha^n (\tilde{\epsilon}^c(0) - \epsilon^c(0)) + \tilde{\delta}^c\right]^2\right\} \\ &\quad + \mu^2 E_{v,x}\left\{\left[\left(\sum_{i=0}^n \alpha^{n-i} \tilde{\nu}^c(i) - \frac{\gamma}{N} \sum_{i=0}^n \frac{1 - \alpha^n}{1 - \alpha}\right)\right]^2\right\}. \end{aligned} \quad (4.40)$$

Note that the second term in the righthand side of (4.40) is just  $\tilde{\varepsilon}_V^c(n)$ . This can be seen from (4.33) and (4.35). We now evaluate this term.

$$\begin{aligned}
\tilde{\varepsilon}_V^c(n) &= \mu^2 E_{v,x} \left\{ \left[ \sum_{i=0}^{n-1} \alpha^{n-i} \tilde{\nu}^c(i) - \frac{\gamma}{N} \left( \frac{1-\alpha^n}{1-\alpha} \right) \right]^2 \right\} \\
&= \mu^2 \left\{ E_{v,x} \left\{ \left[ \sum_{i=0}^{n-1} \alpha^{n-i} \tilde{\nu}^c(i) \right]^2 \right\} - \frac{2\gamma \tilde{\nu}_M^c(i)}{N} \left( \frac{1-\alpha^n}{1-\alpha} \right) \sum_{i=0}^{n-1} \alpha^{n-i} \right. \\
&\quad \left. + \frac{\gamma^2}{N^2} \cdot \left( \frac{1-\alpha^n}{1-\alpha} \right)^2 \right\} \\
&= \mu^2 \left\{ E_{v,x} \left\{ \left[ \sum_{i=0}^{n-1} \alpha^{n-i} \tilde{\nu}^c(i) \right]^2 \right\} - \frac{\gamma^2}{N^2} \left( \frac{1-\alpha^n}{1-\alpha} \right)^2 \right\}. \tag{4.41}
\end{aligned}$$

From (4.41), we can see that we have to find the autocorrelation function of  $\tilde{\nu}^c(i)$ , which is  $E_{v,x} \{ \tilde{\nu}^c(i) \tilde{\nu}^c(j) \}$ . It can be shown that the function have the same value for  $i \neq j$ . Let

$$E_{v,x} \{ \tilde{\nu}^c(i) \tilde{\nu}^c(j) \} = \begin{cases} p_\nu & i = j \\ q_\nu & i \neq j. \end{cases} \tag{4.42}$$

To solve the problem, we first consider a simple two-chip case in which  $N = 2$

$$\tilde{\nu}^c(0) + \tilde{\nu}^c(1) = \gamma \tag{4.43}$$

where the unconstrained variables  $\nu^c(0)$  and  $\nu^c(1)$  are two i.i.d. random variables with zero mean and variance  $\sigma_\nu^2$ . We can evaluate the conditional joint probability function of  $\{ \tilde{\nu}^c(0), \tilde{\nu}^c(1) \}$  as

$$\begin{aligned}
f(\tilde{\nu}^c(0), \tilde{\nu}^c(1)) &= \frac{1}{2\pi\sigma_\nu^2} \exp \left\{ -\frac{(\tilde{\nu}^c(0))^2 + (\tilde{\nu}^c(1))^2}{2\sigma_\nu^2} \right\} \\
&= \frac{1}{2\pi\sigma_\nu^2} \exp \left\{ -\frac{(\tilde{\nu}^c(0))^2 + [\gamma - \tilde{\nu}^c(0)]^2}{2\sigma_\nu^2} \right\} \\
&= \frac{1}{2\pi\sigma_\nu^2} \exp \left\{ -\frac{[(\tilde{\nu}^c(0) - \frac{1}{2}\gamma]^2 + \frac{1}{4}\gamma^2]}{\sigma_\nu^2} \right\} \\
&= C \cdot \frac{1}{\sqrt{2\pi \cdot \sigma_\nu^2/2}} \exp \left\{ -\frac{1}{2} \frac{[\tilde{\nu}^c(0) - \frac{1}{2}\gamma]^2}{\frac{1}{2}\sigma_\nu^2} \right\} \\
&= C f(\tilde{\nu}^c(0)) \tag{4.44}
\end{aligned}$$

where  $C$  is a normalization constant. From (4.44), we can obtain  $\tilde{v}_M^c(0) = \tilde{v}_M^c(1) = \frac{1}{2}\gamma$ , and  $\tilde{v}_V^c(0) = \frac{1}{2}\sigma_\nu^2$ . Multiplying  $\tilde{v}^c(0)$  and taking expectation on the both sides of (4.43), we can obtain

$$(\tilde{v}_M^c(0))^2 + \tilde{v}_V^c(0) + q_\nu = \gamma \tilde{v}_M^c(0). \quad (4.45)$$

Instituting the result of  $\tilde{v}_M^c(0)$  into (4.45), we can obtain  $q_\nu$  as

$$q_\nu = \frac{\gamma^2}{4} - \frac{\sigma_\nu^2}{2} = \frac{\gamma^2}{4} - \frac{\sigma^2}{2N}. \quad (4.46)$$

Direct extension of the above derivation to  $N > 2$  is difficult since we have to evaluate multi-dimensional integrations. We now use a simple method to overcome this problem. First, we let  $N$  be even and rewrite the  $\gamma$ -constrained equation as

$$\tilde{\theta}^c(0) + \tilde{\theta}^c(1) = \gamma, \quad \begin{cases} \tilde{\theta}^c(0) = \sum_{i=0}^{N/2-1} \tilde{v}^c(i) \\ \tilde{\theta}^c(1) = \sum_{i=N/2}^{N-1} \tilde{v}^c(i) \end{cases} \quad (4.47)$$

where the unconstrained variables  $\theta^c(0)$  and  $\theta^c(1)$  are i.i.d. random variables with the same distribution. We can then apply the result in (4.45) and obtain

$$\left(\tilde{\theta}_M^c(0)\right)^2 + \tilde{\theta}_V^c(0) + q_\theta = \gamma \cdot \tilde{\theta}_M^c(0). \quad (4.48)$$

Note that  $\tilde{\theta}_V^c(0) = \frac{1}{2}\theta_V^c(0)$  with  $\theta_V^c(0) = N\sigma_\nu^2/2$ , and  $\tilde{\theta}_M^c(0) = \gamma/2$ . Combing with (4.48), we can then obtain  $q_\theta$ . Note that

$$\begin{aligned} q_\theta &= E_{v,x} \left\{ \sum_{i=0}^{N/2-1} \sum_{j=N/2}^{N-1} \tilde{v}^c(i)\tilde{v}^c(j) \right\} \\ &= \left(\frac{N}{2}\right)^2 q_\nu. \end{aligned} \quad (4.49)$$

Thus, from (4.49) we can obtain the crosscorrelation  $q_\nu$  for  $N > 2$  as

$$q_\nu = \frac{\gamma^2}{N^2} - \frac{\sigma_\nu^2}{N}. \quad (4.50)$$

Multiplying  $\tilde{\nu}^c(i)$  on both sides of (4.47) and taking expectation, we have

$$p_\nu + (N - 1)q_\nu = \frac{\gamma^2}{N}. \quad (4.51)$$

Finally, we obtain

$$p_\nu = \frac{\gamma^2}{N} + \frac{N - 1}{N}\sigma_\nu^2. \quad (4.52)$$

Simulation results show that the result (derived for an even  $N$ ) is also very accurate for an odd  $N$ . We can then have an explicit expression of the first summation term on the righthand side of (4.41) as

$$E_{v,x} \left\{ \left[ \sum_{i=0}^n \alpha^{n-i} \tilde{\nu}^c(i) \right]^2 \right\} = q_\nu \left( \frac{1 - \alpha^n}{1 - \alpha} \right)^2 + (p_\nu - q_\nu) \left( \frac{1 - \alpha^{2n}}{1 - \alpha^2} \right). \quad (4.53)$$

Thus, combining (4.41), (4.50), (4.52) and (4.53), we have

$$\begin{aligned} \tilde{\varepsilon}_V^c(n) &= \mu^2 \left\{ \sigma_\nu^2 \left( \frac{1 - \alpha^{2n}}{1 - \alpha^2} \right) - \frac{\sigma_\nu^2}{N} \left( \frac{1 - \alpha^n}{1 - \alpha} \right)^2 \right\} \\ &= \frac{\mu^2}{N^2} \left\{ N\sigma^2 \left( \frac{1 - \alpha^{2n}}{1 - \alpha^2} \right) - \sigma^2 \left( \frac{1 - \alpha^n}{1 - \alpha} \right)^2 \right\}. \end{aligned} \quad (4.54)$$

By definition and (4.40), we have

$$\varepsilon_V^c(n) = E_\gamma \left\{ \left[ \alpha^n \left( \tilde{\varepsilon}^c(0) - \varepsilon^c(0) \right) + \tilde{\delta}^c \right]^2 \right\} + \varepsilon_V^c(n). \quad (4.55)$$

Note that the result in (4.54) is independent of  $\gamma$ ; it is a function of noise variance and the step size only. Thus,  $\varepsilon_V^c(n) = E_\gamma \{ \tilde{\varepsilon}_V^c(n) \} = \tilde{\varepsilon}_V^c(n)$ . Thus, the second term in the righthand side of (4.55) can be evaluate using (4.54). Denote the first term in (4.55) as  $\delta_V^c$ . Then,

$$\varepsilon_V^c(n) = \delta_V^c + \varepsilon_V^c(n). \quad (4.56)$$

The term  $\delta_V^c$  can be further evaluated as

$$\begin{aligned} \delta_V^c &= E_\gamma \left\{ \left[ \alpha^n \left( \tilde{\varepsilon}^c(0) - \varepsilon^c(0) \right) + \tilde{\delta}^c \right]^2 \right\} \\ &= (1 - \alpha^n)^2 E_\gamma \left\{ \left( \tilde{w}_{opt}^c - w_{opt}^c \right)^2 \right\} \\ &= (1 - \alpha^n)^2 \left( E_\gamma \left\{ \left[ \tilde{w}_{opt}^c \right]^2 \right\} - \left[ w_{opt}^c \right]^2 \right) \end{aligned} \quad (4.57)$$

where the second moment of  $\tilde{w}_{opt}^c$  is given by

$$E_{\gamma} \left\{ \left[ \tilde{w}_{opt}^c \right]^2 \right\} = E_{\gamma} \left\{ (a + \gamma)^2 \mid \gamma \in \mathbb{V}^c \right\}. \quad (4.58)$$

Thus, we can obtain the weight error power shown in (4.38) using (4.36), (4.54), (4.55) and (4.57) as

$$E \left\{ \left[ \tilde{\epsilon}^c(n) \right]^2 \right\} = \alpha^{2n} \left[ \epsilon^c(0) \right]^2 + \delta_V^c + \tilde{\epsilon}_V^c(n). \quad (4.59)$$

Similarly, the weight error power for the erroneous decision described in (4.39) can be obtained as

$$E \left\{ \left[ \tilde{\epsilon}^e(n) \right]^2 \right\} = \alpha^{2n} \left[ \epsilon^e(0) \right]^2 + \delta_V^e + \tilde{\epsilon}_V^e(n). \quad (4.60)$$

The second term in the righthand side of (4.60) can be expanded as

$$\delta_V^e = (1 - \alpha^n)^2 \left( E_{\gamma} \left\{ \left[ \tilde{w}_{opt}^e \right]^2 \right\} - \left[ w_{opt}^e \right]^2 \right) \quad (4.61)$$

where the second moment of  $\tilde{w}_{opt}^e$  is given by

$$E_{\gamma} \left\{ \left[ \tilde{w}_{opt}^e \right]^2 \right\} = E_{\gamma} \left\{ (a + \gamma)^2 \mid \gamma \in \mathbb{V}^e \right\}. \quad (4.62)$$

As mentioned, the result in (4.54) is independent of  $\gamma$ . Thus, we have  $\tilde{\epsilon}_V^e(n) = \tilde{\epsilon}_V^c(n)$  and  $\epsilon_V^e(n) = \tilde{\epsilon}_V^c(n)$ . The third term in the righthand side of (4.60) can be evaluated using (4.54).

### § 4.3 Exact Analysis for Two-user Scenario

Extending the procedure developed in the previous section, we now proceed to analyze the two-user case. Only the optimal weights and convergent weight error means are considered since the closed form expression for the weight error variance is difficult to obtain. In most cases, we only represent the result for the correct decision (denoted with superscript ‘c’). The derivation for erroneous decision is summarized in Appendix D.

### § 4.3.1 Optimal Weight Analysis

Define  $\mathbf{x}(n) = [x_1(n), x_2(n)]^T$  and the matrix formed by  $\mathbf{x}(n)$  as  $\mathbf{R}(n) \triangleq \{\mathbf{x}(n)\mathbf{x}(n)^T\}$ . Then, the time-averaged correlation matrix is obtained as

$$\mathbf{R} \triangleq \frac{1}{N} \sum_{n=0}^{N-1} \mathbf{R}(n). \quad (4.63)$$

The time-averaged correlation between these two users' codes is given by

$$\rho = \sum_{n=0}^{N-1} x_1(n)x_2(n). \quad (4.64)$$

Note that  $N\rho$  is an integer. It is simple to show that

$$\mathbf{R} = \frac{1}{N} \begin{bmatrix} 1 & \rho \\ \rho & 1 \end{bmatrix}. \quad (4.65)$$

The matched filter output vector, denoted by  $\mathbf{y}^{(1)} = [y_1^{(1)}, y_2^{(1)}]^T$ , is then

$$\begin{aligned} \mathbf{y}^{(1)} &= \sum_{n=0}^{N-1} \mathbf{x}(n)r(n) \\ &= \sum_{n=0}^{N-1} \mathbf{x}(n)(a_1b_1x_1(n) + a_2b_2x_2(n) + v(n)) \\ &= N\mathbf{R}\mathbf{A}\mathbf{b} + \sum_{n=0}^{N-1} \mathbf{x}(n)v(n) \\ &= N\mathbf{R}\mathbf{A}\mathbf{b} + \sum_{n=0}^{N-1} \boldsymbol{\nu}(n) \end{aligned} \quad (4.66)$$

where  $\mathbf{b} = [b_1, b_2]^T$  is the data bit vector,  $\mathbf{A} = \text{diag}\{a_1, a_2\}$  is the channel amplitude matrix, and  $\boldsymbol{\nu}(n) = [\nu_1(n), \nu_2(n)]^T$  is the noise vector after code multiplication. Let the second term in the righthand side of (4.66) be denoted as  $\boldsymbol{\gamma} = [\gamma_1, \gamma_2]^T$ . Then

$$\boldsymbol{\gamma} = \sum_{n=0}^{N-1} \boldsymbol{\nu}(n), \quad (4.67)$$

and

$$\mathbf{y}^{(1)} = N\mathbf{R}\mathbf{A}\mathbf{b} + \boldsymbol{\gamma}. \quad (4.68)$$

As that in the single user case, the decision in the first stage depends on the value of  $\boldsymbol{\gamma}$ . However, the problem here become more involved since the distribution of  $\boldsymbol{\gamma}$  depends on  $\rho$ . It can be shown that the joint probability density function for the random vector  $\boldsymbol{\gamma}$  is Gaussian and

$$f(\boldsymbol{\gamma}) = \frac{1}{2\pi|\mathbf{C}_\boldsymbol{\gamma}|^{1/2}} \exp\left\{-\frac{1}{2}\boldsymbol{\gamma}^T\mathbf{C}_\boldsymbol{\gamma}^{-1}\boldsymbol{\gamma}\right\} \quad (4.69)$$

where the covariance matrix is given as

$$\mathbf{C}_\boldsymbol{\gamma} \triangleq E\{\boldsymbol{\gamma}\boldsymbol{\gamma}^T\} = \begin{bmatrix} \sigma^2 & \rho\sigma^2 \\ \rho\sigma^2 & \sigma^2 \end{bmatrix}. \quad (4.70)$$

Note that now the number of bits for decision is two and the number of the decision patterns becomes four. Let  $j = 3 - k$  and  $k$  can be 1 or 2. Define the set for which User  $k$ 's decision is correct as

$$\begin{aligned} \mathbb{V}_k^c &\triangleq \{\boldsymbol{\gamma}_k | b_k = \hat{b}_k\} \\ &= \begin{cases} \boldsymbol{\gamma}_k > -(a_k + a_j b_j \rho) & \text{for } b_k = 1 \\ \boldsymbol{\gamma}_k < a_k - a_j b_j \rho & \text{for } b_k = -1. \end{cases} \end{aligned} \quad (4.71)$$

Similarly the noise subset for making erroneous decision is represented as

$$\begin{aligned} \mathbb{V}_k^e &\triangleq \{\boldsymbol{\gamma}_k | b_k \neq \hat{b}_k\} \\ &= \begin{cases} \boldsymbol{\gamma}_k < -(a_k + a_j b_j \rho) & \text{for } b_k = 1 \\ \boldsymbol{\gamma}_k > a_k - a_j b_j \rho & \text{for } b_k = -1. \end{cases} \end{aligned} \quad (4.72)$$

We then extend our notations defined in the previous section. Let a random variable  $z$  conditioned on  $\boldsymbol{\gamma}$  and then on  $\rho$  be denoted as  $\tilde{z}$ , i.e.,  $\tilde{z} = \{z|\boldsymbol{\gamma}|\rho\}$ . Also let  $\tilde{z}_M = E_{v,x}\{\tilde{z}\}$ ,  $\tilde{z}_M = E_\boldsymbol{\gamma}\{\tilde{z}_M\}$ ,  $z_M = E_\rho\{\tilde{z}_M\}$ . We then have  $z_M = E\{z\}$ . Using the similar rule, we define the optimal weight conditioned on  $\boldsymbol{\gamma}$  and then on  $\rho$  as  $\tilde{\mathbf{w}}_{opt}$ , the optimal weight conditioned on  $\rho$  as  $\tilde{\mathbf{w}}_{opt}$ , and the optimal weight as  $\mathbf{w}_{opt}$ . We then have  $\tilde{\mathbf{w}}_{opt} = E_\boldsymbol{\gamma}\{\tilde{\mathbf{w}}_{opt}\}$  and  $\mathbf{w}_{opt} = E_\rho\{\tilde{\mathbf{w}}_{opt}\}$ .



The optimal weight conditioned on  $\gamma$  and then on  $\rho$  can be represented as

$$\tilde{\mathbf{w}}_{opt} = \tilde{\mathbf{Q}}^{-1} \tilde{\mathbf{p}} \quad (4.73)$$

where the correlation matrix of input signals is expressed by

$$\begin{aligned} \tilde{\mathbf{Q}} &= E_{v,x} \{ \tilde{\boldsymbol{\chi}}(n) \tilde{\boldsymbol{\chi}}(n)^T \} \\ &= \frac{1}{N} \begin{bmatrix} 1 & \hat{b}_1 \hat{b}_2 \rho \\ \hat{b}_1 \hat{b}_2 \rho & 1 \end{bmatrix}. \end{aligned} \quad (4.74)$$

The crosscorrelation vector is given by

$$\begin{aligned} \tilde{\mathbf{p}} &\triangleq E_{v,x} \{ \tilde{\boldsymbol{\chi}}(n) \tilde{r}(n) \} \\ &= E_{v,x} \{ \hat{\mathbf{B}} \tilde{\mathbf{x}}(n) [a_1 b_1 \tilde{x}_1(n) + a_2 b_2 \tilde{x}_2(n) + \tilde{v}(n)] \}. \end{aligned} \quad (4.75)$$

Thus, the conditional optimal weight vector is

$$\begin{aligned} \tilde{\mathbf{w}}_{opt} &= \frac{N}{1 - \rho^2} \begin{bmatrix} 1 & -\hat{b}_1 \hat{b}_2 \rho \\ -\hat{b}_1 \hat{b}_2 \rho & 1 \end{bmatrix} \cdot \frac{1}{N} \begin{bmatrix} a_1 b_1 \hat{b}_1 + a_2 \hat{b}_1 b_2 \rho + \hat{b}_1 \tilde{\gamma}_1 \\ a_2 b_2 \hat{b}_2 + a_1 \hat{b}_2 b_1 \rho + \hat{b}_2 \tilde{\gamma}_2 \end{bmatrix} \\ &= \mathbf{A} \hat{\mathbf{B}} \mathbf{b} + \frac{1}{N} \hat{\mathbf{B}} \mathbf{R}^{-1} \tilde{\boldsymbol{\gamma}}. \end{aligned} \quad (4.76)$$

As we can see from (4.76), the optimal weights depends on the decision patterns in  $\hat{\mathbf{B}}$ . There are four decision patterns, i.e.,  $\{\hat{b}_1 = b_1, \hat{b}_2 = b_2\}$ ,  $\{\hat{b}_1 = b_1, \hat{b}_2 \neq b_2\}$ ,  $\{\hat{b}_1 \neq b_1, \hat{b}_2 = b_2\}$ , and  $\{\hat{b}_1 \neq b_1, \hat{b}_2 \neq b_2\}$ . Note that for each decision pattern, we have two bit patterns that  $b_1 = b_2$  and  $b_1 \neq b_2$ . Let  $\mathbb{U}^{ij}$  denote the set of  $\gamma$  yielding the  $i$ th decision for the  $j$ th bit pattern. For example,

$$\mathbb{U}^{11} = \{ \gamma | \gamma_1 \in \mathbb{V}_1^c, \gamma_2 \in \mathbb{V}_2^c, b_1 = b_2 \} \quad (4.77)$$

$$\mathbb{U}^{12} = \{ \gamma | \gamma_1 \in \mathbb{V}_1^c, \gamma_2 \in \mathbb{V}_2^c, b_1 \neq b_2 \}. \quad (4.78)$$

Let  $\tilde{z}^{ij} = \{z | \gamma \in \mathbb{U}^{ij} | \rho\}$ . Also let  $\tilde{z}_M^{ij} = E_{v,x} \{ \tilde{z}^{ij} \}$ . We can have similar notation for optimal weights. Let the optimal weight conditioned on  $\gamma \in \mathbb{U}^{ij}$  and then on  $\rho$  as  $\tilde{\mathbf{w}}_{opt}^{ij}$  and  $\check{\mathbf{w}}_{opt}^{ij} = E_{\gamma} \{ \tilde{\mathbf{w}}_{opt}^{ij} \}$ . Then,

$$\tilde{\mathbf{w}}_{opt}^{ij} = \mathbf{A} \hat{\mathbf{B}}^i \mathbf{b}^j + \frac{1}{N} \hat{\mathbf{B}}^i \mathbf{R}^{-1} E_{\gamma} \{ \tilde{\boldsymbol{\gamma}}^{ij} \} \quad (4.79)$$

where  $\hat{\mathbf{B}}^i$  denotes the  $i$ th decision pattern, and  $\mathbf{b}^j$  denotes the  $j$ th bit pattern.

If we further assume that  $b_1 = 1$ , we have

$$\mathbb{U}^{11} = \{\gamma | \gamma_1 \in \mathbb{V}_1^c, \gamma_2 \in \mathbb{V}_2^c, b_1 = 1 = b_2\} \quad (4.80)$$

$$= \{\gamma | \gamma_1 > -(a_1 + a_2\rho), \gamma_2 > -(a_2 + a_1\rho)\} \quad (4.81)$$

and

$$\mathbb{U}^{12} = \{\gamma | \gamma_1 \in \mathbb{V}_1^c, \gamma_2 \in \mathbb{V}_2^c, b_1 = 1 \neq b_2\} \quad (4.82)$$

$$= \{\gamma | \gamma_1 > -(a_1 - a_2\rho), \gamma_2 > -(a_2 - a_1\rho)\}. \quad (4.83)$$

The optimal weights for  $\hat{\mathbf{B}}^1$  becomes

$$\check{\mathbf{w}}_{opt}^{11} = \mathbf{a} + \frac{1}{N} \mathbf{R}^{-1} E_{\gamma} \{\tilde{\gamma}^{11}\} \quad (4.84)$$

$$\check{\mathbf{w}}_{opt}^{12} = \mathbf{a} + \frac{1}{N} \mathbf{J} \mathbf{R}^{-1} E_{\gamma} \{\tilde{\gamma}^{12}\}$$

where  $\mathbf{a} = [a_1, a_2]^T$  and  $\mathbf{J} \triangleq \text{diag}\{1, -1\}$ . The result in (4.84) for  $b = -1$  is identical for  $b_1 = 1$  since in (4.79) the product in  $\hat{\mathbf{B}}^i \mathbf{b}^j$  or  $\hat{\mathbf{B}}^i E_{\gamma}^{ij} \{\gamma\}$  is independent of the value of  $b_1$ . The components in  $E_{\gamma}^{ij} \{\gamma\}$  are given by

$$E_{\gamma} \{\tilde{\gamma}^{ij}\} = \frac{\int_{\mathbb{U}^{ij}} \gamma f(\gamma) d\gamma}{\int_{\mathbb{U}^{ij}} f(\gamma) d\gamma}. \quad (4.85)$$

The complete set of  $\gamma$  for all decision and bit patterns is shown in Table 4.1. The complete set of conditional optimal weights is given in Table 4.2.

Our objective is to determine  $\check{\mathbf{w}}_{opt}^c$  and  $\check{\mathbf{w}}_{opt}^e$  by taking expectation on  $\check{\mathbf{w}}_{opt}^c$  and  $\check{\mathbf{w}}_{opt}^e$ . As seen in Table 4.1, the region of  $\gamma_1$  for correct decision is different from that of  $\gamma_2$ . Thus we have to determine the components of  $\check{\mathbf{w}}_{opt}^c$  user by user. The union of noise subsets for the first user to have correct decision is then

$$\mathbb{C}_1 = \mathbb{U}^{11} \cup \mathbb{U}^{12} \cup \mathbb{U}^{21} \cup \mathbb{U}^{22}. \quad (4.86)$$

The occurrence probability for  $\mathbb{U}^{ij}$  is obtained as

$$P_{ij} = \int_{\mathbb{U}^{ij}} f(\gamma) d\gamma. \quad (4.87)$$

Table 4.1: Sets of  $\gamma$  for all decision and bit patterns

$\mathbb{U}^{ij}$	$\hat{\mathbf{B}}^i \mathbf{b}^j$	Range for $\gamma_1$	Range for $\gamma_2$
$\mathbb{U}^{11}$	$\begin{bmatrix} 1 \\ 1 \end{bmatrix}$	$\gamma_1 > -(a_1 + a_2\rho)$	$\gamma_2 > -(a_1\rho + a_2)$
$\mathbb{U}^{12}$	$\begin{bmatrix} 1 \\ 1 \end{bmatrix}$	$\gamma_1 > -(a_1 - a_2\rho)$	$\gamma_2 < -(a_1\rho - a_2)$
$\mathbb{U}^{21}$	$\begin{bmatrix} 1 \\ -1 \end{bmatrix}$	$\gamma_1 > -(a_1 + a_2\rho)$	$\gamma_2 < -(a_2 + a_1\rho)$
$\mathbb{U}^{22}$	$\begin{bmatrix} 1 \\ -1 \end{bmatrix}$	$\gamma_1 > -(a_1 - a_2\rho)$	$\gamma_2 > -(a_1\rho - a_2)$
$\mathbb{U}^{31}$	$\begin{bmatrix} -1 \\ -1 \end{bmatrix}$	$\gamma_1 < -(a_1 + a_2\rho)$	$\gamma_2 < -a_2 + a_1\rho$
$\mathbb{U}^{32}$	$\begin{bmatrix} -1 \\ -1 \end{bmatrix}$	$\gamma_1 < -(a_1 - a_2\rho)$	$\gamma_2 > -(a_1\rho - a_2)$
$\mathbb{U}^{41}$	$\begin{bmatrix} -1 \\ 1 \end{bmatrix}$	$\gamma_1 < -(a_1 + a_2\rho)$	$\gamma_2 > -(a_2 + a_1\rho)$
$\mathbb{U}^{42}$	$\begin{bmatrix} -1 \\ 1 \end{bmatrix}$	$\gamma_1 < -(a_1 - a_2\rho)$	$\gamma_2 < -(a_1\rho - a_2)$

The first user optimal weight for correct decision and a given  $\rho$  is

$$\check{w}_{opt,1}^c = \frac{1}{P_{\mathcal{C}_1}} \sum_{\mathcal{C}_1} \check{w}_{opt,1}^{ij} P_{ij} \quad (4.88)$$

where

$$P_{\mathcal{C}_1} = P_{11} + P_{12} + P_{21} + P_{22}. \quad (4.89)$$

The second user optimal weight for correct decision and a given  $\rho$  is

$$\check{w}_{opt,2}^c = \frac{1}{P_{\mathcal{C}_2}} \sum_{\mathcal{C}_2} \check{w}_{opt,2}^{ij} P_{ij} \quad (4.90)$$

where

$$\mathcal{C}_2 = \mathbb{U}^{11} \cup \mathbb{U}^{12} \cup \mathbb{U}^{41} \cup \mathbb{U}^{42} \quad (4.91)$$

$$P_{\mathcal{C}_2} = P_{11} + P_{12} + P_{41} + P_{42}. \quad (4.92)$$

Table 4.2: Complete list of conditional optimal weights

$\check{\mathbf{w}}_{opt}^{11} = \mathbf{a} + \frac{1}{N}\mathbf{R}^{-1}E_{\gamma}\{\tilde{\gamma}^{11}\}$	$\check{\mathbf{w}}_{opt}^{12} = \mathbf{a} + \frac{1}{N}\mathbf{J}\mathbf{R}^{-1}E_{\gamma}\{\tilde{\gamma}^{12}\}$
$\check{\mathbf{w}}_{opt}^{21} = -\mathbf{a} + \frac{1}{N}\mathbf{J}\mathbf{R}^{-1}E_{\gamma}\{\tilde{\gamma}^{21}\}$	$\check{\mathbf{w}}_{opt}^{22} = -\mathbf{a} + \frac{1}{N}\mathbf{R}^{-1}E_{\gamma}\{\tilde{\gamma}^{22}\}$
$\check{\mathbf{w}}_{opt}^{31} = \mathbf{J}\mathbf{a} - \frac{1}{N}\mathbf{J}\mathbf{R}^{-1}E_{\gamma}\{\tilde{\gamma}^{31}\}$	$\check{\mathbf{w}}_{opt}^{32} = \mathbf{J}\mathbf{a} - \frac{1}{N}\mathbf{R}^{-1}E_{\gamma}\{\tilde{\gamma}^{32}\}$
$\check{\mathbf{w}}_{opt}^{41} = -\mathbf{J}\mathbf{a} - \frac{1}{N}\mathbf{J}\mathbf{R}^{-1}E_{\gamma}\{\tilde{\gamma}^{41}\}$	$\check{\mathbf{w}}_{opt}^{42} = -\mathbf{J}\mathbf{a} - \frac{1}{N}\mathbf{R}^{-1}E_{\gamma}\{\tilde{\gamma}^{42}\}$

The optimal weight is obtained through averaging  $\check{\mathbf{w}}_{opt}^c$  over all  $\rho$  values by

$$w_{opt,i}^c = E_{\rho}\{\check{w}_{opt,i}^c\} = \frac{\sum_{\rho} \check{w}_{opt,i}^c P_{\rho} P_{C_i}}{\sum_{\rho} P_{\rho} P_{C_i}} \quad (4.93)$$

where  $i = 1, 2$  and the distribution for the correlation coefficient is given by

$$P_{\rho} = \frac{1}{2^N} \binom{N}{N(1+\rho)/2}. \quad (4.94)$$

The optimal weights for erroneous decision can be obtained in a similar way and summarized in Appendix D.

### § 4.3.2 Weight Error Mean Analysis

The LMS update equation for a two-user scenario is rewritten as

$$\begin{aligned} \hat{r}(n) &= \boldsymbol{\chi}(n)^T \mathbf{w}(n) \\ e(n) &= r(n) - \hat{r}(n) \\ \mathbf{w}(n+1) &= \mathbf{w}(n) + \mu e(n) \boldsymbol{\chi}(n) \end{aligned} \quad (4.95)$$

where  $\mathbf{w}(n) = [w_1(n), w_2(n)]^T$ . Define two weight errors as

$$\begin{aligned} \tilde{\epsilon}_i^c(n) &= \tilde{w}_i^c(n) - w_{opt,i}^c \\ \tilde{\epsilon}_i^e(n) &= \tilde{w}_i^e(n) - w_{opt,i}^e \end{aligned} \quad i = 1, 2. \quad (4.96)$$

From the optimal weight results of the two-user case, we know  $\check{\mathbf{w}}_{opt}^c$  and  $\check{\mathbf{w}}_{opt}^e$  are obtained from  $\check{\mathbf{w}}_{opt}^{ij}$ 's. Thus we also give the conditional weight errors as

$$\tilde{\epsilon}^{ij}(n) = \tilde{\mathbf{w}}^{ij}(n) - \check{\mathbf{w}}_{opt}^{ij} \quad (4.97)$$

where the conditional weights are defined as

$$\tilde{\mathbf{w}}^{ij}(n) = \{\mathbf{w}(n) | \gamma \in \mathbb{U}^{ij}\}. \quad (4.98)$$

As in the single-user case, our goal is to determine close-form expressions of  $E\{\epsilon_i^c(n)\}$  and  $E\{\epsilon_i^e(n)\}$ . It is obtained by  $E\{\epsilon_i^c(n)\} = E_\rho\{\tilde{\epsilon}_{M,i}^c(n)\}$  and  $E\{\epsilon_i^e(n)\} = E_\rho\{\tilde{\epsilon}_{M,i}^e(n)\}$ . By definition  $\tilde{\mathbf{w}}_{opt}^{ij} = E_\gamma\{\tilde{\mathbf{w}}_{opt}^{ij}\}$ . We express the conditional weight error for  $\tilde{\mathbf{w}}_{opt}^{ij}$  as

$$\begin{aligned} \tilde{\epsilon}^{ij}(n) &= \tilde{\mathbf{w}}^{ij}(n) - \tilde{\mathbf{w}}_{opt}^{ij} \\ &= \tilde{\mathbf{w}}^{ij}(n) - \tilde{\mathbf{w}}_{opt}^{ij} + \tilde{\mathbf{w}}_{opt}^{ij} - \tilde{\mathbf{w}}_{opt}^{ij}. \end{aligned} \quad (4.99)$$

We then define

$$\begin{aligned} \tilde{\epsilon}^{ij}(n) &= \tilde{\mathbf{w}}^{ij}(n) - \tilde{\mathbf{w}}_{opt}^{ij} \\ \tilde{\delta}^{ij} &= \tilde{\mathbf{w}}_{opt}^{ij} - \tilde{\mathbf{w}}_{opt}^{ij}. \end{aligned} \quad (4.100)$$

From (4.99) and (4.100) we have

$$\tilde{\epsilon}^{ij}(n) = \tilde{\epsilon}^{ij}(n) + \tilde{\delta}^{ij}. \quad (4.101)$$

It is obvious that

$$\tilde{\delta}_M^{ij} = [0 \ 0]^T. \quad (4.102)$$

Thus we obtain that

$$\tilde{\epsilon}_M^{ij}(n) = \tilde{\epsilon}_M^{ij}(n). \quad (4.103)$$

Thus  $\check{\epsilon}_M^{ij}(n) = \tilde{\epsilon}_M^{ij}(n) = E_\gamma\{\tilde{\epsilon}_M^{ij}(n)\}$ . We then have

$$\begin{aligned} \tilde{\epsilon}^{ij}(n) &= \tilde{\mathbf{w}}^{ij}(n) - \tilde{\mathbf{w}}_{opt}^{ij} \\ &= \tilde{\mathbf{w}}^{ij}(n-1) - \tilde{\mathbf{w}}_{opt}^{ij} + \mu \tilde{\chi}^{ij}(n-1) \tilde{\epsilon}^{ij}(n-1) \\ &= \tilde{\epsilon}^{ij}(n-1) + \mu \tilde{\chi}^{ij}(n-1) (\tilde{r}^{ij}(n-1) - \tilde{\chi}^{ij}(n-1)^T \tilde{\mathbf{w}}^{ij}(n-1)) \\ &= (\mathbf{I} - \mu \tilde{\mathbf{Q}}^{ij}(n-1)) \tilde{\epsilon}^{ij}(n-1) + \mu (\tilde{\chi}^{ij}(n-1) \tilde{r}^{ij}(n-1) - \tilde{\mathbf{Q}}^{ij}(n-1) \tilde{\mathbf{w}}_{opt}^{ij}) \\ &= (\mathbf{I} - \mu \tilde{\mathbf{Q}}^{ij}(n-1)) \tilde{\epsilon}^{ij}(n-1) + \mu \tilde{\Psi}^{ij}(n-1) \end{aligned} \quad (4.104)$$

where  $\tilde{\mathbf{Q}}^{ij}(n) = \{\tilde{\boldsymbol{\chi}}^{ij}(n)\tilde{\boldsymbol{\chi}}^{ij}(n)^T\}$  and the parameter  $\tilde{\boldsymbol{\Psi}}^{ij}(n)$  in the second term on the righthand side of the above equation is defined as

$$\tilde{\boldsymbol{\Psi}}^{ij}(n) \triangleq \tilde{\boldsymbol{\chi}}^{ij}(n)\tilde{r}^{ij}(n) - \tilde{\mathbf{Q}}^{ij}(n)\tilde{\mathbf{w}}_{opt}^{ij}. \quad (4.105)$$

It can be easily shown by deduction that the recursive weight error given  $\gamma$  and  $\rho$  is

$$\begin{aligned} \tilde{\boldsymbol{\epsilon}}^{ij}(n) &= \prod_{m=0}^{n-1} \left( \mathbf{I} - \mu \tilde{\mathbf{Q}}^{ij}(m) \right) \tilde{\boldsymbol{\epsilon}}^{ij}(0) \\ &\quad + \mu \sum_{m=0}^{n-1} \prod_{l=m+1}^{n-1} \left( \mathbf{I} - \mu \tilde{\mathbf{Q}}^{ij}(l) \right) \tilde{\boldsymbol{\Psi}}^{ij}(m). \end{aligned} \quad (4.106)$$

By combining (4.105) and (4.106) with the institution that

$$\tilde{\mathbf{W}}^{ij}(n, m) \triangleq \prod_{l=m+1}^n \left( \mathbf{I} - \mu \tilde{\mathbf{Q}}^{ij}(l) \right) \quad (4.107)$$

we obtain the conditional weight error as

$$\begin{aligned} \tilde{\boldsymbol{\epsilon}}^{ij}(n) &= \tilde{\mathbf{W}}^{ij}(n, -1)\tilde{\boldsymbol{\epsilon}}^{ij}(0) + \mu \sum_{m=0}^{n-1} \tilde{\mathbf{W}}^{ij}(n, m)\tilde{\boldsymbol{\Psi}}^{ij}(m) \\ &= \tilde{\mathbf{W}}^{ij}(n, -1)\tilde{\boldsymbol{\epsilon}}^{ij}(0) + \mu \sum_{m=0}^{n-1} \tilde{\mathbf{W}}^{ij}(n, m) \left( \tilde{\boldsymbol{\chi}}^{ij}(m)\tilde{r}^{ij}(m) - \tilde{\mathbf{Q}}^{ij}(m)\tilde{\mathbf{w}}_{opt}^{ij} \right) \\ &= \tilde{\mathbf{W}}^{ij}(n, -1)\tilde{\boldsymbol{\epsilon}}^{ij}(0) \\ &\quad + \mu \sum_{m=0}^{n-1} \tilde{\mathbf{W}}^{ij}(n, m) \left( \tilde{\boldsymbol{\chi}}^{ij}(m) [a_1 b_1 \tilde{x}_1^{ij}(m) + a_2 b_2 \tilde{x}_2^{ij}(m) + \tilde{v}^{ij}(m)] \right. \\ &\quad \left. - \tilde{\boldsymbol{\chi}}^{ij}(m)\tilde{\boldsymbol{\chi}}^{ij}(m)^T \left[ \mathbf{A}\hat{\mathbf{B}}^i \mathbf{b}^j + \frac{1}{N} \mathbf{R}^{-1} \hat{\mathbf{B}}^i \tilde{\boldsymbol{\gamma}}^{ij} \right] \right). \end{aligned} \quad (4.108)$$

Note that by some algebraic computations we obtain

$$\tilde{\boldsymbol{\chi}}^{ij}(m) [a_1 b_1 \tilde{x}_1^{ij}(m) + a_2 b_2 \tilde{x}_2^{ij}(m)] - \tilde{\boldsymbol{\chi}}^{ij}(m)\tilde{\boldsymbol{\chi}}^{ij}(m)^T \mathbf{A}\hat{\mathbf{B}}^i \mathbf{b}^j = \begin{bmatrix} 0 \\ 0 \end{bmatrix}, \quad (4.109)$$

and then we can express the weight error as

$$\begin{aligned} \tilde{\boldsymbol{\epsilon}}^{ij}(n) &= \tilde{\mathbf{W}}^{ij}(n, -1)\tilde{\boldsymbol{\epsilon}}^{ij}(0) \\ &\quad + \mu \sum_{m=0}^{n-1} \tilde{\mathbf{W}}^{ij}(n, m) \left( \tilde{\boldsymbol{\chi}}^{ij}(m)\tilde{v}^{ij}(m) - \frac{1}{N} \tilde{\boldsymbol{\chi}}^{ij}(m)\tilde{\boldsymbol{\chi}}^{ij}(m)^T \mathbf{R}^{-1} \hat{\mathbf{B}}^i \tilde{\boldsymbol{\gamma}}^{ij} \right) \end{aligned} \quad (4.110)$$

From the above definition, we know  $\tilde{\epsilon}_M^{ij}(n) = E_\gamma\{\tilde{\epsilon}_M^{ij}(n)\} = E_\gamma\{E_{v,x}\{\tilde{\epsilon}^{ij}(n)\}\}$ . The expectation for the first term on the righthand side of (4.110) can be obtained as

$$\begin{aligned}
& E_\gamma \left\{ E_{v,x} \left\{ \tilde{\mathbf{W}}(n, -1) \tilde{\epsilon}^{ij}(0) \right\} \right\} \\
&= E_\gamma \left\{ E_{v,x} \left\{ \prod_{m=0}^{n-1} (\mathbf{I} - \mu \tilde{\mathbf{Q}}^{ij}(m)) \right\} \tilde{\epsilon}_M^{ij}(0) \right\} \\
&= E_\gamma \left\{ (\mathbf{I} - \mu \tilde{\mathbf{Q}}^{ij})^n \right\} \tilde{\epsilon}_M^{ij}(0) \\
&= (\mathbf{I} - \mu \tilde{\mathbf{Q}}^{ij})^n \tilde{\epsilon}_M^{ij}(0)
\end{aligned} \tag{4.111}$$

where  $\tilde{\mathbf{Q}}^{ij} = E\{\tilde{\chi}^{ij}(n)\tilde{\chi}^{ij}(n)^T | \gamma \in \mathbb{U}^{ij}\}$ . Note that  $\tilde{\epsilon}_M^{ij}(0) = \tilde{\mathbf{w}}^{ij}(0) - \tilde{\mathbf{w}}_{opt}^{ij}$  and  $\mathbf{w}^{ij}(0) = \mathbf{w}(0)$  is a deterministic term. The conditional expectation for the second term can be obtained as

$$\begin{aligned}
& E_\gamma \left\{ E_{v,x} \left\{ \sum_{m=0}^{n-1} \tilde{\mathbf{W}}^{ij}(n, m) \tilde{\chi}^{ij}(m) \tilde{v}^{ij}(m) \right\} \right\} \\
&= E_\gamma \left\{ E_{v,x} \left\{ \sum_{m=0}^{n-1} \tilde{\mathbf{W}}^{ij}(n, m) \hat{\mathbf{B}}^i \tilde{\nu}^{ij}(i) \right\} \right\} \\
&= E_{v,x} \left\{ \sum_{m=0}^{n-1} \tilde{\mathbf{W}}^{ij}(n, m) \right\} \frac{\hat{\mathbf{B}}^i \tilde{\gamma}^{ij}}{N}.
\end{aligned} \tag{4.112}$$

The conditional expectation for the third term can be obtained as

$$\begin{aligned}
& E_\gamma \left\{ E_{v,x} \left\{ \sum_{m=0}^{n-1} \tilde{\mathbf{W}}^{ij}(n, m) \frac{1}{N} \tilde{\chi}^{ij}(m) \tilde{\chi}^{ij}(m)^T \mathbf{R}^{-1} \hat{\mathbf{B}}^i \tilde{\gamma}^{ij} \right\} \right\} \\
&= E_{v,x} \left\{ \sum_{m=0}^{n-1} \tilde{\mathbf{W}}^{ij}(n, m) \hat{\mathbf{B}}^i \mathbf{R}(m) [\hat{\mathbf{B}}^i]^T \mathbf{R}^{-1} \hat{\mathbf{B}}^i \frac{\tilde{\gamma}^{ij}}{N} \right\} \\
&\simeq E_{v,x} \left\{ \sum_{m=0}^{n-1} \tilde{\mathbf{W}}^{ij}(n, m) \right\} \hat{\mathbf{B}}^i E_x \{ \mathbf{R}(m) \} \mathbf{R}^{-1} \frac{\tilde{\gamma}^{ij}}{N} \\
&= E_{v,x} \left\{ \sum_{m=0}^{n-1} \tilde{\mathbf{W}}^{ij}(n, m) \right\} \hat{\mathbf{B}}^i \frac{\tilde{\gamma}^{ij}}{N}
\end{aligned} \tag{4.113}$$

where the independence between  $\widetilde{\mathbf{W}}^{ij}(n, m)$  and  $\mathbf{R}(m)$  is assumed. Combining the expectation terms through (4.111)-(4.113) the weight error mean vector conditioned on  $\gamma$  and  $\rho$  is given by

$$\tilde{\epsilon}_M^{ij}(n) = \left(\mathbf{I} - \mu \tilde{\mathbf{Q}}^{ij}\right)^n \tilde{\epsilon}_M^{ij}(0). \quad (4.114)$$

It has to be noted that in (4.114) the evaluation of  $\tilde{\mathbf{Q}}^{ij}$  varies for different  $\mathbb{U}^{ij}$  as expressed by

$$\tilde{\mathbf{Q}}^{ij} = \begin{cases} \mathbf{R}_+ = \frac{1}{N} \begin{bmatrix} 1 & +\rho \\ +\rho & 1 \end{bmatrix}, \{ij\} = \{11, 22, 31, 42\} \\ \mathbf{R}_- = \frac{1}{N} \begin{bmatrix} 1 & -\rho \\ -\rho & 1 \end{bmatrix}, \{ij\} = \{12, 21, 32, 41\}. \end{cases} \quad (4.115)$$

Let  $\tilde{\epsilon}_M^{ij}(n) = [\tilde{\epsilon}_{M,1}^{ij}(n), \tilde{\epsilon}_{M,2}^{ij}(n)]^T$ . The weight error mean for the first user conditioned on only the correct decision and  $\rho$  is represented by

$$\epsilon_{M,1}^c(n) = \frac{1}{P_{\mathbb{C}_1}} \sum_{\mathbb{C}_1} \tilde{\epsilon}_{M,1}^{ij}(n) P_{ij} \quad (4.116)$$

where  $\mathbb{C}_1$  is given in (4.86). Similarly the weight error mean for the second user is represented as

$$\epsilon_{M,2}^c(n) = \frac{1}{P_{\mathbb{C}_2}} \sum_{\mathbb{C}_2} \tilde{\epsilon}_{M,2}^{ij}(n) P_{ij} \quad (4.117)$$

where  $\mathbb{C}_2$  is given in (4.91). Then the averaged weight error mean for correct decision over  $\rho$  can be obtain by

$$\begin{aligned} E\{\epsilon_i^c(n)\} &= E_\rho\{\tilde{\epsilon}_{M,i}^c(n)\} \\ &= \frac{\sum_\rho \tilde{\epsilon}_{M,i}^c(n) P_\rho P_{\mathbb{C}_i}}{\sum_\rho P_\rho P_{\mathbb{C}_i}} \end{aligned} \quad (4.118)$$

for  $i = 1, 2$ .

## § 4.4 Approximate Analysis for $K$ -user Scenario

In prior two sections, we have derived the exact analytical results for the optimal weight, the weight error mean, and the weight error variance for the single-user case, and the optimal



weights, the weight error means for the two-user case. In this section, we will extend the results to accommodate the general  $K$ -user case. Due to the difficulty of the problem, we will seek approximate rather exact solutions. In most cases, we will only give the result for correct decision (denoted with superscript ‘c’) and omit the derivation of erroneous decision.

First note that the received despread signal of each user composes of three parts, i.e., the desired signal, the MAI, and noise. The key to reduce the analysis complexity is to consider each user individually and treat all other  $K - 1$  interfering users as an equivalent user. By doing so, we can transfer the general  $K$ -user case to a two-user case. In other words, we let

$$\sum_{j \neq k} a_j b_j \rho_{jk} \simeq a_I b_I \rho \quad (4.119)$$

where  $b_I \in \{\pm 1\}$  and  $a_I = (\sum_{j \neq 1} a_j^2)^{1/2}$ . Here,  $a_I$  represent the equivalent amplitude and  $\rho$  the equivalent correlation. Using this model, we can have equivalent interference second order statistics. Also note that  $b_I$  is virtual and we do not need its actual values in derivation. In the following analysis, we assume that the desired user is the first user. Thus, the matched filter output is then

$$y_1^{(1)} \simeq a_1 b_1 + a_I b_I \rho + \gamma_1. \quad (4.120)$$

Thus, we can keep the computational complexity comparable to the two-user case.

#### § 4.4.1 Optimal Weight Analysis

We use two methods to approximate optimal weights. The first method directly uses the two-user model in (4.120). All we have to do is to let the amplitude of the second user be equal to  $a_I = (\sum_{j \neq 1} a_j^2)^{1/2}$ ; optimal weights can be obtained readily. In what follows the similar derivation for optimal weights applies, which is termed as  $\mathbf{w}_{opt}^c$  for correct decision and  $\mathbf{w}_{opt}^e$  for erroneous decision. The associated equations are listed below with the same noise integration ranges  $\mathbb{U}^{ij}$  in Table 4.1. The conditional optimal weights given  $\rho$  and  $\mathbb{U}^{ij}$  is represented as

$$\tilde{\mathbf{w}}_{opt}^{ij} = \mathbf{A} \hat{\mathbf{B}}^i \mathbf{b}^j + \frac{1}{N} \mathbf{R}^{-1} \hat{\mathbf{B}}^i E_{\gamma} \{ \tilde{\gamma}^{ij} \} \quad (4.121)$$

where  $\mathbf{A} = \text{diag}\{a_1, a_I\}$ . The optimal weights for correct decision of the first user given  $\rho$  is similar to (4.88) as expressed by

$$\check{w}_{opt,1}^c = \frac{1}{P_{\mathbb{C}_1}} \sum_{\mathbb{C}_1} \check{w}_{opt,1}^{ij} P_{ij} \quad (4.122)$$

with  $\mathbb{C}_1$  given in (4.86). The approximate optimal weight of correct decision analogous to (4.93) is obtained by

$$w_{opt,1}^c = E_\rho\{\check{w}_{opt,1}^c\} = \frac{\sum_\rho \check{w}_{opt,1}^c P_\rho P_{\mathbb{C}_1}}{\sum_\rho P_\rho P_{\mathbb{C}_1}} \quad (4.123)$$

with  $P_\rho$  defined in (4.94). This method is referred to as the optimal weight approximation one (OWA1). Similar procedures for  $w_{opt,1}^e$  can be easily repeated.

The second method simplifies the result one step further. In the preceding optimal weight approximation, it is necessary to derive the optimal weights  $\check{w}_{opt}^{ij}$  according to different noise subspaces  $\mathbb{U}^{ij}$ . It can be seen that the optimal weights of the two-user case are coupled with each other. For this reason the optimal solution for the first user requires bit decision information pertaining to the second user, thus the long list of Table 4.1 results. If we can ignore some coupling relationship, the optimal weight can be calculated more easily. Here we ignore the decision coupling between two users. In other words, the first user decision is independent of the second user decision. In this case, the decision patterns are degenerated into two,  $b_1 = \hat{b}_1$  and  $b_1 \neq \hat{b}_1$ . We denote these patterns as the fifth and the sixth pattern. For each decision pattern, we have two bit patterns, i.e.,  $b_1 = b_I$  and  $b_1 \neq b_I$ . The noise space can be partitioned into two subsets accordingly. Thus, for  $b_1 = \hat{b}_1$ , we have two sets as ( $b_1=1$ )

$$\begin{aligned} \mathbb{U}^{51} &= \mathbb{U}^{11} \cup \mathbb{U}^{21}, \quad b_1 = b_I \\ \mathbb{U}^{52} &= \mathbb{U}^{12} \cup \mathbb{U}^{22}, \quad b_1 \neq b_I. \end{aligned} \quad (4.124)$$

Hence the conditional optimal weight on  $\mathbb{U}^{5j}$  for correct decision is obtained to be

$$\begin{aligned} \check{w}_{opt,1}^{5j} &= E_\gamma\{\check{w}_{opt,1}^{5j}\} \\ &= a_1 + E_\gamma\{\tilde{\gamma}_1^{5j}\}, \quad j = 1, 2. \end{aligned} \quad (4.125)$$

Note that (4.125) only involves one-dimensional integration instead of two-dimensional integration. Then the optimal weight for correct decision of the first user conditioned on  $\rho$  in (4.122) can be approximated as

$$\tilde{w}_{opt,1}^c = \frac{\tilde{w}_{opt,1}^{51} P_{51} + \tilde{w}_{B,1}^{52} P_{52}}{P_{\mathbb{B}}} \quad (4.126)$$

where the noise integration region and the corresponding occurrence probabilities are defined as

$$\mathbb{B} = \mathbb{U}^{51} \cup \mathbb{U}^{52} \quad (4.127)$$

$$P_{\mathbb{B}} = P_{51} + P_{52}. \quad (4.128)$$

The optimal weight is then

$$w_{opt,1}^c = E_{\rho}\{\tilde{w}_{opt,1}^c\} = \frac{\sum_{\rho} \tilde{w}_{opt,1}^c P_{\rho} P_{\mathbb{B}}}{\sum_{\rho} P_{\rho} P_{\mathbb{B}}} \quad (4.129)$$

where  $P_{\rho}$  is defined in (4.94). This optimal weight approximation method is referred to as the optimal weight approximation two (OWA2).

#### § 4.4.2 Weight Error Mean Analysis

We also develop two methods for weight error mean approximation. The first method follows the same derivation of the mean weight error vector for the two-user case. The weight error mean for the  $K$ -user case can be obtained through the direct substitution of  $a_I$ , and are referred to as  $E\{\epsilon_1^c(n)\}$  and  $E\{\epsilon_1^e(n)\}$  for correct and erroneous decision, respectively. The weight error mean vector given  $\rho$  and  $\mathbb{U}^{ij}$  are represented from (4.114) as

$$\check{\epsilon}_M^{ij}(n) = \left(\mathbf{I} - \mu \tilde{\mathbf{Q}}^{ij}\right)^n (\mathbf{w}(0) - \tilde{\mathbf{w}}_{opt}^{ij}) \quad (4.130)$$

where the optimal weights in (4.130) for the  $K$ -user case can be  $\tilde{\mathbf{w}}_{opt}^{ij}$  if the OWA1 is used or  $\tilde{\mathbf{w}}_{opt}^{5j}$  if the OWA2 is used. The conditional weight error mean given  $\rho$  for correct decision is given by

$$\check{\epsilon}_{M,1}^c(n) = \frac{1}{P_{\mathbb{D}}} \sum_{\mathbb{D}} \check{\epsilon}_{M,1}^{ij}(n) P_{ij} \quad (4.131)$$

where the union of noise subsets  $\mathbb{D}$  is  $\mathbb{C}_1$  in (4.86) for the OWA1 or  $\mathbb{B}$  in (4.127) for the OWA2. Also  $P_{\mathbb{D}}$  is  $P_{\mathbb{C}_1}$  for the OWA1 or  $P_{\mathbb{B}}$  for the OWA2. Finally, the averaged weight error mean is obtained as

$$\begin{aligned}\epsilon_{M,1}^c(n) &= E_{\rho}\{\check{\epsilon}_{M,1}^c(n)\} \\ &= \frac{\sum_{\rho} \check{\epsilon}_{M,1}^c(n) P_{\rho} P_{\mathbb{D}}}{\sum_{\rho} P_{\rho} P_{\mathbb{D}}}.\end{aligned}\quad (4.132)$$

We call this approximation as the weight error mean approximation 1 (WEMA1).

The second method further explores simpler approximation. Note that  $\check{\epsilon}_{M,1}^c(n)$  differs according to different  $\rho$  values. From (4.94), we can find that most of the correlation values fall in the vicinity of  $\rho = 0$ . We would like to simplify the derivation of  $\epsilon_{M,1}^c(n)$  by  $\check{\epsilon}_{M,1}^c(n)$  for  $\rho \simeq 0$ . Expanding (4.116) we have

$$\check{\epsilon}_{M,1}^c(n) = \frac{1}{P_{\mathbb{C}_1}} \left\{ \check{\epsilon}_{M,1}^{11}(n) P_{11} + \check{\epsilon}_{M,1}^{12}(n) P_{12} + \check{\epsilon}_{M,1}^{21}(n) P_{21} + \check{\epsilon}_{M,1}^{22}(n) P_{22} \right\}. \quad (4.133)$$

It should be noted that when  $\rho \rightarrow 0$  (from Table 4.1),

$$\begin{aligned}P_{11} &= P_{12} \\ P_{21} &= P_{22}.\end{aligned}\quad (4.134)$$

Thus we have

$$\epsilon_{M,1}^c(n) = \frac{1}{P_{\mathbb{C}_1}} \left\{ P_{11} (\check{\epsilon}_{M,1}^{11}(n) + \check{\epsilon}_{M,1}^{12}(n)) + P_{21} (\check{\epsilon}_{M,1}^{21}(n) + \check{\epsilon}_{M,1}^{22}(n)) \right\}. \quad (4.135)$$

We rewrite the first summation term in (4.135) of  $\check{\epsilon}_{M,1}^{ij}(n)$  in vector forms using (4.114) and (4.115) as

$$\begin{aligned}\check{\epsilon}_M^{11}(n) + \check{\epsilon}_M^{12}(n) &= (\mathbf{I} - \mu \mathbf{R}_+)^n \check{\epsilon}_M^{11}(0) + (\mathbf{I} - \mu \mathbf{R}_-)^n \check{\epsilon}_M^{12}(0) \\ &= (\mathbf{I} - \mu \mathbf{R}_+)^n (\mathbf{w}^{11}(0) - \check{\mathbf{w}}_{opt}^{11}) + (\mathbf{I} - \mu \mathbf{R}_-)^n (\mathbf{w}^{12}(0) - \check{\mathbf{w}}_{opt}^{12}).\end{aligned}\quad (4.136)$$

Remember that  $\mathbf{w}^{11}(0) = \mathbf{w}^{12}(0) = \mathbf{w}(0)$ . Note that in Table 4.1 that when  $\rho \rightarrow 0$ ,  $\mathbb{U}^{11}$  and  $\mathbb{U}^{12}$  are symmetrical with respect to the  $x$ -axis. In a consequence we have  $\check{w}_{opt,1}^{11} = \check{w}_{opt,1}^{12}$  and

$\check{w}_{opt,2}^{11} = -\check{w}_{opt,2}^{12}$ . Also note that

$$\begin{aligned} (\mathbf{I} - \mu \mathbf{R}_+)^n &\simeq \begin{bmatrix} (1 - \mu/N)^n & \Delta \\ \Delta & (1 - \mu/N)^n \end{bmatrix} \\ (\mathbf{I} - \mu \mathbf{R}_-)^n &\simeq \begin{bmatrix} (1 - \mu/N)^n & -\Delta \\ -\Delta & (1 - \mu/N)^n \end{bmatrix} \end{aligned} \quad (4.137)$$

where  $\Delta \ll (1 - \mu/N)^n$ . Thus we can express the first user component in (4.136) as

$$\begin{aligned} \check{\epsilon}_{M,1}^{11}(n) + \check{\epsilon}_{M,1}^{12}(n) &\simeq 2 \{ (1 - \mu/N)^n (w_1(0) - \check{w}_{opt,1}^{11}) + \Delta (w_2(0) - \check{w}_{opt,1}^{12}) \} \\ &\simeq 2(1 - \mu/N)^n \check{\epsilon}_{M,1}^{11}(0). \end{aligned} \quad (4.138)$$

Similarly we obtain

$$\begin{aligned} \check{\epsilon}_{M,1}^{21}(n) + \check{\epsilon}_{M,1}^{22}(n) &\simeq 2(1 - \mu/N)^n (w_1(0) - \check{w}_{opt,1}^{21}) \\ &= 2(1 - \mu/N)^n \check{\epsilon}_{M,1}^{21}(0). \end{aligned} \quad (4.139)$$

Combining with (4.135), we have the approximation

$$\begin{aligned} \check{\epsilon}_{M,1}^c(n) &= \frac{2(1 - \mu/N)^n}{P_{C_1}} [\check{\epsilon}_{M,1}^{11}(0)P_{11} + \check{\epsilon}_{M,1}^{21}(0)P_{21}] \\ &\simeq (1 - \mu/N)^n \check{\epsilon}_{M,1}^c(0) \\ &= (1 - \mu/N)^n (w_1^c(0) - \check{w}_{opt,1}^c) \end{aligned} \quad (4.140)$$

where  $\check{\epsilon}_{M,1}^c(0) = \frac{2}{P_{C_1}} [\check{\epsilon}_{M,1}^{11}(0)P_{11} + \check{\epsilon}_{M,1}^{21}(0)P_{21}]$  is assumed. The final weight error mean is obtained as

$$\begin{aligned} \epsilon_{M,1}^c(n) &= E_\rho \{ \check{\epsilon}_{M,1}^c(n) \} \\ &\simeq E_\rho \{ \check{\epsilon}_{M,1}^c(n) | \rho \simeq 0 \} \\ &\simeq (1 - \mu/N)^n (w_1^c(0) - w_{opt,1}^c) \end{aligned} \quad (4.141)$$

Note that  $w_{opt,1}^c$  can be that in (4.123) for the OWA1 or in (4.129) for the OWA2. We call this the weight error mean approximation 2 (WEMA2).

### § 4.4.3 Weight Error Variance Analysis

The exact analysis for the weight error variance is difficult even for the two-user case. Thus the analytical result in the single-user case is used to approximate weight error variance in the  $K$ -user scenario. We rewrite (4.56) here as

$$\epsilon_V^c(n) = \delta_V^c + \varepsilon_V^c(n) \quad (4.142)$$

As previously, we first treat the  $K - 1$  user signals as one equivalent interference. Comparing (4.120) with (4.12), we found that the desired user output in this two-user environment has one extra term which is  $a_I b_I \rho$ . As we did in the derivation for the OWA2, we ignore the decision coupling relationship. As a result, the second user can only affect the conditional optimal weight. In other words,  $\varepsilon_V^c(n)$  remain the same for the  $K$ -user case. Only will  $\delta_V^c(n)$  be changed. Note that  $\delta_V^c(n)$  is a function of  $\rho$  and can be obtained by  $\delta_V^c(n) = E_\rho\{\check{\delta}_V^c(n)\}$  where

$$\check{\delta}_V^c(n) = \frac{\check{\delta}_V^{51}(n)P_{51} + \check{\delta}_V^{52}(n)P_{52}}{P_{\mathbb{B}}}. \quad (4.143)$$

Then the term  $\check{\delta}_V^{5j}(n)$  is obtained as

$$\check{\delta}_V^{5j}(n) = (1 - \alpha^n)^2 E_\gamma \left\{ (\tilde{w}_{opt,1}^{5j} - \check{w}_{opt,1}^{5j})^2 \right\} \quad (4.144)$$

where the expectation term with analogy to (4.57) is given as

$$\begin{aligned} & E_\gamma \left\{ (\tilde{w}_{opt,1}^{5j} - \check{w}_{opt,1}^{5j})^2 \right\} \\ = & \begin{cases} E_\gamma \left\{ (a_1 + a_I \rho + \gamma_1 - \tilde{w}_{opt,1}^{5j})^2 | \gamma_1 > -(a_1 + a_I \rho) \right\} & j = 1 \\ E_\gamma \left\{ (a_1 - a_I \rho + \gamma_1 - \tilde{w}_{opt,1}^{5j})^2 | \gamma_1 > -(a_1 - a_I \rho) \right\} & j = 2. \end{cases} \end{aligned} \quad (4.145)$$

Finally the averaged  $\delta_V^c(n)$  is obtained as

$$\delta_V^c(n) = \frac{\sum_\rho \check{\delta}_V^c(n) P_\rho P_{\mathbb{B}}}{\sum_\rho P_\rho P_{\mathbb{B}}}. \quad (4.146)$$

The weight error power for correct decision is expressed as

$$\begin{aligned}
E \{ [\tilde{\epsilon}_1^c(n)]^2 \} &= E \left\{ [\tilde{w}_1^c(n) - w_{opt,1}^c]^2 \right\} \\
&= [\epsilon_{M,1}^c(n)]^2 + \epsilon_V^c(n) \\
&= \alpha^{2n} [\epsilon_{M,1}^c(0)]^2 + \delta_V^c(n) + \epsilon_V^c(n)
\end{aligned} \tag{4.147}$$

where  $\epsilon_{M,1}^c(0)$  can be obtained from the WEMA1 or WEMA2. Similarly the weight error power for erroneous decision can be obtained.

#### § 4.4.4 Output MSE and BER

Since we have derived the approximate weight error power for the adapted weights corresponding to both correct and erroneous decisions, we can then calculate the output MSE and then BER. As mentioned in (4.10) that if the adapted weight of the  $k$ th users is  $a_k$  for  $b_k = \hat{b}_k$  or  $-a_k$  for  $b_k \neq \hat{b}_k$ , its interference to other users can be perfectly canceled. Thus, the MSE for the correct decision, denoted as  $\varpi_k^c(n)$ , introduced to other users when the weight obtained at time  $n$  is used for cancellation is

$$\begin{aligned}
\varpi_k^c(n) &= E \{ [\tilde{w}_k^c(n) b_k x_k(n) - a_k b_k x_k(n)]^2 \} \\
&= E \{ [\tilde{w}_k^c(n) - a_k]^2 \} / N.
\end{aligned} \tag{4.148}$$

As a result, the overall MSE, denoted as  $\varpi_k(n)$ , introduced to other users when the cancellation is performed is then

$$\varpi_k(n) = \frac{1}{N} \left\{ P_{c,k} E \{ [\tilde{w}_k^c(n) - a_k]^2 \} + P_{e,k} E \{ [\tilde{w}_k^e(n) + a_k]^2 \} \right\} \tag{4.149}$$

where  $P_{c,k}$  and  $P_{e,k}$  denote the probability of correct and that of erroneous decision in the first stage for the  $k$ th user, respectively. Note that these probabilities can be easily obtained using Gaussian approximation. Substituting the weight error power in (4.147) into (4.149), we can

obtain  $\varpi_k(n)$  as

$$\begin{aligned} \varpi_k(n) = & \frac{1}{N} \left\{ P_{c,k} \left\{ E \left\{ [\tilde{\epsilon}_k^c(n)]^2 \right\} + 2w_{M,k}^c(n) (w_{opt,k}^c - a_k) + a_k^2 - [w_{opt,k}^c]^2 \right\} \right. \\ & \left. + P_{e,k} \left\{ E \left\{ [\tilde{\epsilon}_k^e(n)]^2 \right\} + 2w_{M,k}^e(n) (w_{opt,k}^e + a_k) + a_k^2 - [w_{opt,k}^e]^2 \right\} \right\}. \end{aligned} \quad (4.150)$$

Note here that we extend our notations defined previously to the  $k$ th user. Assuming that the residual error resulting from imperfect interference cancellation is Gaussian distributed with zero mean and variance  $\varpi_k(N)$ , we can then obtain the BER for the  $k$ th user as

$$P(y_k^{(2)}) = \mathcal{Q} \left\{ \frac{a_k}{\sqrt{\sigma^2 + \sum_{j \neq k}^K \varpi_j(N)}} \right\}. \quad (4.151)$$

Note that the MSE at the end of adaptation is  $\varpi_k(N)$  and it is a function of the step size  $\mu$ . We can then use the numerical method to search for the optimal step size minimizing the MSE. Using the same idea, we can also obtain the optimal step size minimizing the BER. Since minimizing MSE is easier, we use that in later simulations.

## § 4.5 Simulation Results

In this section we report some simulation results to evaluate the validity of our analytical results. We consider an adaptive blind two-stage partial HPIC receiver using the LMS algorithm. We utilized the random codes as the spreading codes and the processing gain is set as  $N = 31$ . Only the AWGN channel was used throughout the simulations. For the first set of simulations, we compared theoretical optimal weights with empirical ones for various  $E_b/N_0$  ( $N_0/2 = \sigma^2$ ). Optimal weights for correct and erroneous decision were considered separately. Note that the channel gain was normalized to unity, i.e., as  $a_k = 1$  for all  $k$ . Thus all weights starting adaptation from  $w_k(0) = 1$ . Figure 4.2 shows the results for a two-user case, which includes exact analytical optimal weights in (4.93), those obtained using the OWA2 in (4.129), and those obtained empirically. It can be seen that both the exact and approximate optimal weights agree



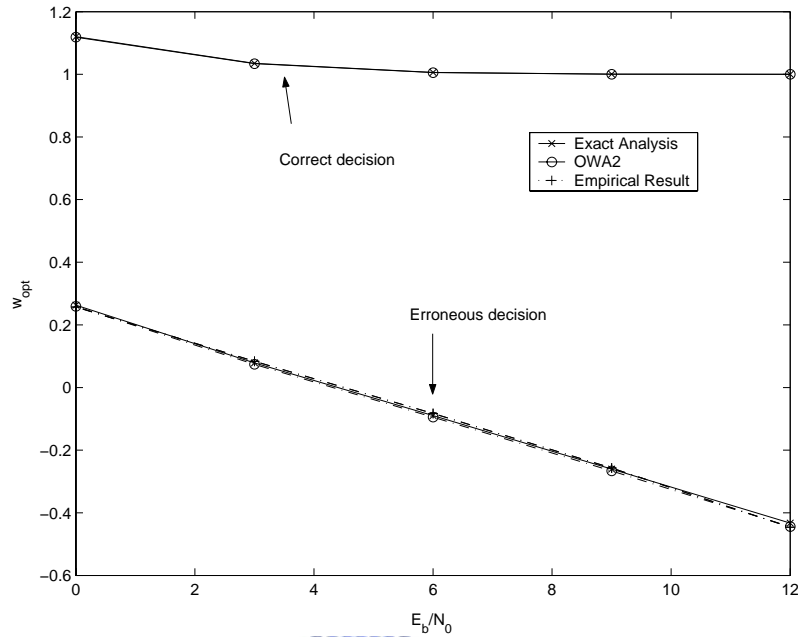


Figure 4.2: Optimal weight comparison for two power-balanced users.

with the empirical ones very well. As depicted in the figure, the optimal weights for correct decision are almost the same as the channel gain, while the weights for erroneous decision is not; its actual value depends on noise variance. The larger the  $E_b/N_0$  ratio, the closer the optimal weight to  $-1$ . We also give optimal weights for 5 and 15 users (with various  $E_b/N_0$ ) in Fig. 4.3 and Fig. 4.4, respectively. In these figures, the results for the OWA1 (using (4.123)) and the OWA2 (using (4.129)) are shown simultaneously. We can see that although these approximates are performed based on the two-user model, the results are very close to the true optimums. From Figure 4.2-Figure 4.4, we can observe that when the  $E_b/N_0$  and the number of users vary, the optimal weights for correct decision keep very close to the channel gains which is one, while those for erroneous decision vary. Also note that the performances of the two approximations are very similar. Since the OWA2 is simpler, it is then desirable to use that whenever necessary.

We next consider the weight convergence of the LMS algorithm. Figure 4.5 presents the analytical mean weights along with the empirical mean weights for a two-user scenario. The powers of these two users are equal and  $E_b/N_0 = 6$  dB. The normalized step size is chosen as

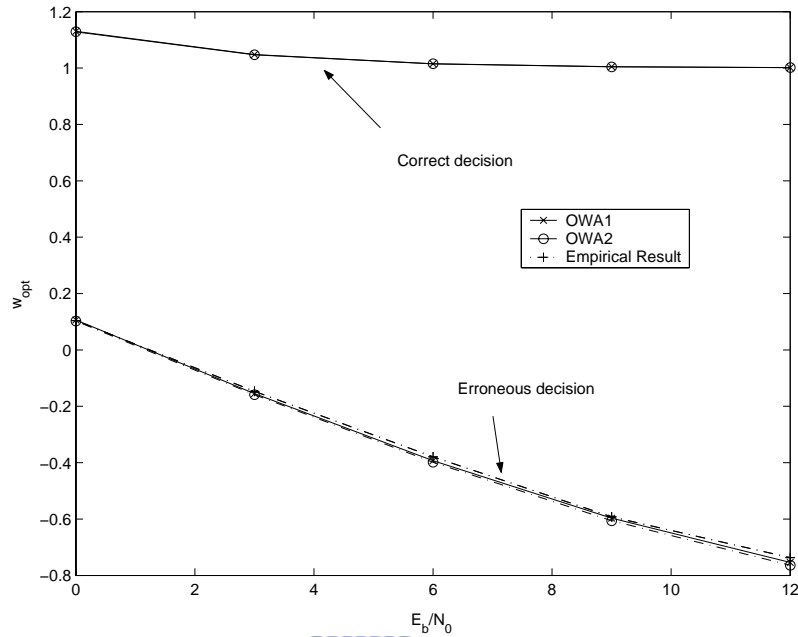


Figure 4.3: Optimal weight comparison for five power-balanced users.

$\mu_0 = \mu/N = 0.02$ . The exact analysis in (4.118) and the WEMA2 in (4.141) with the OWA2 are evaluated. In the figure, we can observe that both analytical results match with the empirical mean weights quit well. Similar comparison for 5 and 15 power-balanced users with  $E_b/N_0 = 6$  dB and  $\mu_0 = 0.02$  are also shown in Figure 4.6 and Figure 4.7, respectively. The WEMA1 in (4.132) with the OWA1 is compared to WEMA2 with the OWA2. We can see that the analytical results are more accurate for the 5-user case. For the 15-user case, there is some discrepancy between analytical and empirical results. From above simulation results, we can conclude that the WEMA2 with the OWA2 is suffice to give satisfactory results. This combination will render less computational complexity. The weight error power comparison for the two-user case with  $E_b/N_0 = 6$  dB and  $\mu_0 = 0.02$  is given in Figure 4.8. It is obvious that the analytic result performs close to simulated results. Also note that the weight error power incurred from correct decision is smaller than that form erroneous decision. This is because the weights for erroneous decision converges slower. The similar phenomenon can be observed when the user number is larger. In Figures 4.9 and 4.10, the weight error power for 5 and 15 users are examined

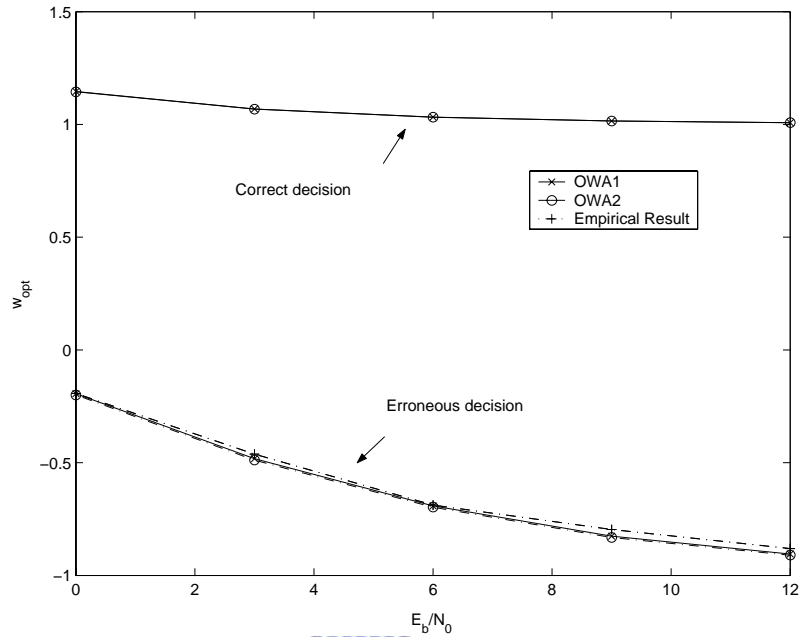


Figure 4.4: Optimal weight comparison for 15 power-balanced users.

( $E_b/N_0 = 6$  dB and  $\mu_0 = 0.02$ ). As we can see, the analytic results are still accurate even for the erroneous decision of the 15-user case where only an estimation error about 20% is produced. Finally, we present the results for step size optimization. Figure 4.11 gives the step size minimizing MSE using (4.150). The figure reveals that the analytically optimized step size is more accurate in low capacity systems. This is reasonable since the approximate analysis is based on the single-user and two-user cases. We also give the BER comparison for the second stage output with different user numbers in Figure 4.12. From the figure, we observe that the analytical and empirical results are similar for low to moderate  $E_b/N_0$ .

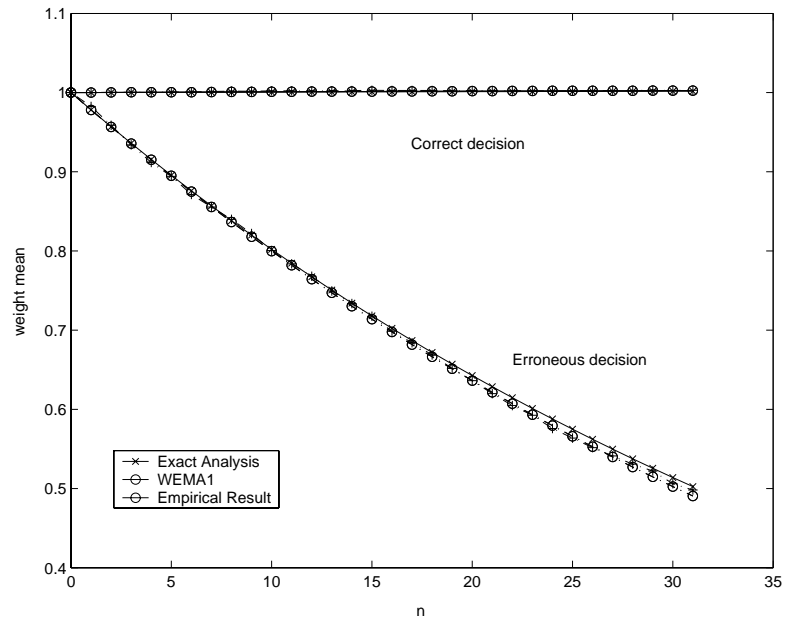


Figure 4.5: Weight mean comparison for two power-balanced users ( $\mu_0 = 0.02$ , and  $E_b/N_0 = 6$  dB).

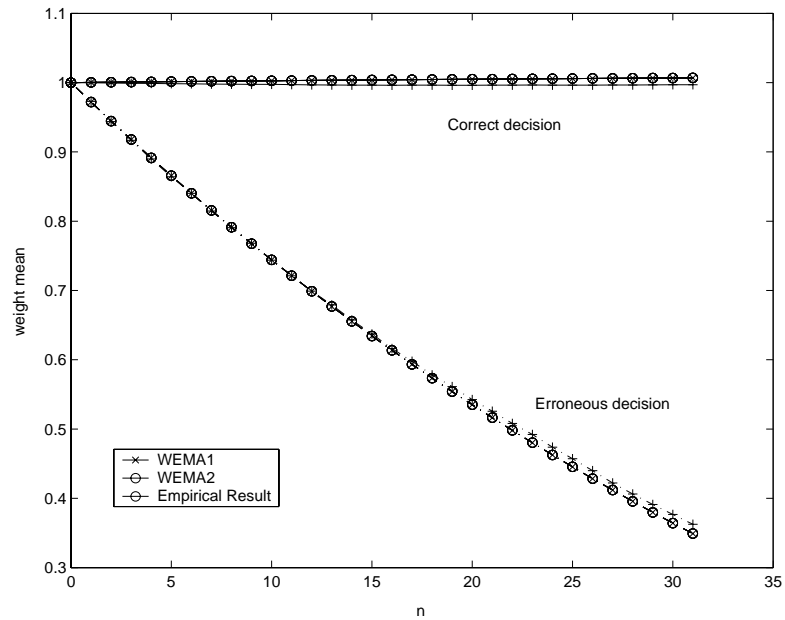


Figure 4.6: Weight mean comparison for five power-balanced users ( $\mu_0 = 0.02$ , and  $E_b/N_0 = 6$  dB).

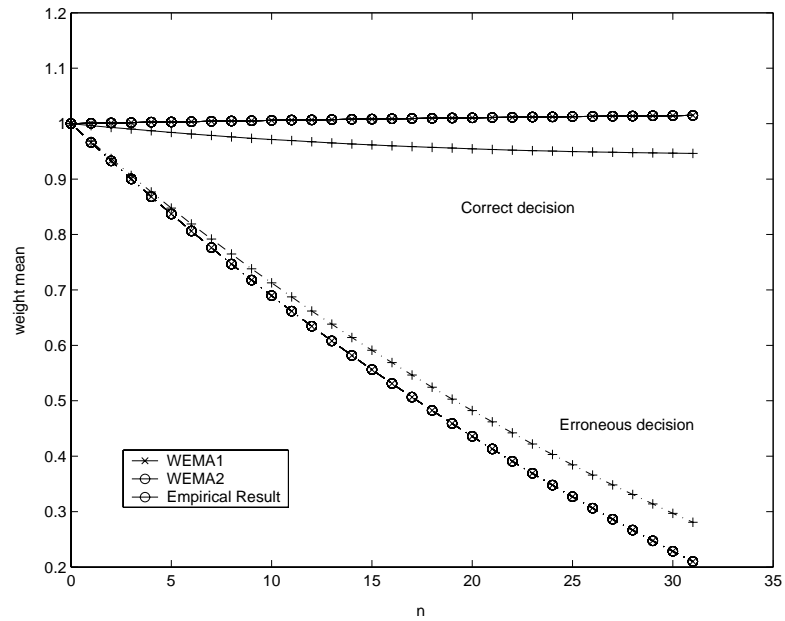


Figure 4.7: Weight mean comparison for 15 power-balanced users ( $\mu_0 = 0.02$ , and  $E_b/N_0 = 6$  dB).

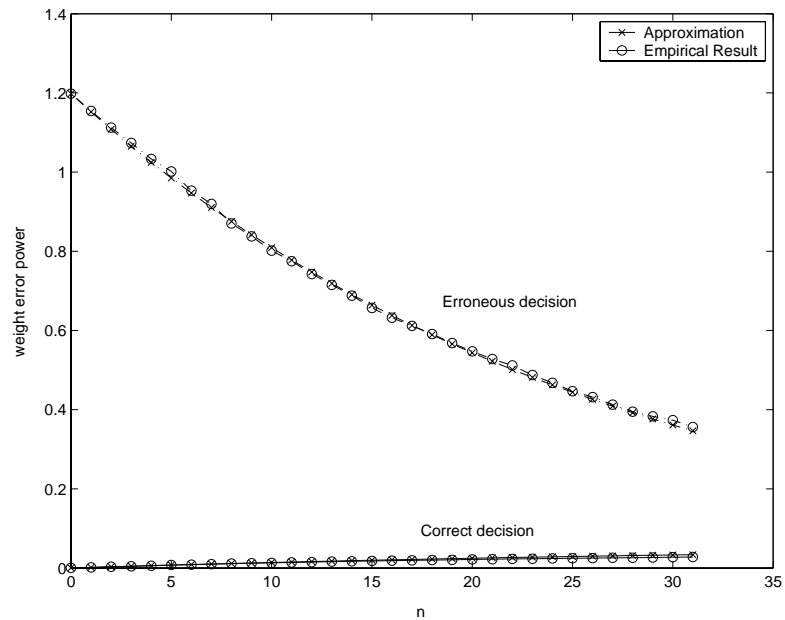


Figure 4.8: Weight error power comparison for two power-balanced users ( $\mu_0 = 0.02$ , and  $E_b/N_0 = 6$  dB).

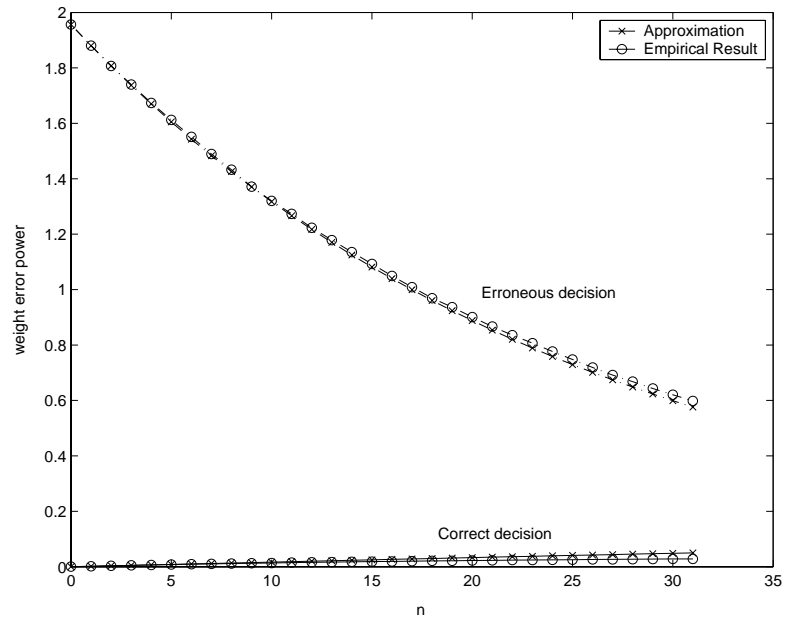


Figure 4.9: Weight error power comparison for five power-balanced users ( $\mu_0 = 0.02$ , and  $E_b/N_0 = 6$  dB).

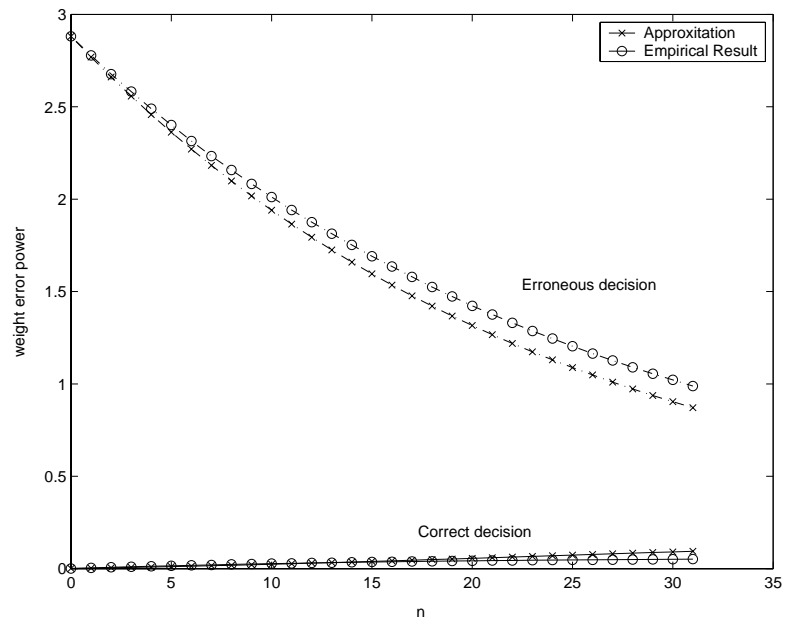


Figure 4.10: Weight error power comparison for 15 power-balanced users ( $\mu_0 = 0.02$ , and  $E_b/N_0 = 6$  dB).

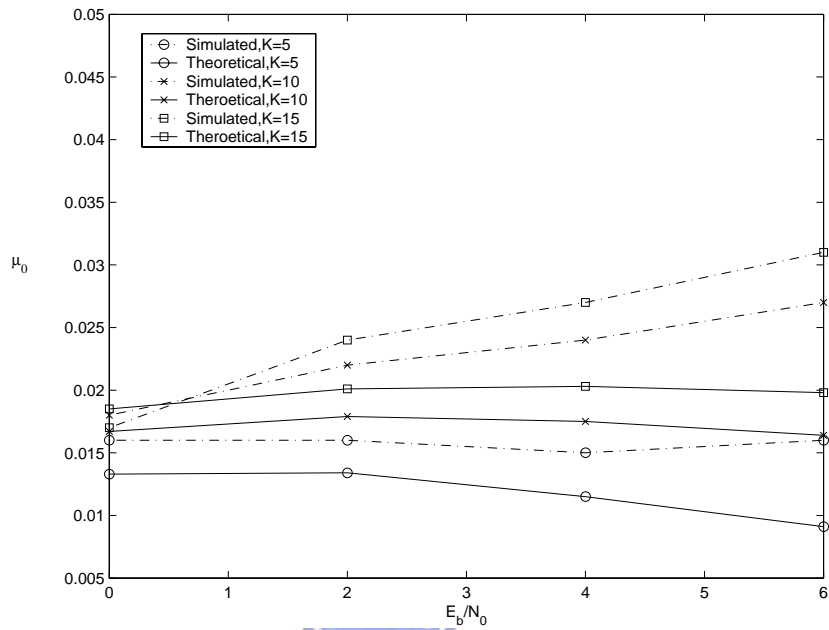


Figure 4.11: Optimal step-size comparison for different user numbers.

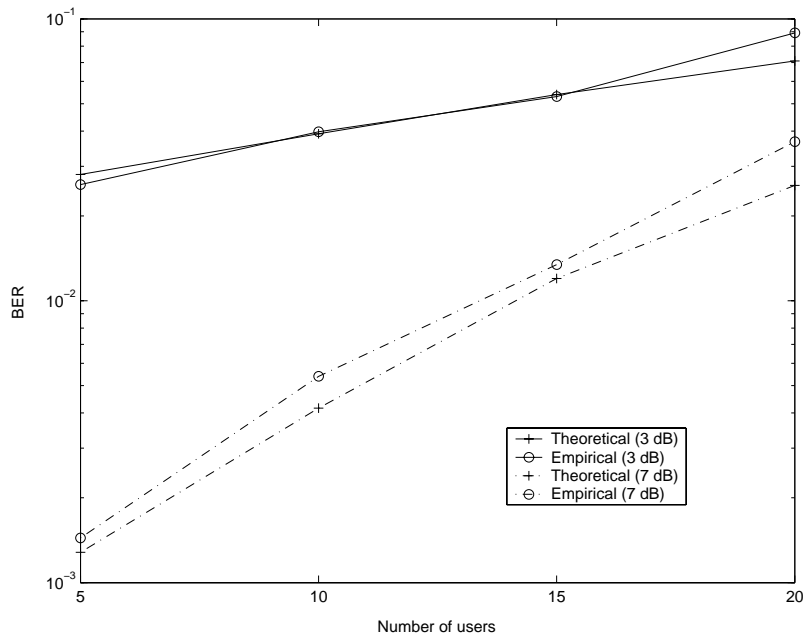



Figure 4.12: Second-stage BER comparison for power-balanced cases ( $\mu_0 = 0.02$ ).

## Chapter 5

# Improved Adaptive Blind Partial HPIC Receivers



This chapter proposes improved algorithms for adaptive blind partial HPIC receivers. The basic idea is to reduce the excess MSE introduced by the LMS algorithm. We use two procedures to implement this idea. The first one is developed to reduce the number of weights in the LMS algorithm. It is known that the excess MSE is proportional to the number of tap weights adapted. If the number of weights can be reduced, the excess MSE can be reduced. The second procedure is used to further process the adapted weights such that the weight variance can be reduced. Section 1 describes the conventional adaptive blind partial HPIC receiver for completeness. In Section 2, we then detail the proposed enhancement algorithm. In Section 3, we analyze the performance of the proposed algorithm, which include the output MSE and the corresponding BER. Finally, we report simulation results in Section 4.



## § 5.1 Adaptive Blind Partial HPIC Receivers

Consider a synchronous system operated in a AWGN channel. The received signal in a certain bit interval can be expressed as

$$\begin{aligned} r(n) &= \sum_{k=1}^K s_k(n) + v(n) \\ &= \sum_{k=1}^K a_k b_k x_k(n) + v(n), \quad 0 \leq n \leq N-1 \end{aligned} \quad (5.1)$$

where  $a_k$  and  $b_k$  are the  $k$ th user's amplitude and data bit,  $x_k(n)$  denotes its signature sequence, and  $N$  is the processing gain  $N$ . The matched filter output, which is the first stage output, can be represented as

$$\begin{aligned} y_k^{(1)} &= \sum_{n=0}^{N-1} r(n) x_k(n) \\ &= a_k b_k + \sum_{j \neq k} a_j b_j \rho_{jk} + \gamma_k. \end{aligned} \quad (5.2)$$

Let  $\hat{r}_k^{(i)}(n)$  denote an interference-subtracted signal for User  $k$  in the  $i$ th stage. Then,

$$\hat{r}_k^{(i)}(n) = r(n) - \sum_{j \neq k} C_j^{(i)} \cdot \hat{s}_j^{(i)}(n) \quad (5.3)$$

where  $C_j^{(i)}$  denote the PCFs for the  $j$ th user in the  $i$ th stage are and  $\hat{s}_j^{(i)}(n)$  is the corresponding interference estimate. We can obtain the estimate as

$$\hat{s}_j^{(i)}(n) = a_j \hat{b}_j^{(i-1)} \cdot x_j(n) \quad (5.4)$$

where  $\hat{b}_j^{(1)} = \text{sgn}[y_j^{(1)}]$ . Thus, the output signal in Stage  $i$  is then

$$y_k^{(i)} = \sum_{n=0}^{N-1} \hat{r}_k^{(i)}(n) x_k(n). \quad (5.5)$$

Finally, we can obtain the  $i$ th stage detected bit as

$$\hat{b}_k^{(i)} = \text{sgn}[y_k^{(i)}]. \quad (5.6)$$

A more compact form for the despread signal is given by

$$y_k^{(i)} = y_k^{(1)} - \sum_{j \neq k} C_j^{(i)} a_j \hat{b}_j^{(i-1)} \rho_{jk}. \quad (5.7)$$

There is another partial HPIC receiver good for the power-balanced scenario. It uses a decoupled structure [30] and has the output as

$$y_k^{(i)} = C^{(i)} \left( y_k^{(1)} - \sum_{j \neq k} a_j \hat{b}_j^{(i-1)} \rho_{jk} \right) + (1 - C^{(i)}) y_k^{(i-1)}. \quad (5.8)$$

As we can see, all PCFs in the same stage are equal. Comparing (5.7) with (5.8), we can readily find that both expressions are equivalent for the second stage. For higher stages, both structures are different. Obviously, the optimal PCFs may differ for these two partial HPIC. It has been shown that the algorithm of (5.8) performs better than that in (5.7) in power-balanced systems [68]. Thus, we use (5.8) as the conventional partial HPIC whenever comparison is necessary.

As mentioned, optimal PCFs can be obtained using the adaptive blind partial HPIC approach. We first define the error signal as

$$e^{(i)}(n) = r(n) - \hat{r}^{(i)}(n) \quad (5.9)$$

where  $\hat{r}^{(i)}(n)$  is the regenerated received signal and it is expressed as

$$\hat{r}^{(i)}(n) = \sum_k w_k^{(i)}(n) \hat{b}_k^{(i-1)} x_k(n). \quad (5.10)$$

Here,  $w_k^{(i)}(n)$  is the adapted weight for the  $k$ th user in the  $i$ th stage. Consequently, we define the MSE as

$$J^{(i)}(n) = E \left[ (r(n) - \hat{r}^{(i)}(n))^2 \right]. \quad (5.11)$$

Using the stochastic gradient descent method, we can obtain the weight update equation as

$$w_k^{(i)}(n+1) = w_k^{(i)}(n) + \mu^{(i)} \chi_k^{(i)}(n) e^{(i)}(n) \quad (5.12)$$

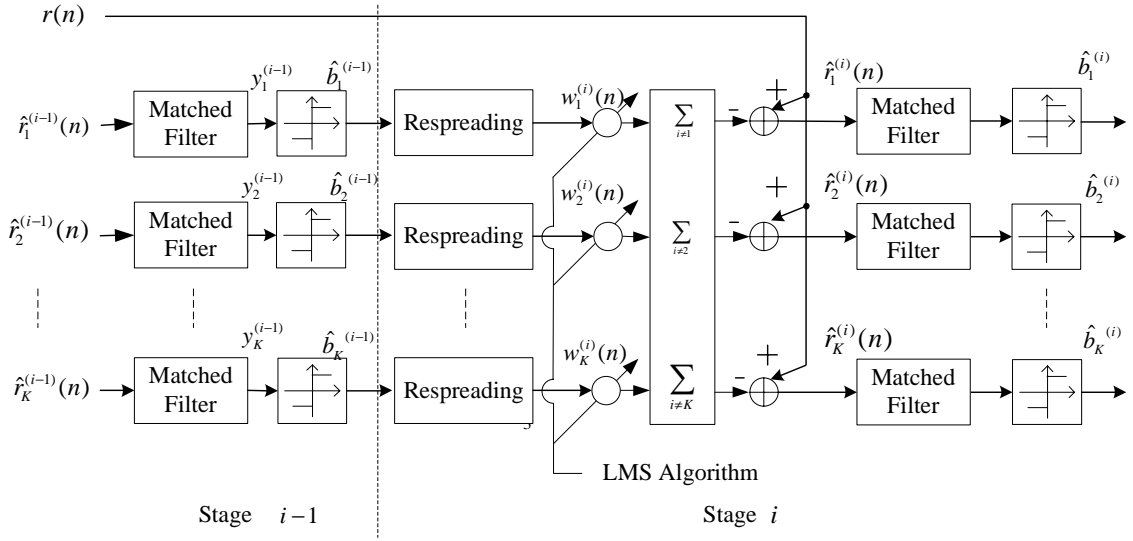


Figure 5.1: Adaptive blind partial HPIC receivers.

where  $\mu^{(i)}$  is the step size in Stage  $i$ . The interference-subtracted signal for the  $k$ th user is then

$$\hat{r}_k^{(i)}(n) = r(n) - \sum_{j \neq k} \chi_j^{(i)}(n) w_j^{(i)}(n). \quad (5.13)$$

We then have the detected bit as

$$\hat{b}_k^{(i)} = \text{sgn} [y_k^{(i)}] \quad (5.14)$$

where  $y_k^{(i)}$  is the matched filter output in the  $i$ th stage and it is given by

$$y_k^{(i)} = \sum_{n=0}^{N-1} \hat{r}_k^{(i)}(n) x_k(n). \quad (5.15)$$

The structure of the adaptive blind partial HPIC receiver for a certain stage is shown in Figure 5.1.

In practical CDMA systems, users often transmit data through multipath fading channels. Thus, it is necessary to take the multipath effect into account. Denote transfer function of the channel impulse response for the  $k$ th user as

$$\mathcal{W}_k(z) = \sum_{l=1}^L h_{k,l} z^{-\tau_{k,l}} \quad (5.16)$$

where  $h_{k,l}$  and  $\tau_{k,l}$  are the path gain and path delay of the  $l$ th path for the  $k$ th user, respectively, and  $L$  is the number of paths. Without loss of generality, we assume that  $\tau_{k,1} \leq \tau_{k,2} \leq \dots \leq \tau_{k,L}$ . In the receiving end, we can use a matched filter with a maximal ratio combining (MRC) to demodulate the signal. Let the equivalent baseband received signal be expressed by

$$r(n) = \sum_{l=1}^L \sum_{k=1}^K x_k(n - \tau_{k,l}) b_k a_k h_{k,l}. \quad (5.17)$$

The first stage output signal can be represented as

$$y_k^{(1)} = \sum_{l=1}^L y_{k,l}^{(1)} h_{k,l} \quad (5.18)$$

where the branch output from the MRC can be formed by

$$y_{k,l}^{(1)} = \sum_{n=0}^{N-1} r(n) x_k(n - \tau_{k,l}). \quad (5.19)$$

Following the signal model for the AWGN channel, we can formulate the error signal as that in (5.9). We first obtain the regenerated received signal as

$$\hat{r}^{(i)}(n) = \sum_{l=1}^L \sum_{k=1}^K \chi_k^{(i)}(n - \tau_{k,l}) w_{k,l}^{(i)}(n) \quad (5.20)$$

where  $w_{k,l}^{(i)}(n)$  denotes the weight for the  $l$ th path of the  $k$ th user in the  $i$ th stage. Then, the counterpart of  $\hat{r}_k^{(i)}(n)$  in (5.10) for the multipath scenario is

$$\hat{r}_k^{(i)}(n) = r(n) - \sum_{l=1}^L \sum_{j \neq k}^K \chi_j^{(i)}(n - \tau_{k,l}) w_{j,l}^{(i)}(N). \quad (5.21)$$

The matched output using the MRC is then

$$y_k^{(i)} = \sum_{l=1}^L \sum_{n=0}^{N-1} \hat{r}_k^{(i)}(n) x_k(n - \tau_{k,l}) h_{k,l}. \quad (5.22)$$

## § 5.2 Proposed Algorithm

As mentioned, the adaptive blind partial HPIC essentially performs system identification. As a consequence, if the training period is long enough (all weights converge), the mean value for the  $k$ th weight will be

$$w_k^{(i)} = \begin{cases} [w_{opt,k}^c]^{(i)}, & \hat{b}_k^{(i)} = b_k \\ [w_{opt,k}^e]^{(i)}, & \hat{b}_k^{(i)} \neq b_k. \end{cases} \quad (5.23)$$

In the previous chapter, we have analyzed the adaptive two-stage partial HPIC receiver. The result reveals that the performance of the adapted weights are determined by several factors listed as follows.

- Number of weights
- Step size
- Number of training data
- Noise variance
- Weight initials



Note that these factors may interact one another. Here, we will manipulate the first two factors, the weight numbers and the step size to obtain improved performance. We propose an algorithm that can reduce the number of adapted weight as well as its variance. At the same time, the step size can be increased to accelerate convergence. First, we will show that the MSE of the adaptive blind partial HPIC is proportional to the number of weights adapted in the LMS algorithm. Assume that the first user is the desired user. From (4.150), we have the output MSE as

$$\begin{aligned} \varpi_1(n) = & P_{c,1} \left\{ E \{ [\tilde{\epsilon}_1^c(n)]^2 \} + 2w_{M,1}^c(n) (w_{opt,1}^c - a_1) + a_1^2 - [w_{opt,1}^c]^2 \right\} \\ & + P_{e,1} \left\{ E \{ [\tilde{\epsilon}_1^e(n)]^2 \} + 2w_{M,1}^e(n) (w_{opt,1}^e + a_1) + a_1^2 - [w_{opt,1}^e]^2 \right\}. \end{aligned} \quad (5.24)$$

Since  $P_{e,1}$  is usually no more than 0.1, the total MSE is dominated by the part with correct decision. Note that  $w_{opt,k}^c$  is usually close to the desired weight value  $a_k$  even when  $K$  is large. Thus the MSE can be simplified to

$$E \{ [\tilde{\epsilon}_1^c(n)]^2 \} = \alpha^{2n} [\epsilon_{M,1}^c(0)]^2 + \delta_V^c(n) + \varepsilon_V^c(n). \quad (5.25)$$

The first term  $[\epsilon_{M,1}^c(0)]^2$  can be neglected since optimal weights and initials are close to  $a_1$ . The term  $\varepsilon_V^c(n)$  is a function of step size and noise variance only.

$$\varepsilon_V^c(n) = \frac{\mu^2}{N^2} \left\{ N\sigma^2 \left( \frac{1 - \alpha^{2n}}{1 - \alpha^2} \right) - \sigma^2 \left( \frac{1 - \alpha^n}{1 - \alpha} \right)^2 \right\}. \quad (5.26)$$

Thus the major term in the output MSE is  $\delta_V^c(n)$ . We first represent this variance function given  $\rho$  as

$$\tilde{\delta}_V^c(n) = \frac{\tilde{\delta}_V^{51}(n)P_{51} + \tilde{\delta}_V^{52}(n)P_{52}}{P_B} \quad (5.27)$$

where the components  $\tilde{\delta}_V^{5j}(n)$ ,  $j = 1, 2$  are given by

$$\tilde{\delta}_V^{5j}(n) = (1 - \alpha^n)^2 E_\gamma \left\{ (\tilde{w}_{opt,1}^{5j} - \check{w}_{opt,1}^{5j})^2 \right\}. \quad (5.28)$$

Taking the expectation on (5.28), we have

$$\begin{aligned} E_\gamma \left\{ (\tilde{w}_{opt,1}^{51} - \check{w}_{opt,1}^{51})^2 \right\} &= E_\gamma \left\{ (a_1 + a_I\rho + \gamma_1 - \check{w}_{opt,1}^{51})^2 | \gamma_1 > -(a_1 + a_I\rho) \right\} \\ E_\gamma \left\{ (\tilde{w}_{opt,1}^{52} - \check{w}_{opt,1}^{52})^2 \right\} &= E_\gamma \left\{ (a_1 - a_I\rho + \gamma_1 - \check{w}_{opt,1}^{52})^2 | \gamma_1 > -(a_1 - a_I\rho) \right\}. \end{aligned} \quad (5.29)$$

For the correct decision scenario, the conditional optimal weights are close to the ideal values, i.e.,  $\tilde{w}_{opt,1}^{5j} \simeq a_1$ . In that case, we can observe that the second moment in (5.29) is increased with  $a_I$  for  $\rho \neq 0$ . In summary, we know that the MSE of the adapted weights increases with  $a_I$ , and thus with  $K$ . One way to improve the system performance is to reduce the weight number trained in the LMS algorithm. This is possible if we know the channel gains. We then propose a procedure to do that. If a user's matched output magnitude exceeds a threshold  $a_k \xi_s^{(i)}$  in the  $i$ th stage, the corresponding decided bit is deemed reliable and the weight corresponds to this

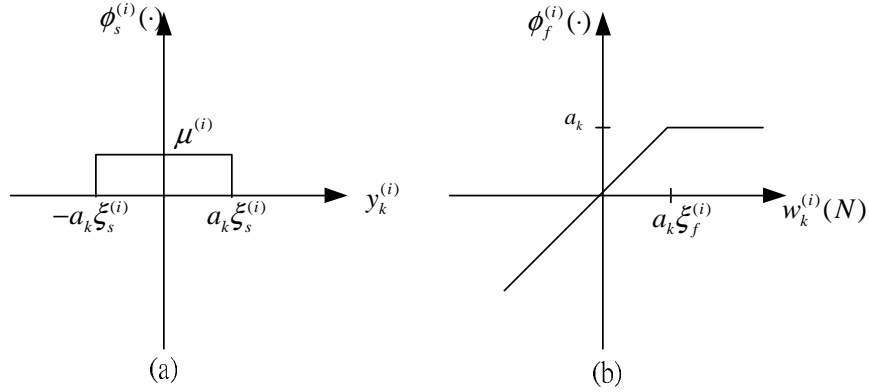


Figure 5.2: Functions used in the proposed algorithm. (a) Weight selection function. (b) Weight post filtering function.

bit is deactivated. In other words, this weight will not be included in the training process. This algorithm can be easily expressed using a two step-size scenario. Let the step size for User  $j$  be  $\mu_j^{(i)}$ . Then,

$$\mu_j^{(i)} = \begin{cases} 0 & \text{if } |y_j^{(i-1)}| > a_k \xi_s^{(i)} \\ \mu^{(i)} & \text{if } |y_j^{(i-1)}| \leq a_k \xi_s^{(i)} \end{cases} . \quad (5.30)$$

The step-size decision function, denoted as  $\phi_s(\cdot)$ , is shown in Figure 5.2(a). Note that there must be some users whose weights are erroneously decided. If this happens, it will increase the noise variance  $\sigma^2$  (in the computation of  $\varepsilon_V^c(n)$ ). The variance increased can be calculated as

$$\begin{aligned} E\{(a_j b_j - \tilde{w}_j^c(N) \hat{b}_j \rho_{jk})^2\} &= E\{(a_j b_j - a_j (-b_j))^2\} E\{\rho_{jk}^2\} \\ &= 4a_j^2/N \\ &= 4a_1^2/N. \end{aligned} \quad (5.31)$$

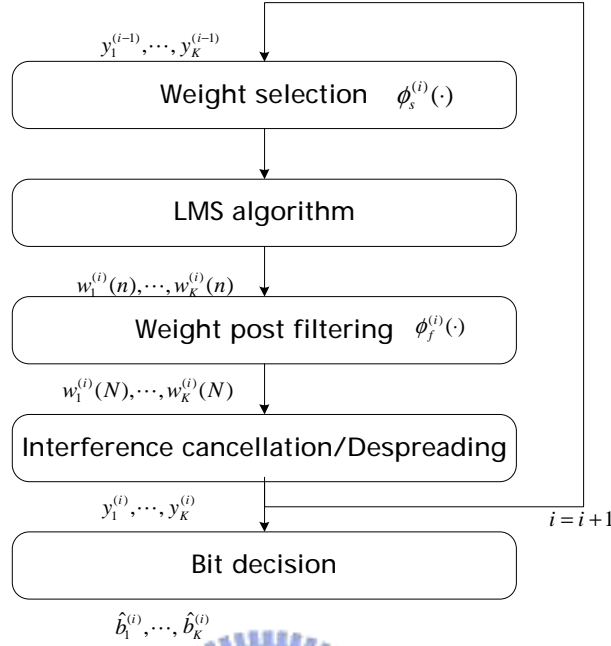


Figure 5.3: Flow chart for the proposed algorithm.

In (5.31),  $E\{\rho_{jk}^2\}$  is obtained by

$$\begin{aligned}
 E\{\rho_{jk}^2\} &= E\left\{\left[\sum_{n=0}^{N-1} x_j(n)x_k(n)\right]^2\right\} \\
 &= \sum_{n=0}^{N-1} E\{x_j(n)^2x_k(n)^2\} \\
 &= 1/N.
 \end{aligned} \tag{5.32}$$

We call this procedure as the weight selection procedure.

It is well known that the convergent weights in the LMS algorithm are random. Thus, if we know the weight distribution, we can perform weight post filtering (estimation). This will enhance the PIC performance furthermore. Figure 5.4 shows a typical probability function for the LMS convergent weight. It is clear that some of weights are greater than the channel gains and some weights are less than the channel gains. Note that given a binary random variable embedded in AWGN, the MMSE estimate corresponds to a transformation with a hyperbolic



tangent function. We can then apply the estimation theory here. To ease the derivation, we make a simplified alternative where a piece-wise linear decision function is used for weight post filtering; we denote this function as  $\phi_f(\cdot)$ . It is shown in Figure 5.2(b) in which a threshold  $a_k \xi_f^{(i)}$  is required. If a trained weight is greater than some threshold, it is decided to be  $a_k$ . Note that no decision is made below  $-a_k$ . This is because the probability that the weights appear in the region is low and it has little impact in overall performance. We call this the weight post filtering procedure.

As mentioned, the weight distribution has different mean values for correct/erroneous decision (in the previous stage). The weight means for erroneous decision bits will approach the corresponding optimal weights if the processing gain  $N$  is large. However, in a practical system,  $N$  is usually not large enough. Thus, we prefer to use a large step size  $\mu^{(i)}$  to speed up the weight adaptation for users with erroneous decisions. However, a larger step size will enlarge the weight variance which adversely affect the final performance. The two procedures propose above can reduce the number of active weights and further filter the convergent weights. As a result, it is possible to use a larger step size without significantly increasing the weight variance. By careful examination, we can find a good compromise among the parameters  $\{\mu_0^{(i)}, \xi_s^{(i)}, \xi_f^{(i)}\}$  ( $\mu_0^{(i)} = \mu^{(i)}/N$ ) such that the weights are determined in an optimal way. The flow chart for the proposed algorithm is depicted in Figure 5.3.

### § 5.2.1 Gradient Guided Search Algorithm

It is well known that the HPIC was proposed based on the ML principle. The HPIC decides the desire user bit polarity with larger likelihood while estimate other user data bits from the previous stage. The procedure of likelihood maximization is performed simultaneously for all users. When the MAI is strong, the full HPIC output will not converge but oscillate in subsequent stages. The partial HPIC relieves the limit cycle phenomenon and finds a local maximum with likelihood higher than that of the full HPIC. There are many methods that can increase the likelihood. One method applied in the full HPIC is to flip parts of the user bits in

one stage and output the pattern giving the highest likelihood. [69],[70]. We call this method the gradient guided search (GGS) algorithm [71], whose procedure is outlined as follows.

- (a) Let  $i = 1$ . Obtain the initial input bits. This is usually performed by the matched filter output as

$$\hat{\mathbf{b}}^{(1)} = \{\hat{b}_k^{(1)} = \text{sgn}[y_k^{(1)}], k = 1, 2, \dots, K\}. \quad (5.33)$$

- (b) Flip the user bit one by one and compute the  $K$  log-likelihood functions  $\mathcal{L}(\bar{\mathbf{b}}_k^{(i)})$ ,  $k = 1, 2, \dots, K$  using (2.3). The input bit sequence is then

$$\bar{\mathbf{b}}_k^{(i)} = [\hat{b}_1^{(i)}, \hat{b}_2^{(i)}, \dots, \hat{b}_{k-1}^{(i)}, -\hat{b}_k^{(i)}, \hat{b}_{k+1}^{(i)}, \dots, \hat{b}_K^{(i)}]^T. \quad (5.34)$$

- (c) Choose one pattern whose log-likelihood function is the largest among  $K$  likelihood functions. Note that this likelihood must be greater than that for the initial bit pattern.

$$\hat{\mathbf{b}}^{(i+1)} = \max_{\bar{\mathbf{b}}_k^{(i)}} \{\mathcal{L}(\bar{\mathbf{b}}_k^{(i)}), k = 1, 2, \dots, K\}. \quad (5.35)$$

If no one log-likelihood function exceeds that of the original bit pattern, all user bits are keep unchanged and the algorithm terminates.

- (b) Update the initial bit pattern with the new one and proceed to the next stage from (b) with stage number  $i + 1$ .

In this chapter, the GGS algorithm is utilized as a post processing algorithm to further improve the performance of the adaptive partial HPIC.

### § 5.3 Performance Analysis of the Proposed Algorithm

We will analyze the performance of the proposed algorithm for a two-stage HPIC. Specifically, we will derive the output MSE and the BER. As previously, we assume the AWGN channel and

the power-balanced scenario. Substituting  $C_j^{(i)} = w_j^{(i)}$  in (5.2) and (5.7), we have the second stage despread output signal for the first user as

$$y_1^{(2)} = a_1 b_1 + \sum_{j \neq 1} (a_j b_j - w_j \hat{b}_j) \rho_{j1} + \gamma_1 \quad (5.36)$$

where  $w_j = w_j^{(2)}$  and  $\hat{b}_j = \hat{b}_j^{(1)}$ . Approximating interference signal as Gaussian distribution, we can have the BER, denoted as  $P_e$ , for the desired user in the first stage as

$$P_e = Q \left( \frac{a_1}{\sqrt{\sigma^2 + (K-1)/N}} \right) \quad (5.37)$$

where  $Q(\cdot)$  is the Q-function. The probability that the user has correct decision in the first stage and its output is greater than the threshold ( $y_1^{(1)} > \xi_s^{(2)} a_1, \hat{b}_1^{(1)} = b_1$ ) is

$$P_s = Q \left( \frac{a_1 (\xi_s^{(2)} - 1)}{\sqrt{\sigma^2 + (K-1)/N}} \right). \quad (5.38)$$

In other words,  $P_s$  is the probability of correct weight selection. The probability of erroneous weight selection ( $y_1^{(1)} > \xi_s^{(2)} a_1$  and  $\hat{b}_1^{(1)} \neq b_1$ ) is

$$P_z = Q \left( \frac{a_1 (\xi_s^{(2)} + 1)}{\sqrt{\sigma^2 + (K-1)/N}} \right). \quad (5.39)$$

If the first stage output is greater than  $\xi_s^{(2)} a_1$ , the corresponding weight will not be adjusted. The effective number of weights is reduced from  $K$  to  $K_l$  where  $K_l$  is given by

$$K_l = K(1 - P_s - P_z). \quad (5.40)$$

Note that  $K_l$  may not be an integer since it represents an rough estimate of the averaged weight number. If the weight selected for non-adaptive is erroneous, it will increase the noise variance when the LMS algorithm is applied. The amount increased is

$$\begin{aligned} E\{(a_j b_j - \tilde{w}_j^c(N) \hat{b}_j)^2\} &= E\{(a_j b_j + a_j b_j)^2\} \\ &= 4a_j^2 \\ &= 4a_1^2. \end{aligned} \quad (5.41)$$

Let the enlarged noise variance be  $\sigma_l^2$ , Then,

$$\begin{aligned}\sigma_l^2 &= \sigma^2 + KP_z E\{(a_j b_j - \tilde{w}_j^c(N) \hat{b}_j \rho_{jk})^2\} \\ &= \sigma^2 + KP_z \cdot 4a_1^2/N\end{aligned}\quad (5.42)$$

The convergence analysis for the LMS algorithm developed in Chapter 4 can be directly applied here. However, we have to change the weight number from  $K$  to  $K_l$  and the noise variance from  $\sigma^2$  to  $\sigma_l^2$ . As we have seen, the number of user direct influence the equivalent interference gain.

$$a_l = a_1 \sqrt{K_l - 1} \quad (5.43)$$

We denote the adapted weights in the second stage for correct or erroneous first stage decision as  $\tilde{w}_1^c(n)$  or  $\tilde{w}_1^e(n)$ , respectively. We omit the superscript of stage number for simplicity. Assuming that  $y_1^{(2)}$  is a Gaussian random variable, we can estimate the BER in the second stage output. Note that we have the mean of  $y_1^{(2)}$  as  $a_1$ . If cancellation is perfect, the variance of  $y_1^{(2)}$  is just  $\sigma^2$ . However, since the cancellation is not perfect, the variance will be increased. There are two types of erroneous cancellation. The first one is due to cancellation from users with erroneous selected weights (non-adaptive), denoted by  $V_z$ . The second one is due to cancellation of adapted weights, denoted by  $V_w$ . Thus, the overall noise variance is

$$V_y = \sigma^2 + V_z + V_w \quad (5.44)$$

Using  $\tilde{w}_j^c(N) = a_j$  and (5.39), we have

$$\begin{aligned}V_z &= \frac{KP_z}{N} (a_j b_j - \tilde{w}_j^c(N) \hat{b}_j)^2 \\ &= \frac{KP_z}{N} (a_j b_j - a_j (-b_j))^2 \\ &= \frac{4a_j^2 KP_z}{N}.\end{aligned}\quad (5.45)$$

Since we have performed weight post filtering, various conditions for the second type of cancellation has to be considered. We treat  $V_w$  as the sum of two components  $V_c$  and  $V_e$ ; one is contributed from  $\tilde{w}_1^c$  and the other is from  $\tilde{w}_1^e$ . Denoted their corresponding density function

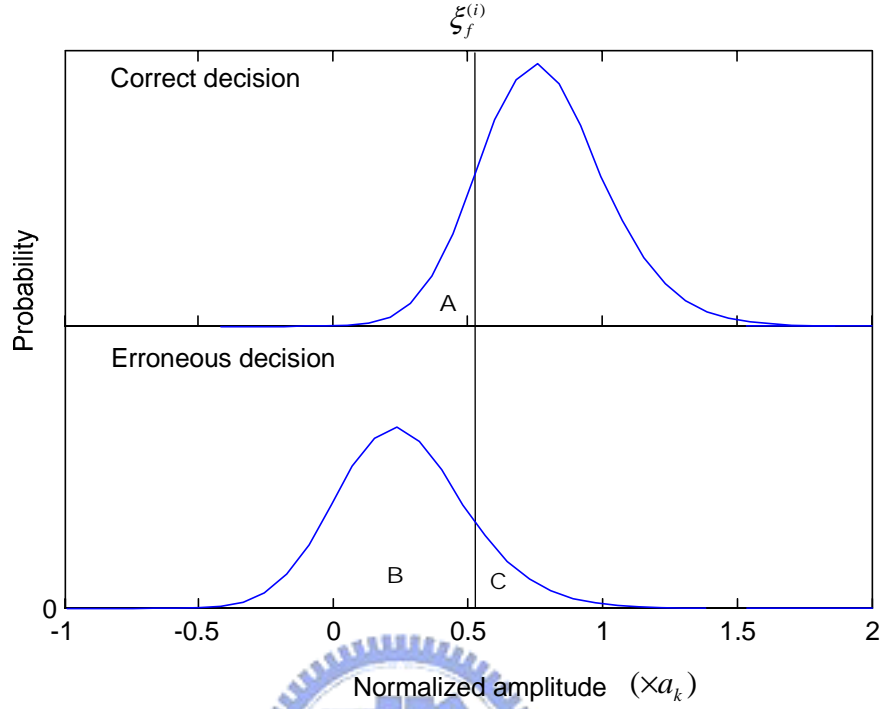


Figure 5.4: Probability density function for adapted weights from LMS algorithm.

as  $f(\tilde{w}_1^c)$  and  $f(\tilde{w}_1^e)$ , respectively. Figure 5.4 gives an example of simulated distributions. Due to weight post filtering, no cancellation error is induced when  $\tilde{w}_1^c > \zeta_d a_1$ . Only the region represented by the 'A' area in Figure 5.4 will introduce error. Thus,

$$V_c = \frac{K_l - 1}{N} \int_{-\infty}^{\xi_f a_1} (\tilde{w}_1^c - a_1)^2 f(\tilde{w}_1^c) d\tilde{w}_1^c \quad (5.46)$$

As to  $\tilde{w}_1^e$ , erroneous weight decision occurs when  $\tilde{w}_1^e > \zeta_d a_1$ , i.e.,  $\phi_f(\tilde{w}_1^e) = a_1$  and  $(a_j b_j - \tilde{w}_j^e (N) \hat{b}_j)^2 = (a_j b_j - (a_j)(-b_j))^2 = 4a_j^2 = 4a_1^2$ . Thus,

$$V_e = \frac{K_l - 1}{N} \int_{-\infty}^{\xi_f a_1} (\tilde{w}_1^e + a_1)^2 f(\tilde{w}_1^e) d\tilde{w}_1^e + \frac{4a_1^2 (K_l - 1)}{N} \int_{\xi_f a_1}^{\infty} f(\tilde{w}_1^e) d\tilde{w}_1^e \quad (5.47)$$

The integration areas are represented by 'B' and 'C' in Figure 5.4, respectively. Then,  $V_c$  and  $V_e$  can be combined as

$$V_w = \frac{V_c(1 - P_e - P_s) + V_e(P_e - P_z)}{1 - P_s - P_z} \quad (5.48)$$

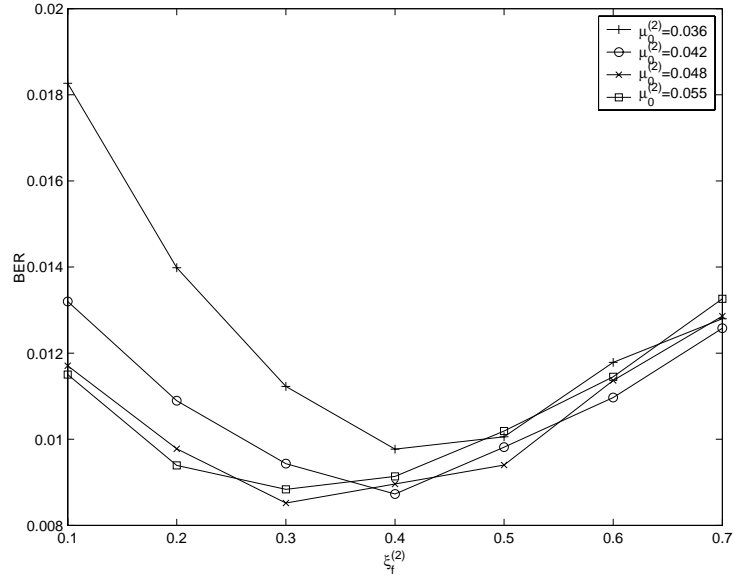


Figure 5.5: Second stage parameter optimization for the proposed algorithm. (Weight selection is not performed).

Finally, we can express the BER in the second stage HPIC output as

$$P(y_k^{(2)}) = \mathcal{Q} \left( \frac{a_k}{\sqrt{\sigma^2 + V_z + V_w}} \right). \quad (5.49)$$

## § 5.4 Simulation Results

### A. Parameter optimization

In this section, we will report simulation results to demonstrate the effectiveness of the proposed algorithm. We have used random codes of length 31 as spreading sequences. Partial HPIC receivers up to five stages are considered. First, we determine the optimal parameters for each receiver in order to obtain the best system performance. We let the user number be  $K = 20$ ,  $E_b/N_0 = 7$  dB, and power was balanced. For the conventional partial HPIC, we have empirically found the optimal PCFs for stage 2 to 5 as  $\{0.7, 0.8, 0.85, 0.9\}$ . As to the adaptive blind partial HPIC, the normalized step sizes, defined as  $\mu_0^{(i)} = \mu^{(i)}/N$ , are

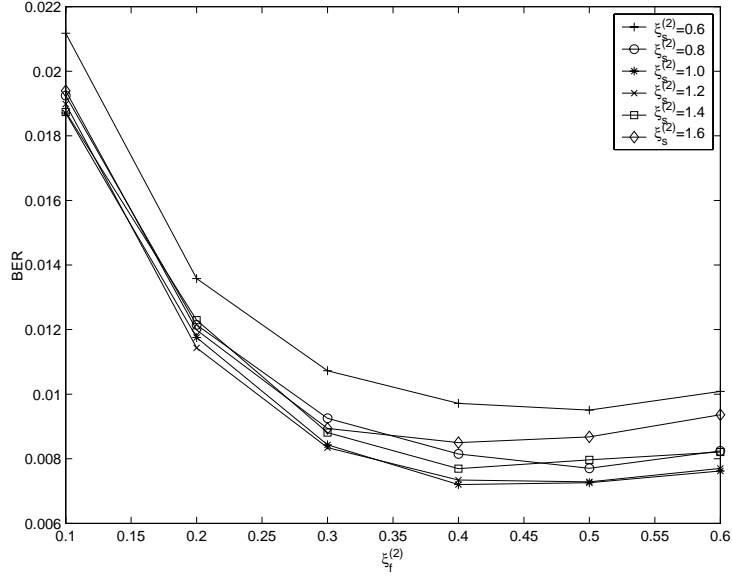


Figure 5.6: Second stage parameter optimization for the proposed algorithm ( $\mu_0^{(2)} = 0.048$ ).

$\{0.022, 0.013, 0.007, 0.003\}$ . For the proposed algorithm, we have additional two parameters  $\xi_s^{(i)}$  and  $\xi_f^{(i)}$ . To simplify the problem, we do not perform weight selection and determine  $\xi_f^{(i)}$  first. Figure 5.5 shows the BER performance vs.  $\xi_f^{(i)}$  and  $\mu^{(2)}$  for the second stage output. From the figure, we can see that the optimal step size is around 0.048 that is larger than the step size used in the conventional approach. This is because the weight post filtering operation removes some weight noise for users regarded reliable. The weight variance is then decreased and the resulting interference cancellation is more accurate. Thus, a larger step size is permitted for faster convergence. We then incorporate the weight selection operation into the parameter optimization. The result is shown in Fig. 5.6. Here, we let the step size be fixed as 0.048. In the figure, we can observe that the optimal parameter setting is  $\xi_s^{(2)} = 1.2$  and  $\xi_f^{(2)} = 0.4$ . Note that the system performance is not sensitive for higher  $\xi_f^{(2)}$  values. This is because most reliable weights have been selected during weight selection. The theoretical BER in (5.49) for the proposed algorithm is also evaluated in Figure 5.7. We can observe that our analysis resembles performance trend as the simulated results; however, there exhibits some gaps in between. The inaccuracy may be due to the Gaussian assumption used in the calculation. Optimal parame-

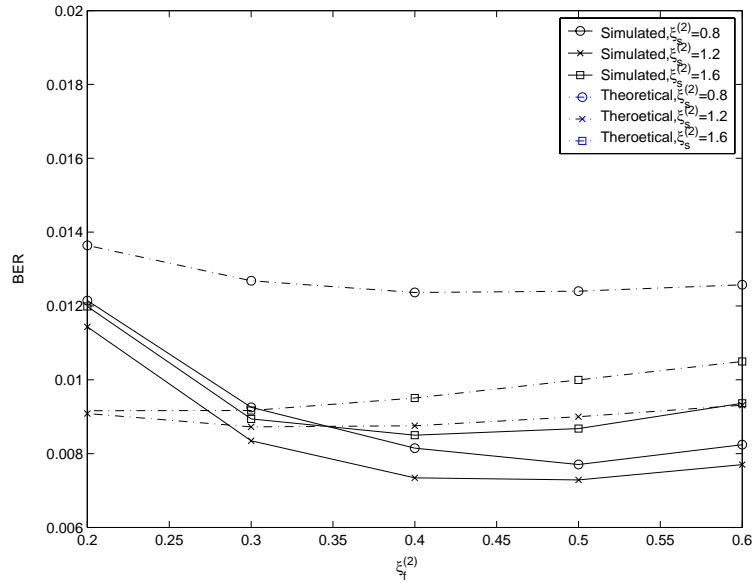


Figure 5.7: Second stage BER performance for the proposed algorithm ( $K = 20$ ,  $\mu_0^{(2)} = 0.048$ , and  $E_b/N_0 = 7$  dB).

ters found in a specific stage may not be optimal for all the stages. However, the optimization will be cumbersome. For simplicity, we will use the parameters found in the second stage for all stages. The superscript on parameters for denoting the stage number is then omitted in the sequel. In the fading channels; however, those parameters should be tuned again to obtain the best performance.

### B. Performance comparison

In the following, we present the performance comparison for various multiuser receivers which include the conventional matched filter, the non-adaptive partial HPIC (referred to as PHPIC), the adaptive blind partial HPIC (referred to as the AHPIC), the proposed algorithm, and the GGS algorithm. The GGS algorithm serves as a post-processor for both the AHPIC and the proposed algorithm. Note that we let the GGS only perform one iteration (one bit correction) in each cancellation stage. Figure 5.8 expresses the second stage performance of the proposed algorithm and other methods vs. different user numbers ( $E_b/N_0 = 7$  dB). We



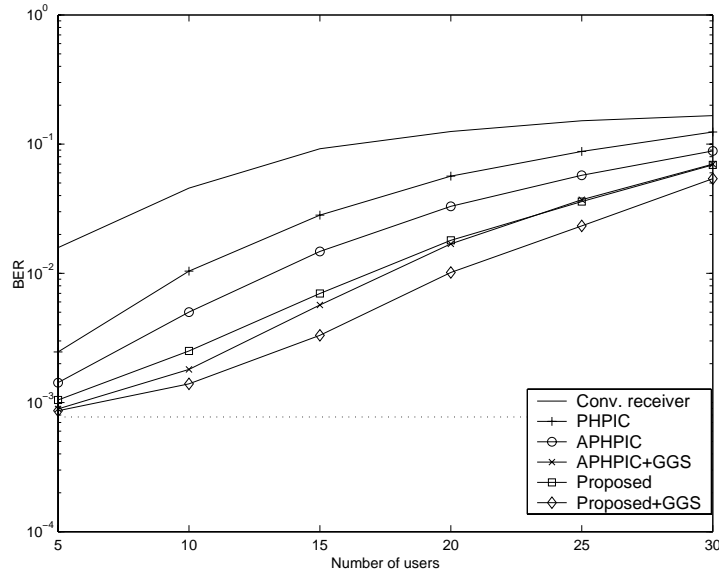


Figure 5.8: Second stage BER performance comparison vs. user numbers ( $\xi_s = 1.2$ ,  $\xi_f = 0.4$ ,  $\mu_0 = 0.048$ , and  $E_b/N_0 = 7$  dB).

can find that the conventional matched filter receiver perform worst due to the heavy MAI. The PHPIC performs worse than the AHPIC and the proposed algorithm. The combined AHPIC and GGS receivers provides more performance improvement in light loading condition. This is because the GGS algorithm performs at most one bit correction in one stage; it is more effective for low error rate scenario. The proposed algorithm is better than the AHPIC and the post GGS processing enhances the proposed algorithm in all cases. We also show the performance for higher stage processing in Figures 5.9-5.11. As we can see, the GGS algorithm gives less and less improvement as the stage number increases. All adaptive partial HPIC receivers perform close to the single user bound when the number of users is small. However, adaptive receivers degrade in heavy loading scenarios. If we want to further improve the performance, we have to increase the adaptation length and decrease the step size. In such a way, we can reduce the weight variance from inaccurate interference cancellation. We then compare the proposed algorithm with other methods under different  $E_b/N_0$  (ten users). Fig. 5.12 and 5.13 show the results for the second and the fifth stage, respectively. We observe that the performance

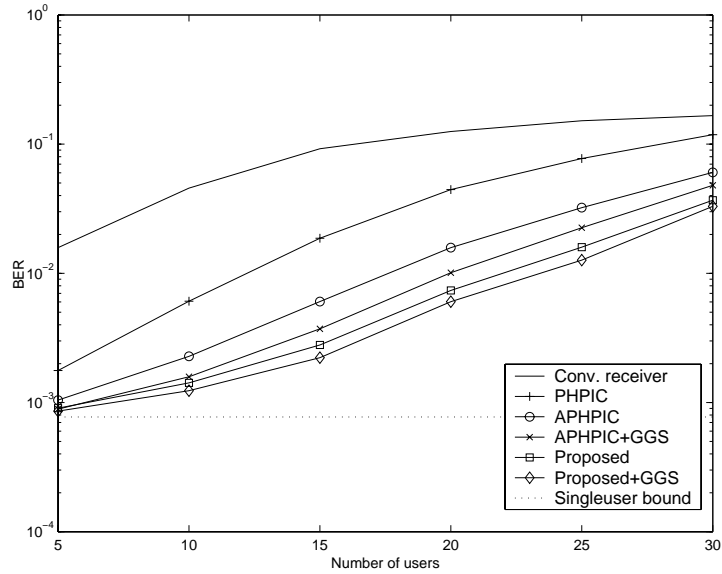


Figure 5.9: Third stage BER performance comparison vs. user numbers (the parameter setting is the same as that in Figure 5.8 for all stages).

of the proposed algorithm is close to the single user bound when the number stage is five and  $E_b/N_0$  is low to median. We also compare the system performance under the power-imbalanced scenario. The user powers are equally distributed and the power ratio between the strongest and weakest users is 15 dB. In Fig.5.14 and Fig.5.15, we present the BER performance for the weakest user in the second and fifth stage. It can be seen that the proposed algorithm provides a significant performance gain in the fifth stage, especially when the user number is large. Note that the proposed algorithm makes the performance of the weakest user indistinguishable as compared to that of the single user case when the user number is less than twenty. The reason for this superior performance may be due to the weight selection process where stronger users are almost all recognized and excluded from the training phase. This results is similar to the behavior in SIC, where the most reliable user is first detected and subtracted from the received signal. In the following, we consider the performance of the HPIC receivers under the fading channel environment. Figure 5.16 demonstrates the performance comparison of 5-stage receivers for a single-path rician fading channel. The reflect-to-diffuse ratio was set 7 dB and

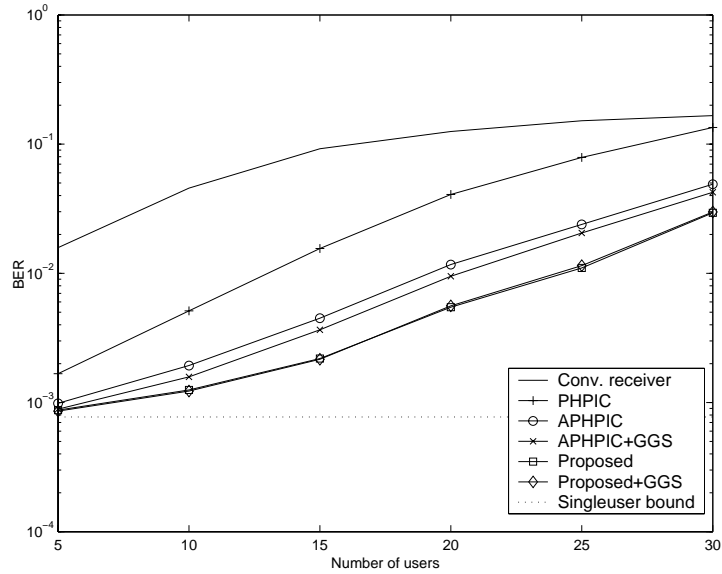


Figure 5.10: Fourth stage BER performance comparison vs. user numbers (the parameter setting is the same as that in Figure 5.8 for all stages).

$E_b/N_0 = 7$  dB. Note that the channel gain was constant during a bit interval and varied bit by bit independently. We can observe that the proposed algorithm outperforms the PHPIC and APHPIC receivers. We next use a two-path fading channel; the second path is one chip delay with respect to the main path, and each path gain is Gaussian distributed with zero mean. The result is shown in Figure 5.17. The proposed algorithm still has the best performance. The GGS algorithm is not employed here since it is not suitable for the bit-asynchronous systems.

### C. Effect of channel estimation error

In the adaptive HPIC receiver scenario, channel information is necessary for initial setting and for interference cancellation. The proposed algorithm also requires channel information to determine the optimal parameters. All of the simulations conducted above have assumed perfect channel estimation. However, in practice, channel estimation cannot be perfect and its error has to be taken into account. Consider a model for channel estimation error as

$$\hat{a}_k = a_k + \Delta_a \quad (5.50)$$

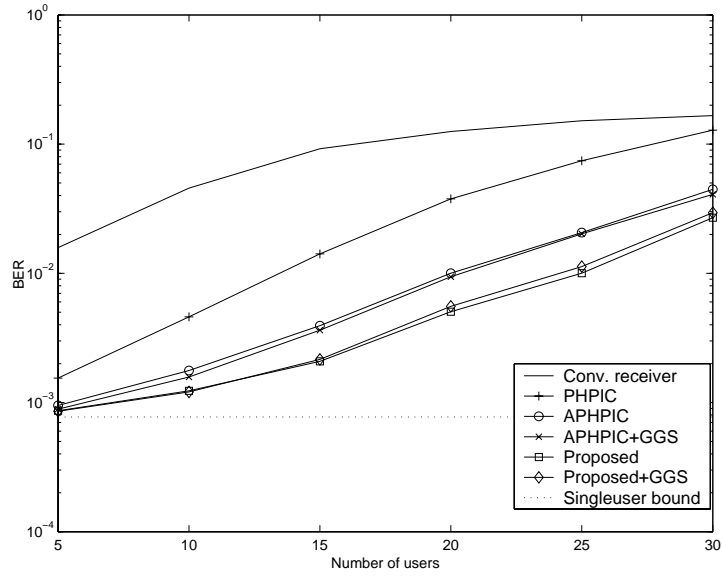


Figure 5.11: Fifth stage BER performance comparison vs. user numbers (the parameter setting is the same as that in Figure 5.8 for all stages).

where  $\Delta_a$  is a Gaussian distributed random variable with zeros mean and standard deviation  $\sigma_a$ . We then use  $\hat{a}_k$  instead of  $a_k$  in the receiver. Figure 5.18 show the simulation results. As seen from the figure, the proposed algorithm always performs better than the AHPIC under different channel estimation error scenarios. Note that the GGS algorithm will fail when the channel estimation error is large. The proposed algorithm is the most robust one among the multiuser receivers compared.

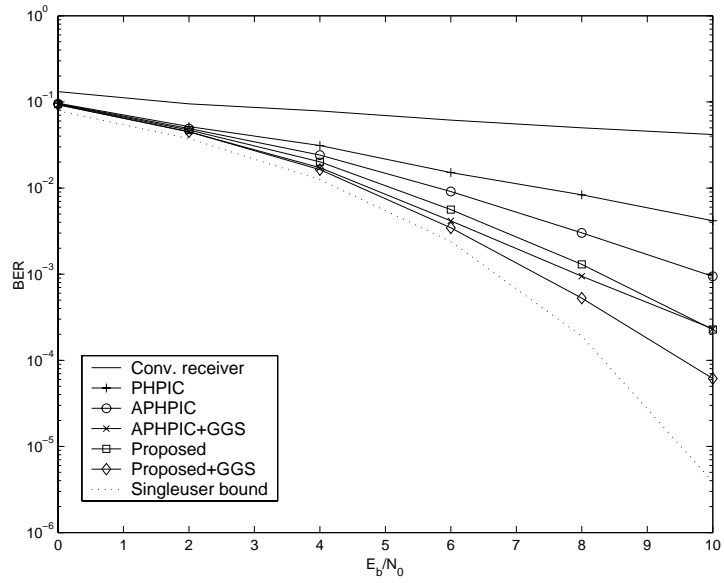


Figure 5.12: Second stage BER performance comparison vs.  $E_b/N_0$  ratios ( $K = 10$ , and the parameter setting is the same as that in Figure 5.8 for all stages).

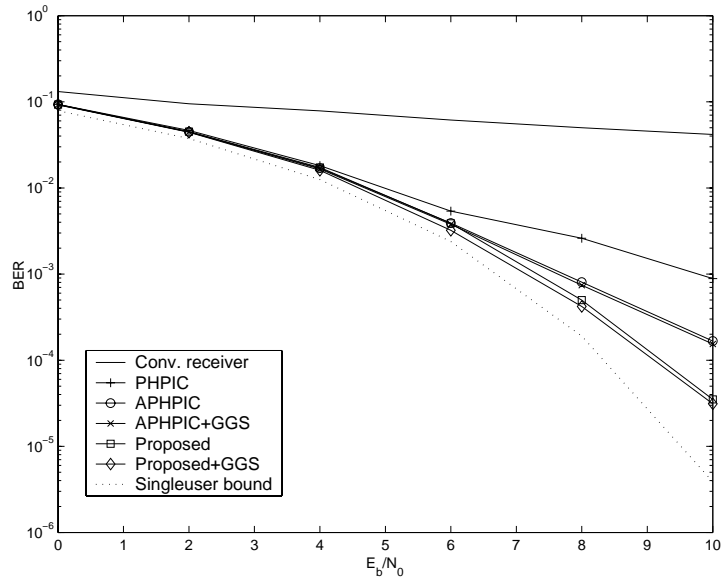


Figure 5.13: Fifth stage BER performance comparison vs.  $E_b/N_0$  ratios ( $K = 10$ , and the parameter setting is the same as that in Fig. 5.8).

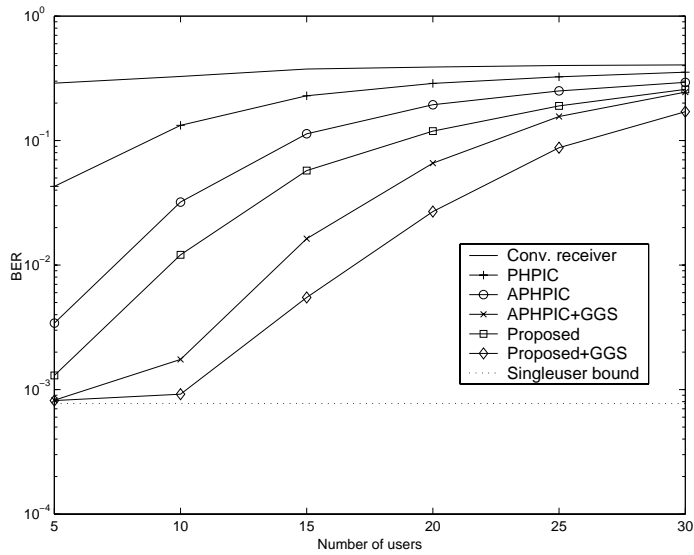


Figure 5.14: Second stage BER performance comparison for the weakest user (power-imbalanced,  $E_b/N_0 = 7$  dB, and the parameter setting is the same as that in Fig. 5.8).

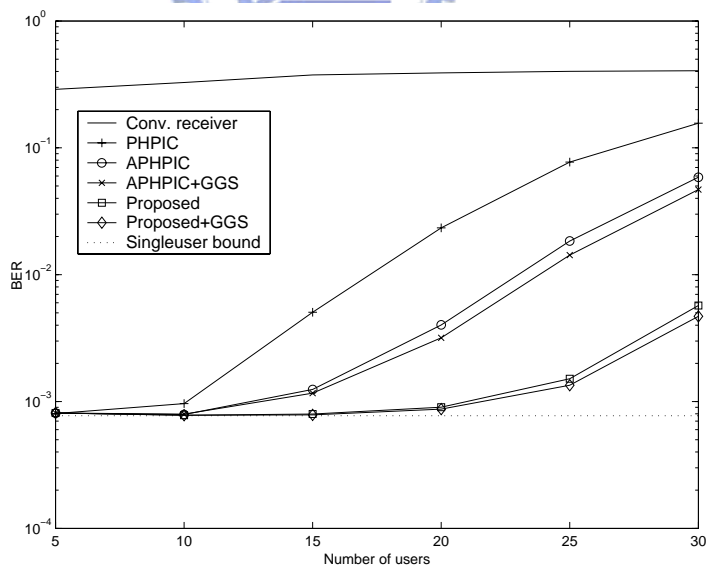


Figure 5.15: Fifth stage BER performance comparison for the weakest user (power-imbalanced,  $E_b/N_0 = 7$  dB and the parameter setting is the same as that in Fig. 5.8).

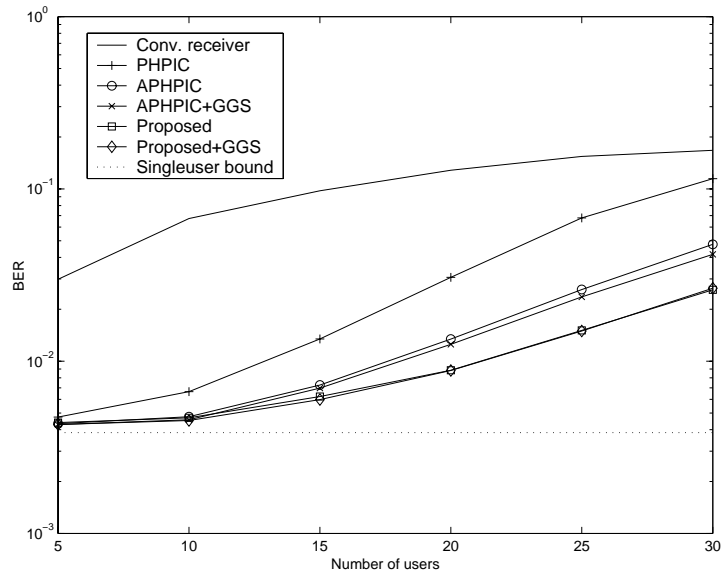


Figure 5.16: Fifth stage BER performance comparison for single-path rician fading channels ( $E_b/N_0 = 7$  dB,  $\xi_s = 1.4$ , and  $\xi_f = 0.3$  for all stages).

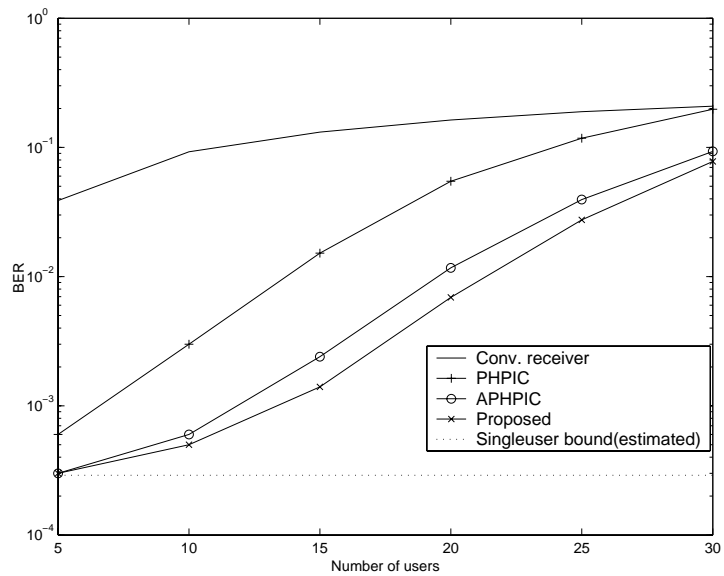


Figure 5.17: Fifth stage BER performance comparison for two-ray multipath fading channels ( $E_b/N_0 = 17$  dB,  $\xi_s = 5$ , and  $\xi_f = 0.5$  for all stages).

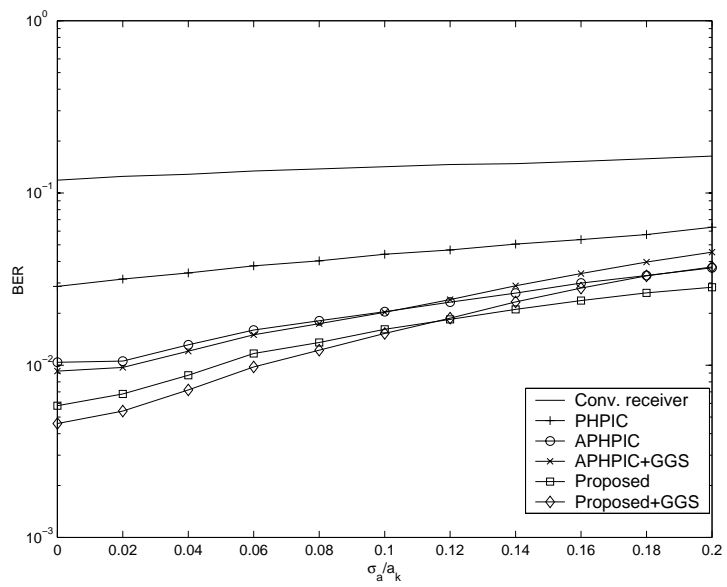


Figure 5.18: Fifth stage BER performance comparison vs. channel estimation errors ( $K = 20$ ,  $E_b/N_0 = 7$  dB,  $\mu_0 = 0.048$ ,  $\xi_s = 1.5$ , and  $\xi_f = 0.5$  for all stages).



# Chapter 6

## Conclusions

In DS-CDMA communication systems, MAI is considered as the main factor limiting the system performance. Among many multiuser detection schemes, the PIC receiver is considered as a simple yet effective approach. It has been shown that the performance of the PIC can be further improved if interference is not fully cancelled. The performance of a partial PIC depends heavily on the PCFs. Thus, how to determine PCFs optimally is of great concern.

In this dissertation, we have studied two types of partial PICs. Using the BER criterion, We first develop a two-stage decoupled partial SPIC and derive a set of closed-form solutions for optimal PCFs. These PCFs are useful for periodic and aperiodic spreading codes in additive white Gaussian noise channels, and for those in multipath channels. Simulation results show that the derived optimal PCFs agree closely with empirical optimal PCFs. The optimal two-stage partial SPIC outperforms a conventional matched filter detector, a two-stage full SPIC detector, and even a three-stage full SPIC. Simulations have also shown that the derived decoupled partial SPIC performs similarly to the optimal two-stage partial SPIC with coupled structure. We have also shown that the derived PCFs are not sensitive to parameter estimation errors. It can be noted that the optimal PCFs for aperiodic spreading code systems in AWGN channels have a simple expression. This will be a great advantage for real-world applications since the optimal PCFs can be calculated efficiently on-line in a time-varying environment.

We then conduct performance analysis for a two-stage adaptive blind partial HPIC receiver in the AWGN channel. We first derive the analytical result for the optimal weight, the adapted weight mean, and the adapted weight variance in a single-user case. Then, we derive the optimal weights and adapted weight mean for a two-user case. Finally, we extend the result to a general  $K$ -user case. With the results obtained above, we are able to derive the formula for the output MSE and the BER. Using the output MSE criterion, the optimal step size can then be obtained. Simulation results show that the analytical results are accurate. In the final part of the dissertation, we propose an improved adaptive blind partial HPIC receiver. The main idea is to reduce weight variance introduced by the LMS algorithm so as to reduce the output MSE. We use two approaches; the first is to reduce the number of adapted weights and the second is further process the convergent weights. To implement these ideas, we propose the weight selection and weight post filtering schemes. Simulation results show that the proposed algorithm outperforms the conventional adaptive approach in all scenarios. In power-imbalanced systems, the proposed algorithm can approach the optimum performance. We also derive analytical results for the proposed algorithm which include output MSE and BER. It has been shown that the analysis results are reasonably accurate.

In concluding this dissertation, we suggest some topics for further research. The optimal PCFs derived for the SPIC in the multipath scenarios are complicated and not suitable for real-time calculations. We then need a simpler approximate expression. Also, we are mainly concerned with BPSK modulation. Note that the same result can be extended to accommodate QAM modulation. In this case, however, we have to take the interference between inphase and quadrature components into account. It turns out that for the inphase or quadrature component of one user, we may treat the number of interfering users as  $2K - 1$ .

In the analysis of adaptive blind HPIC, we do not derive the weight variance for the two-user case. As an alternative, we use the result from the single user to perform  $K$ -user approximation. This contribute resultant inaccuracy significantly. Since we use the two-user result in weight mean analysis, the analytical weight mean is more accurate than the analytical weight variance.

The other problem is that we do not consider the multipath scenario. It seems that we can extend our results to the scenario; however, the derivation may become much more complex.

The proposed improved adaptive algorithm has not taken full information we have. The weight selection process only consider the two-stepsize case. It can be expected that a continuous step size will give even better result. Also, we have not considered the initial value problem. If the first stage decision is likely to be erroneous, the initial should be close to zero. On the other hands, it should be close to  $\pm a_k$ . The weight post filtering does not achieve its optimal performance either. As we mentioned, the optimal filtering function consists of a hyperbolic tangent function. The parameters of the function should depend on the weight variance. So, it will be different stage by stage. The information we have is the channel gain which is  $\pm a_k$ . Whether or not the processing schemes mentioned above can fully explore the information deserves further study.



## Appendix A

# Periodic Code System Optimal PCFs for Asynchronous AWGN Channels

Let  $b_{k,i}$  denote the  $i$ th bit for the  $k$ th user and  $\tau_k$  the user delay. Then the received signal for asynchronous channels can then be represented by

$$r(t) = \sum_k \sum_i b_{k,i} a_k(t - iT - \tau_k) \Pi_T(t - iT - \tau_k) + n(t). \quad (\text{A.1})$$

We further define the relative delay between User  $j$  and  $k$  as  $\tau_{jk} = \tau_j - \tau_k$ , and the cross-correlation functions are given by

$$\rho_{jk}(\tau_{jk}) = \begin{cases} \int_{T+\tau_{jk}}^T a_j(t - \tau_{jk} - T) a_k(t) dt & , \tau_{jk} < 0 \\ \int_{\tau_{jk}}^T a_j(t - \tau_{jk}) a_k(t) dt & , \tau_{jk} \geq 0, \end{cases} \quad (\text{A.2})$$

and

$$\hat{\rho}_{jk}(\tau_{jk}) = \begin{cases} \int_0^{T+\tau_{jk}} a_j(t - \tau_{jk}) a_k(t) dt & , \tau_{jk} < 0 \\ \int_0^{\tau_{jk}} a_j(t - \tau_{jk} + T) a_k(t) dt & , \tau_{jk} \geq 0. \end{cases} \quad (\text{A.3})$$

For simplicity we use  $\rho_{jk}$  and  $\hat{\rho}_{jk}$  instead of  $\rho_{jk}(\tau_{jk})$  and  $\hat{\rho}_{jk}(\tau_{jk})$  in the sequel. The matched filter output for the  $k$ th users'  $i$ th bit is obtained as

$$\begin{aligned} y_{k,i} &= \int_{iT+\tau_k}^{(i+1)T+\tau_k} r(t)a_k(t-\tau_k)dt \\ &= A_k b_{k,i} + \sum_{j \neq k} A_j \left( b_{j,i-l_{jk}} \hat{\rho}_{jk} + b_{j,i-l_{jk}+1} \rho_{jk} \right) + \eta_{k,i} \end{aligned} \quad (\text{A.4})$$

where the delay index and noise term are expressed as  $l_{jk}$  and  $\eta_{k,i}$ . They are defined as

$$l_{jk} \triangleq \begin{cases} 1, & \tau_{jk} \geq 0 \\ 0, & \text{otherwise,} \end{cases} \quad (\text{A.5})$$

and

$$\eta_{k,i} = \int_{iT+\tau_k}^{(i+1)T+\tau_k} n(t)a_k(t-\tau_k)dt. \quad (\text{A.6})$$

The regenerated received signal using partial SPIC is given by

$$\hat{r}_k(t) = r(t) - C_k \sum_{j \neq k} \sum_i y_{j,i} a_j(t - iT - \tau_j) \Pi_T(t - iT - \tau_j). \quad (\text{A.7})$$

Thus, the second stage output is obtained as

$$\begin{aligned} z_{k,i} &= \int_{iT+\tau_k}^{(i+1)T+\tau_k} \hat{r}(t)a_k(t-\tau_k)dt \\ &= y_{k,i} - C_k \sum_{j \neq k} \left( y_{j,i-l_{jk}} \hat{\rho}_{jk} + y_{j,i-l_{jk}+1} \rho_{jk} \right) \\ &= A_k b_{k,i} + \sum_{j \neq k} A_j \left( b_{j,i-l_{jk}} \hat{\rho}_{jk} + b_{j,i-l_{jk}+1} \rho_{jk} \right) + \eta_{k,i} \\ &\quad - C_k \sum_{j \neq k} \left\{ A_j \left( b_{j,i-l_{jk}} \hat{\rho}_{jk} + b_{j,i-l_{jk}+1} \rho_{jk} \right) \right. \\ &\quad \quad \left. + \sum_{m \neq j} A_m \left( b_{m,i-l_{mj}-l_{jk}} \hat{\rho}_{mj} \hat{\rho}_{jk} + b_{m,i-l_{mj}-l_{jk}+1} \rho_{mj} \hat{\rho}_{jk} \right) \right. \\ &\quad \quad \left. + b_{m,i-l_{mj}-l_{jk}+1} \hat{\rho}_{mj} \rho_{jk} + b_{m,i-l_{mj}-l_{jk}+2} \rho_{mj} \rho_{jk} \right) \\ &\quad \quad \left. + \eta_{j,i-l_{jk}} \hat{\rho}_{jk} + \eta_{j,i-l_{jk}+1} \rho_{jk} \right\}. \end{aligned} \quad (\text{A.8})$$

Without loss of generality, we may assume that  $\tau_j \geq \tau_k, j \neq k$ . Then  $l_{jk} = 1$  for all  $j$ 's and the result can be simplified to

$$\begin{aligned}
z_{k,i} = & A_k b_{k,i} \left\{ 1 - C_k \sum_{j \neq k} (\hat{\rho}_{jk}^2 + \rho_{jk}^2) \right\} - A_k C_k \sum_{j \neq k} (b_{k,i-1} + b_{k,i+1}) \hat{\rho}_{jk} \rho_{jk} \\
& - C_k \sum_{j \neq k} \sum_{m \neq j,k}^{\tau_m \leq \tau_j} A_j b_{j,i-2} \hat{\rho}_{jm} \hat{\rho}_{mk} - C_k \sum_{j \neq k} \sum_{m \neq j,k}^{\tau_m > \tau_j} A_j b_{j,i+1} \rho_{jm} \rho_{mk} \\
& + \sum_{j \neq k} A_j b_{j,i-1} \Phi_{jk} + \sum_{j \neq k} A_j b_{j,i} \Psi_{jk} + \eta_{k,i} \\
& - C_k \sum_{j \neq k} (\eta_{j,i-l_{jk}} \hat{\rho}_{jk} + \eta_{j,i-l_{jk}+1} \rho_{jk})
\end{aligned} \tag{A.9}$$

where  $\Phi_{jk}$  and  $\Psi_{jk}$  are defined as

$$\begin{aligned}
\Phi_{jk} &= \hat{\rho}_{jk}(1 - C_k) - C_k \left\{ \sum_{m \neq j,k}^{\tau_m > \tau_j} \hat{\rho}_{jm} \hat{\rho}_{mk} + \sum_{m \neq j,k}^{\tau_m \leq \tau_j} (\rho_{jm} \hat{\rho}_{mk} + \hat{\rho}_{jm} \rho_{mk}) \right\} \\
\Psi_{jk} &= \rho_{jk}(1 - C_k) - C_k \left\{ \sum_{m \neq j,k}^{\tau_m \leq \tau_j} \rho_{jm} \rho_{mk} + \sum_{m \neq j,k}^{\tau_m > \tau_j} (\rho_{jm} \hat{\rho}_{mk} + \hat{\rho}_{jm} \rho_{mk}) \right\}.
\end{aligned} \tag{A.10}$$

The squared-mean for  $z_{k,i}$  is obtained from (3.17) and (A.9) as

$$\mathcal{M}_k = A_k^2 (1 - C_k \Lambda_k)^2 \tag{A.11}$$

where

$$\Lambda_k \triangleq \sum_{j \neq k} (\hat{\rho}_{jk}^2 + \rho_{jk}^2). \tag{A.12}$$

Similarly, the variance can also be obtained as

$$\mathcal{V}_k = \sigma^2 (\Omega_{1,k} C_k^2 - 2\Omega_{2,k} C_k + \Omega_{3,k}) \tag{A.13}$$

where  $\Omega_{i,k}$ ,  $1 \leq i \leq 3$ , are defined as

$$\begin{aligned}
\Omega_{1,k} = & 2\gamma_k^2 \sum_{j \neq k} \hat{\rho}_{jk}^2 \rho_{jk}^2 + \sum_{j \neq k} \gamma_j^2 \left( \Phi_{jk}^2 + \Psi_{jk}^2 \right) + \left( \sum_{j \neq k} \sum_{m \neq j,k}^{\tau_m \leq \tau_j} \gamma_j^2 \hat{\rho}_{jm} \hat{\rho}_{mk} \right)^2 \\
& + \left( \sum_{j \neq k} \sum_{m \neq j,k}^{\tau_m > \tau_j} \gamma_j^2 \rho_{jm} \rho_{mk} \right)^2 + \sum_{j \neq k} \left( \hat{\rho}_{jk}^2 + \rho_{jk}^2 \right) \\
& + \sum_{j \neq k} \sum_{m \neq j,k}^{\tau_m < \tau_j} 2 \left( \rho_{jm} \hat{\rho}_{j,k} \hat{\rho}_{m,k} + \rho_{jm} \rho_{jk} \rho_{mk} + \hat{\rho}_{jm} \hat{\rho}_{jk} \rho_{mk} \right) \\
& + \sum_{j \neq k} \sum_{m \neq j,k}^{\tau_m = \tau_j} \left( \rho_{jm} \hat{\rho}_{jk} \hat{\rho}_{mk} + \rho_{jm} \rho_{jk} \rho_{mk} \right), \tag{A.14}
\end{aligned}$$

$$\Omega_{2,k} = \sum_{j \neq k} \gamma_j^2 \left( \hat{\rho}_{jk} \Phi_{jk} + \rho_{jk} \Psi_{jk} \right) + \sum_{j \neq k} \left( \hat{\rho}_{jk}^2 + \rho_{jk}^2 \right), \tag{A.15}$$

$$\Omega_{3,k} = \sum_{j \neq k} \gamma_j^2 \left( \rho_{jk}^2 + \hat{\rho}_{jk}^2 \right) + 1. \tag{A.16}$$

Thus, the optimal PCF can be obtained by substituting (A.12) and (A.14)-(A.16) into (3.27).

## Appendix B

### Expressions for Expected Terms in (3.50)-(3.51)

Extending the definition in (3.62), we have

$$\mathcal{F}_{jk}(p_1, q_1, \dots, p_i, q_i) = N^i E \left\{ \zeta_{jk}(p_1, q_1), \dots, \zeta_{jk}(p_i, q_i) \right\} \quad (\text{B.1})$$

where  $i$  is an integer. To make expression simpler, we let  $\mathbf{w}_i = \{p_i, q_i\}$ . Equation (B.1) can then be rewritten as

$$\mathcal{F}_{jk}(\mathbf{w}_1, \dots, \mathbf{w}_i) = N^i E \left\{ \zeta_{jk}(\mathbf{w}_1), \dots, \zeta_{jk}(\mathbf{w}_i) \right\}. \quad (\text{B.2})$$

We further omit the subscript in  $\mathcal{F}(\cdot)$  and use the following notational substitution

$$\sum_{\mathbf{w}_i=0}^{L^2} \longrightarrow \sum_{p_i=0}^L \sum_{q_i=0}^L. \quad (\text{B.3})$$



In what follows, six expected terms are given without detailed derivation. The first term is

$$\begin{aligned}
E_{\mathcal{L}}\{\varrho_{jk}^2 \varrho_j\} &= \frac{1}{N^3} \sum_{\mathbf{w}_1=1}^{L^2} \sum_{\mathbf{w}_2=1}^{L^2} \sum_{\mathbf{w}_3=1}^{L^2} h_{jk}(\mathbf{w}_1) h_{jk}(\mathbf{w}_2) h_{jj}(\mathbf{w}_3) \mathcal{F}(\mathbf{w}_1, \mathbf{w}_2, \mathbf{w}_3), \\
&\text{IF } \tau_{jk}(\mathbf{w}_1) = \tau_{jk}(\mathbf{w}_2), \tau_{jj}(\mathbf{w}_3) = 0, \\
&\quad \mathcal{F}(\mathbf{w}_1, \mathbf{w}_2, \mathbf{w}_3) = N \left( N - |\tau_{jk}(\mathbf{w}_1)| \right). \\
&\text{ELSE IF } |\tau_{jk}(\mathbf{w}_1) - \tau_{jk}(\mathbf{w}_2)| = |\tau_{jj}(\mathbf{w}_3)|, \\
&\quad \mathcal{F}(\mathbf{w}_1, \mathbf{w}_2, \mathbf{w}_3) = N - \max \left\{ |\tau_{jk}(\mathbf{w}_1)|, |\tau_{jk}(\mathbf{w}_2)|, |\tau_{jj}(\mathbf{w}_3)| \right\}. \\
&\text{ELSE} \\
&\quad \mathcal{F}(\mathbf{w}_1, \mathbf{w}_2, \mathbf{w}_3) = 0 \\
&\text{END.} \tag{B.4}
\end{aligned}$$

The second term is

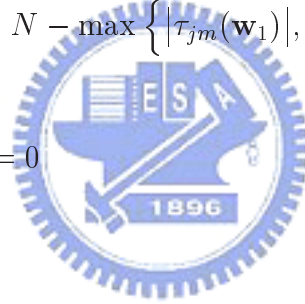
$$\begin{aligned}
E_{\mathcal{L}}\{\varrho_{jk} \varrho_{jm} \varrho_{mk}\} &= \frac{1}{N^3} \sum_{\mathbf{w}_1=1}^{L^2} \sum_{\mathbf{w}_2=1}^{L^2} \sum_{\mathbf{w}_3=1}^{L^2} h_{jk}(\mathbf{w}_1) h_{jm}(\mathbf{w}_2) h_{mk}(\mathbf{w}_3) \mathcal{F}(\mathbf{w}_1, \mathbf{w}_2, \mathbf{w}_3), \\
&\text{IF } \tau_{jm}(\mathbf{w}_1) + \tau_{mk}(\mathbf{w}_2) = \tau_{jk}(\mathbf{w}_3), \\
&\quad \mathcal{F}(\mathbf{w}_1, \mathbf{w}_2, \mathbf{w}_3) = N - \max \left\{ |\tau_{jk}(\mathbf{w}_1)|, |\tau_{jm}(\mathbf{w}_2)|, |\tau_{mk}(\mathbf{w}_3)| \right\}. \\
&\text{ELSE} \\
&\quad \mathcal{F}(\mathbf{w}_1, \mathbf{w}_2, \mathbf{w}_3) = 0 \\
&\text{END.} \tag{B.5}
\end{aligned}$$

The third term is

$$\begin{aligned}
E_{\mathcal{L}}\{\varrho_{jk}^2 \varrho_j^2\} &= \frac{1}{N^4} \sum_{\mathbf{w}_1=1}^{L^2} \sum_{\mathbf{w}_2=1}^{L^2} \sum_{\mathbf{w}_3=1}^{L^2} \sum_{\mathbf{w}_4=1}^{L^2} h_{jk}(\mathbf{w}_1) h_{jk}(\mathbf{w}_2) h_{jj}(\mathbf{w}_3) h_{jj}(\mathbf{w}_4) \mathcal{F}(\mathbf{w}_1, \mathbf{w}_2, \mathbf{w}_3, \mathbf{w}_4), \\
&\text{IF } \tau_{jk}(\mathbf{w}_1) = \tau_{jk}(\mathbf{w}_2), \tau_{jj}(\mathbf{w}_3) = \tau_{jj}(\mathbf{w}_4) = 0, \\
&\quad \mathcal{F}(\mathbf{w}_1, \mathbf{w}_2, \mathbf{w}_3, \mathbf{w}_4) = N^2 \left( N - |\tau_{jk}(\mathbf{w}_1)| \right). \\
&\text{ELSE IF } \tau_{jk}(\mathbf{w}_1) = \tau_{jk}(\mathbf{w}_2), \tau_{jj}(\mathbf{w}_3) = \tau_{jj}(\mathbf{w}_4), \\
&\quad \mathcal{F}(\mathbf{w}_1, \mathbf{w}_2, \mathbf{w}_3, \mathbf{w}_4) = \left( N - |\tau_{jk}(\mathbf{w}_1)| \right) \left( N - |\tau_{jj}(\mathbf{w}_3)| \right). \\
&\text{ELSE IF } |\tau_{jk}(\mathbf{w}_1) - \tau_{jk}(\mathbf{w}_2)| = \tau_{jj}(\mathbf{w}_3), \tau_{jj}(\mathbf{w}_4) = 0, \\
&\quad \text{or } |\tau_{jk}(\mathbf{w}_1) - \tau_{jk}(\mathbf{w}_2)| = \tau_{jj}(\mathbf{w}_4), \tau_{jj}(\mathbf{w}_3) = 0, \\
&\quad \mathcal{F}(\mathbf{w}_1, \mathbf{w}_2, \mathbf{w}_3, \mathbf{w}_4) = N - \max \left\{ |\tau_{jk}(\mathbf{w}_1)|, |\tau_{jk}(\mathbf{w}_2)|, |\tau_{jj}(\mathbf{w}_3)|, |\tau_{jj}(\mathbf{w}_4)| \right\}. \\
&\text{ELSE IF } |\tau_{jk}(\mathbf{w}_1) - \tau_{jk}(\mathbf{w}_2)| = |\tau_{jj}(\mathbf{w}_3) \pm \tau_{jj}(\mathbf{w}_4)|, \tau_{jk}(\mathbf{w}_1) \neq 0, \tau_{jk}(\mathbf{w}_2) \neq 0, \\
&\quad \mathcal{F}(\mathbf{w}_1, \mathbf{w}_2, \mathbf{w}_3, \mathbf{w}_4) = N - \max \left\{ |\tau_{jk}(\mathbf{w}_1)|, |\tau_{jk}(\mathbf{w}_2)|, |\tau_{jj}(\mathbf{w}_3)|, |\tau_{jj}(\mathbf{w}_4)|, \right. \\
&\quad \left. |\tau_{jk}(\mathbf{w}_1) - \tau_{jk}(\mathbf{w}_2)|, |\tau_{jk}(\mathbf{w}_1) \pm \tau_{jj}(\mathbf{w}_3)|, |\tau_{jk}(\mathbf{w}_1) \pm \tau_{jj}(\mathbf{w}_4)| \right\}. \\
&\text{ELSE IF } |\tau_{jk}(\mathbf{w}_1) - \tau_{jk}(\mathbf{w}_2)| = |\tau_{jj}(\mathbf{w}_3) \pm \tau_{jj}(\mathbf{w}_4)|, \\
&\quad \mathcal{F}(\mathbf{w}_1, \mathbf{w}_2, \mathbf{w}_3, \mathbf{w}_4) = N - \max \left\{ |\tau_{jk}(\mathbf{w}_1)|, |\tau_{jk}(\mathbf{w}_2)|, |\tau_{jj}(\mathbf{w}_3)|, |\tau_{jj}(\mathbf{w}_4)| \right\}. \\
&\text{ELSE} \\
&\quad \mathcal{F}(\mathbf{w}_1, \mathbf{w}_2, \mathbf{w}_3, \mathbf{w}_4) = 0 \\
&\text{END.} \tag{B.6}
\end{aligned}$$

The fourth term is

$$\begin{aligned}
E_{\mathcal{L}}\{\varrho_{jm}^2 \varrho_{mk}^2\} &= \frac{1}{N^4} \sum_{\mathbf{w}_1=1}^{L^2} \sum_{\mathbf{w}_2=1}^{L^2} \sum_{\mathbf{w}_3=1}^{L^2} \sum_{\mathbf{w}_4=1}^{L^2} h_{jm}(\mathbf{w}_1) h_{jm}(\mathbf{w}_2) h_{mk}(\mathbf{w}_3) h_{mk}(\mathbf{w}_4) \mathcal{F}(\mathbf{w}_1, \mathbf{w}_2, \mathbf{w}_3, \mathbf{w}_4), \\
&\text{IF } \tau_{jm}(\mathbf{w}_1) = \tau_{jm}(\mathbf{w}_2), \tau_{mk}(\mathbf{w}_3) = \tau_{mk}(\mathbf{w}_4), \\
&\quad \mathcal{F}(\mathbf{w}_1, \mathbf{w}_2, \mathbf{w}_3, \mathbf{w}_4) = \left(N - |\tau_{jm}(\mathbf{w}_1)|\right) \left(N - |\tau_{mk}(\mathbf{w}_3)|\right). \\
&\text{ELSE IF } |\tau_{jm}(\mathbf{w}_1) - \tau_{jm}(\mathbf{w}_2)| = |\tau_{mk}(\mathbf{w}_3) - \tau_{mk}(\mathbf{w}_4)|, \tau_{jm}(\mathbf{w}_1) \neq 0, \tau_{jm}(\mathbf{w}_2) \neq 0, \\
&\quad \tau_{mk}(\mathbf{w}_3) \neq 0, \tau_{mk}(\mathbf{w}_4) \neq 0, \\
&\quad \mathcal{F}(\mathbf{w}_1, \mathbf{w}_2, \mathbf{w}_3, \mathbf{w}_4) = N - \max \left\{ |\tau_{jm}(\mathbf{w}_1)|, |\tau_{jm}(\mathbf{w}_2)|, |\tau_{mk}(\mathbf{w}_3)|, |\tau_{mk}(\mathbf{w}_4)|, \right. \\
&\quad \left. |\tau_{jm}(\mathbf{w}_1) - \tau_{jm}(\mathbf{w}_2)|, |\tau_{jm}(\mathbf{w}_1) + \tau_{mk}(\mathbf{w}_3)|, |\tau_{jm}(\mathbf{w}_1) + \tau_{mk}(\mathbf{w}_4)| \right\}. \\
&\text{ELSE IF } |\tau_{jm}(\mathbf{w}_1) - \tau_{jm}(\mathbf{w}_2)| = |\tau_{mk}(\mathbf{w}_3) - \tau_{mk}(\mathbf{w}_4)|, \\
&\quad \mathcal{F}(\mathbf{w}_1, \mathbf{w}_2, \mathbf{w}_3, \mathbf{w}_4) = N - \max \left\{ |\tau_{jm}(\mathbf{w}_1)|, |\tau_{jm}(\mathbf{w}_2)|, |\tau_{mk}(\mathbf{w}_3)|, |\tau_{mk}(\mathbf{w}_4)| \right\}. \\
&\text{ELSE} \\
&\quad \mathcal{F}(\mathbf{w}_1, \mathbf{w}_2, \mathbf{w}_3, \mathbf{w}_4) = 0 \\
&\text{END.}
\end{aligned} \tag{B.7}$$



The fifth term is

$$E_{\mathcal{L}}\{\varrho_{jm}\varrho_{mk}\varrho_{jn}\varrho_{nk}\} = \frac{1}{N^4} \sum_{\mathbf{w}_1=1}^{L^2} \sum_{\mathbf{w}_2=1}^{L^2} \sum_{\mathbf{w}_3=1}^{L^2} \sum_{\mathbf{w}_4=1}^{L^2} h_{jm}(\mathbf{w}_1)h_{mk}(\mathbf{w}_2)h_{jn}(\mathbf{w}_3)h_{nk}(\mathbf{w}_4) \cdot \mathcal{F}(\mathbf{w}_1, \mathbf{w}_2, \mathbf{w}_3, \mathbf{w}_4),$$

$$\text{IF } \tau_{jm}(\mathbf{w}_1) + \tau_{mk}(\mathbf{w}_2) = \tau_{jn}(\mathbf{w}_3) + \tau_{nk}(\mathbf{w}_4), \tau_{jm}(\mathbf{w}_1) \neq 0, \tau_{mk}(\mathbf{w}_2) \neq 0, \tau_{jn}(\mathbf{w}_3) \neq 0, \tau_{nk}(\mathbf{w}_4) \neq 0,$$

$$\mathcal{F}(\mathbf{w}_1, \mathbf{w}_2, \mathbf{w}_3, \mathbf{w}_4) = N - \max \left\{ |\tau_{jm}(\mathbf{w}_1)|, |\tau_{mk}(\mathbf{w}_2)|, |\tau_{jn}(\mathbf{w}_3)|, |\tau_{nk}(\mathbf{w}_4)|, \right. \\ \left. |\tau_{jm}(\mathbf{w}_1) + \tau_{mk}(\mathbf{w}_2)|, |\tau_{jm}(\mathbf{w}_1) - \tau_{jn}(\mathbf{w}_3)| \right\}.$$

$$\text{ELSE IF } \tau_{jm}(\mathbf{w}_1) + \tau_{mk}(\mathbf{w}_2) = \tau_{jn}(\mathbf{w}_3) + \tau_{nk}(\mathbf{w}_4),$$

$$\mathcal{F}(\mathbf{w}_1, \mathbf{w}_2, \mathbf{w}_3, \mathbf{w}_4) = N - \max \left\{ |\tau_{jm}(\mathbf{w}_1)|, |\tau_{mk}(\mathbf{w}_2)|, |\tau_{jn}(\mathbf{w}_3)|, |\tau_{nk}(\mathbf{w}_4)| \right\}.$$

ELSE

$$\mathcal{F}(\mathbf{w}_1, \mathbf{w}_2, \mathbf{w}_3, \mathbf{w}_4) = 0$$

END.



(B.8)

Finally, the sixth term is

$$E_{\mathcal{L}}\{\varrho_{jm}\varrho_{mk}\varrho_{jk}\varrho_{jj}\} = \frac{1}{N^4} \sum_{\mathbf{w}_1=1}^{L^2} \sum_{\mathbf{w}_2=1}^{L^2} \sum_{\mathbf{w}_3=1}^{L^2} \sum_{\mathbf{w}_4=1}^{L^2} h_{jm}(\mathbf{w}_1)h_{mk}(\mathbf{w}_2)h_{jk}(\mathbf{w}_3)h_{jj}(\mathbf{w}_4) \cdot \mathcal{F}(\mathbf{w}_1, \mathbf{w}_2, \mathbf{w}_3, \mathbf{w}_4),$$

$$\text{IF } \tau_{jm}(\mathbf{w}_1) + \tau_{mk}(\mathbf{w}_2) = \tau_{jk}(\mathbf{w}_3), \tau_{jj}(\mathbf{w}_4) = 0,$$

$$\mathcal{F}(\mathbf{w}_1, \mathbf{w}_2, \mathbf{w}_3, \mathbf{w}_4) = N \left( N - \max \left\{ |\tau_{jm}(\mathbf{w}_1)|, |\tau_{mk}(\mathbf{w}_2)|, |\tau_{jk}(\mathbf{w}_3)| \right\} \right).$$

$$\text{ELSE IF } |\tau_{jm}(\mathbf{w}_1) + \tau_{mk}(\mathbf{w}_2) - \tau_{jk}(\mathbf{w}_3)| = |\tau_{jj}(\mathbf{w}_4)|, \tau_{jm}(\mathbf{w}_1) \neq 0, \tau_{mk}(\mathbf{w}_2) \neq 0,$$

$$\tau_{jk}(\mathbf{w}_3) \neq 0,$$

$$\mathcal{F}(\mathbf{w}_1, \mathbf{w}_2, \mathbf{w}_3, \mathbf{w}_4) = N - \max \left\{ |\tau_{jm}(\mathbf{w}_1)|, |\tau_{mk}(\mathbf{w}_2)|, |\tau_{jk}(\mathbf{w}_3)|, |\tau_{jj}(\mathbf{w}_4)|, \right. \\ \left. |\tau_{jm}(\mathbf{w}_1) + \tau_{mk}(\mathbf{w}_2)|, |\tau_{jm}(\mathbf{w}_1) \pm \tau_{jj}(\mathbf{w}_4)| \right\}.$$

$$\text{ELSE IF } |\tau_{jm}(\mathbf{w}_1) + \tau_{mk}(\mathbf{w}_2) - \tau_{jk}(\mathbf{w}_3)| = |\tau_{jj}(\mathbf{w}_4)|,$$

$$\mathcal{F}(\mathbf{w}_1, \mathbf{w}_2, \mathbf{w}_3, \mathbf{w}_4) = N - \max \left\{ |\tau_{jm}(\mathbf{w}_1)|, |\tau_{mk}(\mathbf{w}_2)|, |\tau_{jk}(\mathbf{w}_3)|, |\tau_{jj}(\mathbf{w}_4)| \right\}.$$

ELSE

$$\mathcal{F}(\mathbf{w}_1, \mathbf{w}_2, \mathbf{w}_3, \mathbf{w}_4) = 0$$

END.

(B.9)

## Appendix C

### Optimal PCFs under Fading Channels

In Chapter 3 optimal PCFs for different scenarios are derived under the assumption of static channels. The received user amplitudes are regarded known and to be varying slowly. Now we relax the constraint by taking the user amplitudes as random variables. Take the optimal PCFs for aperiodic codes in AWGN case as an example, the components in the squared mean is refined to be

$$E_{\mathcal{L},\mathcal{A}}\{\mathcal{M}_k^{(l)}\} = \mathbf{g}_k \left( 1 - C_k E_{\mathcal{L}}\{\Lambda_k^{(l)}\} \right)^2 \quad (\text{C.1})$$

where the expectation subscript  $\mathcal{A}$  represents the expectation on user amplitudes and  $\mathbf{g}_k = E_{\mathcal{A}}\{a_k^2\}$  represents the expected user power over the fading channel. Similarly we define the expected interference power as  $l_k = \sum_{j \neq k} E_{\mathcal{A}}\{a_j^2\}/\sigma^2$  and the resulting variance is given by

$$E_{\mathcal{L},\mathcal{A}}\{\mathcal{V}_k^{(l)}\} = \sigma^2 \left( E_{\mathcal{L},\mathcal{A}}\{\Omega_{1,k}^{(l)}\} C_k^2 - 2E_{\mathcal{L},\mathcal{A}}\{\Omega_{2,k}^{(l)}\} C_k + E_{\mathcal{L},\mathcal{A}}\{\Omega_{3,k}^{(l)}\} \right) \quad (\text{C.2})$$

where

$$E_{\mathcal{L},\mathcal{A}}\{\Omega_{1,k}^{(l)}\} = l_k \left( \frac{1}{N} + \frac{3(K-2)}{N^2} + \frac{(K-2)(K-3)}{N^3} \right) + \frac{K-1}{N} + \frac{(K-1)(K-2)}{N^2}, \quad (\text{C.3})$$

$$E_{\mathcal{L},\mathcal{A}}\{\Omega_{2,k}^{(l)}\} = l_k \left( \frac{1}{N} + \frac{K-2}{N^2} \right) + \frac{K-1}{N}, \quad (\text{C.4})$$

$$E_{\mathcal{L},\mathcal{A}} \left\{ \Omega_{3,k}^{(l)} \right\} = \frac{l_k}{N} + 1. \quad (\text{C.5})$$

When the multipath fading channel is considered, it is assumed that each multipath has independent fading distribution for each user. In that case the expectation term in (3.61) can be represented as

$$E_{\mathcal{L},\mathcal{A}} \left\{ \varrho_{jk}^2 \right\} = \sum_{p_1=1}^L \sum_{q_1=1}^L \sum_{p_2=1}^L \sum_{q_2=1}^L E_{\mathcal{A}} \left\{ h_{jk}(p_1, q_1) h_{jk}(p_2, q_2) \right\} E_{\mathcal{L}} \left\{ \zeta_{jk}(p_1, q_1) \zeta_{jk}(p_2, q_2) \right\}. \quad (\text{C.6})$$

When the probability density function of the fading channel has zero mean, the resulting derivation would be simplified as

$$\begin{aligned} E_{\mathcal{L},\mathcal{A}} \left\{ \varrho_{jk}^2 \right\} &= \sum_{p_1=1}^L \sum_{q_1=1}^L \sum_{p_2=1}^L \sum_{q_2=1}^L E_{\mathcal{A}} \left\{ h_{j,p_1} h_{k,q_1} h_{j,p_2} h_{k,q_2} \right\} \cdot \\ &\quad E_{\mathcal{L}} \left\{ \zeta_{jk}(p_1, q_1) \zeta_{jk}(p_2, q_2) \right\} \\ &= \sum_{p_1=1}^L \sum_{q_1=1}^L \mathbf{g}_{j,p_1} \mathbf{g}_{k,q_1} \left( \frac{N - \tau_{jk}(p_1, q_1)}{N^2} \right) \end{aligned} \quad (\text{C.7})$$

where  $\mathbf{g}_{j,p_1} = E_{\mathcal{A}} \{ h_{j,p_1}^2 \}$  denotes the expected branch power of the  $p_1$ th path for the  $j$ th user and  $\sum_{p_1} \mathbf{g}_{j,p_1} = \mathbf{g}_j$ . Other expectation terms can be derived in a similar way.

# Appendix D

## Supplemental Derivation for Analytical Results in Chapter 4

In chapter 4 the optimal weights, weight error means and weight error variance are provided for only the correct decision in most cases. This Appendix completes the analytical result for the erroneous decision and whatever not detailed in chapter 4.

### § D.1 Two-user Scenario

The union of noise subsets for erroneous decision is represented by

$$\mathbb{E}_1 = \mathbb{U}^{31} \cup \mathbb{U}^{32} \cup \mathbb{U}^{41} \cup \mathbb{U}^{42}. \quad (\text{D.1})$$

$$\mathbb{E}_2 = \mathbb{U}^{21} \cup \mathbb{U}^{22} \cup \mathbb{U}^{31} \cup \mathbb{U}^{32}. \quad (\text{D.2})$$

Thus we have

$$\begin{aligned} P_{\mathbb{E}_1} &= P_{31} + P_{32} + P_{41} + P_{42} \\ P_{\mathbb{E}_2} &= P_{21} + P_{22} + P_{31} + P_{32}. \end{aligned} \quad (\text{D.3})$$



We can express the conditional optimal weight for a given  $\rho$  as

$$\check{w}_{opt,l}^e = \frac{1}{P_{\mathbb{E}_l}} \sum_{\mathbb{E}_l} \check{w}_{opt,l}^{ij} P_{ij}, \quad l = 1, 2. \quad (\text{D.4})$$

The finally optimal weights are given as

$$w_{opt,i}^e = E_{\rho} \{ \check{w}_{opt,i}^e \} = \frac{\sum_{\rho} \check{w}_{opt,i}^e P_{\rho} P_{\mathbb{E}_l}}{\sum_{\rho} P_{\rho} P_{\mathbb{E}_l}} \quad (\text{D.5})$$

where  $i = 1, 2$  and  $P_{\rho}$  is defined in (4.94).

The conditional weight error mean can be obtained to be

$$\check{\epsilon}_{M,l}^e(n) = \frac{1}{P_{\mathbb{E}_l}} \sum_{\mathbb{E}_l} \check{\epsilon}_{M,l}^{ij}(n) P_{ij} \quad l = 1, 2 \quad (\text{D.6})$$

where  $\mathbb{E}_l$  is given in (D.1) and (D.2). Then the averaged mean weight error for correct decision over  $\rho$  can be obtain by

$$\begin{aligned} E \{ \epsilon_i^e(n) \} &= E_{\rho} \{ \check{\epsilon}_{M,i}^e(n) \} \\ &= \frac{\sum_{\rho} \check{\epsilon}_{M,i}^e(n) P_{\rho} P_{\mathbb{E}_l}}{\sum_{\rho} P_{\rho} P_{\mathbb{E}_l}} \end{aligned} \quad (\text{D.7})$$

for  $l = 1, 2$ .

## § D.2 $K$ -user Scenario

The derivation for OWA1 is similar to the that in two-user cases and can be obtained from (D.5). As far as OWA2 is concerned, the noise regions for the erroneous decision of the first user is expressed as the sixth pattern as

$$\begin{aligned} \mathbb{U}^{61} &= \mathbb{U}^{31} \cup \mathbb{U}^{41}, \quad b_1 = b_I \\ \mathbb{U}^{62} &= \mathbb{U}^{32} \cup \mathbb{U}^{42}, \quad b_1 \neq b_I. \end{aligned} \quad (\text{D.8})$$

The conditional optimal weight is described as

$$\check{w}_{opt,1}^e = \frac{\check{w}_{opt,1}^{61} P_{61} + \check{w}_{opt,1}^{62} P_{62}}{P_{\mathbb{B}}} \quad (\text{D.9})$$

where the noise domain and the corresponding occurrence probabilities are defined as

$$\mathbb{B} = \mathbb{U}^{61} \cup \mathbb{U}^{62} \quad (\text{D.10})$$

$$P_{\mathbb{B}} = P_{61} + P_{62}. \quad (\text{D.11})$$

The averaged optimal weight is obtained after averaging all correlation coefficients as

$$w_{opt,1}^e = E_{\rho}\{\check{w}_{opt,1}^e\} = \frac{\sum_{\rho} \check{w}_{opt,1}^e P_{\rho} P_{\mathbb{B}}}{\sum_{\rho} P_{\rho} P_{\mathbb{B}}} \quad (\text{D.12})$$

with  $P_{\rho}$  defined in (4.94).

The conditional optimal weights for WEMA1 of the erroneous decision is obtained as

$$\check{\epsilon}_{M,1}^e(n) = \frac{1}{P_{\mathbb{D}}} \sum_{\mathbb{D}} \check{\epsilon}_{M,1}^{ij}(n) P_{ij} \quad (\text{D.13})$$

where the union of noise subsets  $\mathbb{D}$  is  $\mathbb{E}_1$  given is (D.1) for OWA1 or  $\mathbb{B}$  in (D.10) for OWA2. Also  $P_{\mathbb{D}}$  is  $P_{C_1}$  for OWA1 or  $P_{\mathbb{B}}$  for OWA2. Eventually the averaged mean weight error over  $\rho$  is obtained as

$$\begin{aligned} \epsilon_{M,1}^e(n) &= E_{\rho}\{\check{\epsilon}_{M,1}^e(n)\} \\ &= \frac{\sum_{\rho} \check{\epsilon}_{M,1}^e(n) P_{\rho} P_{\mathbb{D}}}{\sum_{\rho} P_{\rho} P_{\mathbb{D}}}. \end{aligned} \quad (\text{D.14})$$

The WEMA2 for the erroneous decision is obtained readily by

$$\epsilon_{M,1}^e(n) = (1 - \mu/N)^n (w_1^e(0) - w_{opt,1}^e). \quad (\text{D.15})$$

# Bibliography

- [1] K. S. Gilhousen, I. M. Jacobs, R. Roberto, A. J. Viterbi, L. A. Weaver, and C. E. Weatley, "On the capacity of a cellular CDMA system," *IEEE Trans. Veh. Technol.*, vol. 40, no. 2, pp. 303-312, May 1991.
- [2] A.J. Viterbi, *CDMA: Principles of spread spectrum communications*, Addison-Wesley, 1995.
- [3] T. Ojanpera and R. Prasad, *Wideband CDMA for third generation mobile communications*, Artech House Publisher, 1998.
- [4] S. Verdu, "Minimum probability of error for asynchronous Gaussian multiple-access channels," *IEEE Trans. Inform. Theory*, vol. IT-32, pp. 85-96, Jan. 1986.
- [5] S. Moshavi, "Multi-user detection for DS-SS communications," *IEEE Commun. Mag.*, vol. 34, pp. 124-136, Oct. 1996.
- [6] A. Duel-Hallen, J. Holtzman, and Z. Zvonar, "Multiuser detection for CDMA systems," *IEEE Personal Commun.*, vol. 2, no. 2, pp. 46-58, Apr. 1995.
- [7] S. Verdu, *Multiuser Detection*, Cambridge U.K.: Cambridge Univ. Press, 1998.
- [8] R. M. Buehrer, N. S. Correal-Mendoza, and B. D. Woerner, "A simulation comparison of multiuser receivers for cellular CDMA," *IEEE Trans. Veh. Technol.*, vol. 59, no. 4, pp. 1065-1085, Jul. 2000.

- [9] J. G. Proakis, *Digital Communications*, McGraw Hill, New York, 1995.
- [10] R. Lupas and S. Verdu, "Linear multiuser detectors for asynchronous code-division multiple-access channels," *IEEE Trans. Inform. Theory*, vol.35, no. 1, pp.123-136, Jan. 1989.
- [11] Z. Xie, R. T. Short, and C. K. Ruthforth, "A family of suboptimum detector for coherent multiuser communications," *IEEE J. Select. Areas Commun.*, vol. 8, no. 4, pp. 683-690, May 1990.
- [12] R. Lupas and S. Verdu, "Near-far resistance of multi-user detectors in asynchronous channels," *IEEE Trans. Commun.*, vol.35, no. 4, pp. 496-508, Apr. 1990.
- [13] H. V. Poor and S. Verdu, "Probability of error in MMSE multiuser detection," *IEEE Trans. Inform. Theory*, vol. 43, no. 3, pp. 858-871, May 1997.
- [14] D. Guo, S. Verdu and L. K. Rasmussen, "Asymptotic normality of linear multiuser receiver outputs," *IEEE Trans. Inform. Theory*, vol. 48, pp. 3080-3095, Dec. 2002.
- [15] M. J. Juntti, B. Aazhang, and J. O. Lilleberg, "Iterative implementation of linear multiusers detection for dynamic asynchronous CDMA systems," *IEEE Trans. Commun.*, vol. 46, no. 4, pp. 503-508, Apr. 1998.
- [16] P. H. Tan and L. K. Rasmussen, "Linear interference cancellation in CDMA based on iterative techniques for linear equation systems," *IEEE Trans. Commun.*, vol. 48, no. 12, pp. 2099-2108, Dec. 2000.
- [17] U. Madhow and M. L. Honig, "MMSE interference suppression for direct-sequence spread-spectrum CDMA," *IEEE Trans. Commun.*, vol. 42, no. 12, pp. 3178-3188, Dec. 1994.
- [18] P. B. Rapajic and B. S. Vucetic, "Adaptive receiver structure for asynchronous CDMA systems," *IEEE J. Select. Areas Commun.*, vol. 12, pp. 685-697, May 1994.

- [19] S. L. Miller, "An adaptive direct-sequence code-division multiple-access receiver for multiuser interference rejection," *IEEE Trans. Commun.*, vol. 43, pp. 1746-1755, Feb./Mar./Apr. 1995.
- [20] B. Zhu; N. Ansari, and Z. Siveski, "Convergence and stability analysis of a synchronous adaptive CDMA receiver," *IEEE Trans. Commun.*, vol. 43, no. 12, pp. 3073-3079, Dec. 1995.
- [21] D. S. Chen, and S. Roy, "An adaptive multi-user receiver for CDMA systems." *IEEE J. Select. Areas Commun.*, vol.12, pp.808-816, June 1994.
- [22] T. J. Lim, L. K. Rasmussen, and H. Sugimoto, "An adaptive asynchronous multiuser CDMA detector based on the Kalman filter," *IEEE J. Select. Areas Commun.*, vol. 16, no. 9, pp. 1711-1722, Dec. 1998.
- [23] A. J. Viterbi, "Very low rate convolutional codes for maximum theoretical performance of spread-spectrum multiple-access channels," *IEEE J. Select. Areas Commun.*, vol. 8, no. 4, pp. 641-649, May 1990.
- [24] J. M. Holtzman, "Successive interference cancellation for direct sequence code division multiple access," *IEEE Trans. Commun.*, vol. 19, no. 5, pp. 997-793, Oct. 1994.
- [25] P. Patel and J. M. Holtzman, "Analysis of simple successive interference cancellation scheme in DS/CDMA system," *IEEE J. Selet. Areas Commun.*, vol. 12, pp. 796-807, June 1994.
- [26] M. K. Varanasi and B. Aazhang, "Multistage detection in asynchronous code-division multiple-access communications," *IEEE Trans. Commun.*, vol. 38, no. 4, pp. 509-519, Apr. 1990.

- [27] R. Kohno, H. Imai, M. Hatori, and S. Pasupathy, "An adaptive canceller of cochannel interference for spread-spectrum multiple-access communication networks in a power line," *IEEE J. Select. Areas. Commun.*, vol. 8, no. 4, pp. 691-699, Jun. 1990.
- [28] Y. C. Yoon, R. Kohno, and H. Imai, "A spread-spectrum multiaccess system with cochannel interference cancellation," *IEEE J. Select. Areas Commun.*, vol. 11, no. 7, pp. 1067-1075, Sep. 1993.
- [29] T.-B. Oon, R. Steele, and Y. Li, "Performance of an adaptive successive serial-parallel CDMA cancellation scheme in flat Rayleigh fading channels," *IEEE Trans. Veh. Technol.*, vol. 49, no. 1, pp. 130-147, Jan. 2000.
- [30] D. Divsalar, M. K. Simon, and D. Raphaeli, "Improved parallel interference cancellation for CDMA," *IEEE Trans. Commun.*, vol. 46, no. 2, pp. 258-268, Feb. 1998.
- [31] Wei Zha and S. D. Blostein, "Soft-decision multistage multiuser interference cancellation," *IEEE Trans. Veh. Technol.*, vol. 52, no. 2, pp. 380-389, Mar. 2003.
- [32] R. M. Buehrer, S. P. Nicoloso, and S. Gollamudi, "Linear versus non-linear interference cancellation," *J. Commun. Networks*, vol. 1, no. 2, pp. 118-133, Jun. 1999.
- [33] S. Striglis, A. Kaul, N. Yang, and B. D. Woerner, "A multistage RAKE receiver for improved capacity of CDMA systems," in *IEEE 44th Vehicular Technology Conference*, vol. 2, pp. 789-793, June 1994.
- [34] R. M. Buehrer and B. D. Woerner, "Analysis of adaptive multistage interference cancellation for CDMA using an improved Gaussian approximation," *IEEE Trans. Commun.*, vol. 44, no. 10, pp. 1308-1320, Oct. 1996.
- [35] R. M. Buehrer, "Equal BER performance in linear successive interference cancellation for CDMA systems," *IEEE Trans. Commun.*, vol. 49, no. 7, pp. 1250-1258, July 2001.

- [36] H. Elders-Boll, H. D. Schotten, and A. Busboom, "Efficient implementation of linear multiuser detection for asynchronous CDMA systems by linear interference cancellation," *Eur. Trans. Telecommun.*, vol. 9, no. 4, pp. 427-437, Sept.-Nov. 1998.
- [37] N. B. Mandayam and S. Verdu, "Analysis of an approximate decorrelating detector," *Wireless Personal Commun.*, vol. 6 no. 1-2, pp. 97-111, Jan. 1998.
- [38] A. Kaul and B. D. Woerner, "An analysis of adaptive multistage interference cancellation for CDMA," in *Proc. IEEE Veh. Technol. Conf.*, pp. 82-86, Chicago, IL, July 26-28 1995.
- [39] R. B. Buehrer and B. D. Woener, "Analysis of DS-SS parallel interference cancellation with phase and timing errors," *IEEE J. Select. Areas. Commun.*, vol. 14, no. 8, pp. 1522-1535, Oct. 1996.
- [40] D. R. Brown, M. Matani, V. V. Veeravalli, H. V. Poor, and C. R. Johnson, "On the performance of linear parallel interference cancellation," *IEEE Trans. Inform. Theory*, vol. 47, no. 5, pp. 1957-1970, July 2001.
- [41] M. K. Varanasi and B. Aazhang, "Near-optimum detection in synchronous code-division multiple-access systems," *IEEE Trans. Commun.*, vol. 39, no. 5, pp. 725-736, May 1991.
- [42] M. J. Juntti and M. Latva-aho, "Multiuser receivers for CDMA systems in Rayleigh fading channels," *IEEE Trans. Veh. Technol.*, vol. 49, no. 3, pp. 885-899, May 2000.
- [43] J. F. Weng, G. Q. Xue, T. Le-Ngoc, and S. Tahar, "Multistage interference cancellation with diversity reception for asynchronous QPSK DS/SS systems over multipath fading channels," *IEEE J. Select. Areas Commun.*, vol. 17, pp. 2162-2180, Dec. 1999.
- [44] J. F. Weng, T. Le-ngoc, G. Q. Xue, and S. Tahar, "Performance of various multistage interference cancellation schemes for asynchronous QPSK/DS/SS over multipath rayleigh fading hannels," *IEEE Trans. Commun.*, vol. 49, no. 5, pp.774-778, May 2001.

- [45] G. Xue; J. F. Weng, Tho Le-Ngoc, and S. Tahar, "An analytical model for performance evaluation of parallel interference cancellers in CDMA systems," *IEEE Commun. Letters*, vol. 4, no. 6, pp. 184-186, June 2000.
- [46] D. R. Brown III and C. R. Johnson Jr., "SINR, power efficiency, and theoretical system capacity for parallel interference cancellation," *J. Commun. Networks*, vol. 3, no. 3, pp. 228-237, Sep. 2001.
- [47] J. H. Ko, J. S. Joo, and Y. H. Lee, "On the use of sigmoid functions for multistage detection in asynchronous CDMA systems," *IEEE Trans. Veh. Technol.*, vol. 48, no. 2, pp. 522-526, Mar. 1999.
- [48] R. Fantacci, "Proposal of an interference cancellation receiver with low complexity for DS/CDMA mobile communication systems," *IEEE Trans. Veh. Technol.*, vol. 48, no. 4, pp. 1039-1046, July 1999.
- [49] J. Bae, I. Song, and D. H. Won, "A selective and adaptive interference cancellation scheme for code division multiple access systems," *Signal Processing*, vol. 83, no. 2, pp. 259-273, Feb. 2003.
- [50] L. C. Hui and K. B. Letaief, "Successive interference cancellation for multiuser asynchronous DS/CDMA detectors in multipath fading links," *IEEE Trans. Commun.*, vol. 46, pp. 384-391, Mar. 1998.
- [51] R. Cusani, M. Di Felice, and J. Mattila, "A simple Bayesian multistage interference canceller for multiuser detection in TDD-CDMA receivers," *IEEE Trans. Veh. Technol.*, vol. 50, no. 4, pp. 920-924, July 2001.
- [52] D. Guo, L. K. Rasmussen, and T. J. Lim, "Linear parallel interference cancellation in long-code CDMA multiuser detection," *IEEE J. Select. Areas Commun.*, vol. 17, no. 12, pp. 2074-2081, Dec. 1999.



- [53] D. Guo; L. K. Rasmussen, S. Sun and T. J. Lim, "A matrix-algebraic approach to linear parallel interference cancellation in CDMA," *IEEE Trans. Commun.*, vol. 48, no. 1, pp. 152-161, Jan. 2000.
- [54] Y. Li, M. Chen and S. Cheng, "Determination of cancellation factors for soft-decision partial PIC detector in DS/CDMA systems," *Electron. Letters*, vol. 36, no. 3, Feb. 2000.
- [55] N. S. Correal, R. M. Buehrer, and B. D. Worner, "A DSP-based DS-CDMA multiuser receiver employing partial parallel interference cancellation," *IEEE J. Select. Areas Commun.*, vol. 17, no. 4, pp. 613-630, Apr. 1999.
- [56] R. B. Buehrer and S. P. Nicoloso, "Comments on "Partial Parallel Interference Cancellation for CDMA"", *IEEE Trans. Commun.*, vol. 47, no. 5, pp. 658-661, May 1999.
- [57] B. S. Abrams, A. E. Zeger, and T. E. Jones, "Efficiently structured CDMA receiver with near-far immunity," *IEEE Trans. Veh. Technol.*, vol. 44, no. 1, pp. 1-13, Feb. 1995.
- [58] X. Gao and C. Li, "Performance of partial parallel interference cancellation in DS-CDMA system with delay estimation errors," in *Proc. 11th Int. Symp. Personal, Indoor and Mobile Radio Communications*, pp.724-727, London, UK, Sept. 18-21, 2000.
- [59] J. Chen, J. Wang, and M. Sawahashi, "MCI cancellation for multicode wideband CDMA systems," *IEEE J. Select. Areas Commun.*, vol. 20, no. 2, pp. 450-462, Feb. 2002.
- [60] S. Marinkovic, B. S. Vucetic, and J. Evans, "Improved iterative parallel interference cancellation for coded CDMA systems," in *Proc. 2001 IEEE International Symposium on Information Theory*, pp. 34, June 2001.
- [61] P. G. Renucci and B. D. Woerner, "Optimization of soft interference cancellation for DS-CDMA," *Electron. Letters*, vol. 34, no. 8, pp. 731-733, Apr. 1998.

- [62] G. Xue, J. Weng, T. Le-Ngoc, and S. Tahar, "Adaptive multistage parallel interference cancellation for CDMA," *IEEE J. Select. Areas Commun.*, vol. 17, no. 10, pp. 1815-1827, Oct. 1999.
- [63] S. R. Kim, I. Choi, S. Kang, and J. G. Lee, "Adaptive weighted parallel interference cancellation for CDMA systems," *Electron. Letters*, vol. 34, no. 22, pp. 2085 -2086, Oct. 1998.
- [64] K.-C. Lai and J. J. Shynk, "Steady-state analysis of the adaptive successive interference canceler for DS/CDMA signals ," *IEEE Trans. Signal Processing.*, Vol. 49 no. 10, pp. 2345 -2362, Oct. 2001.
- [65] L. Hanzo, *Single and multi-carrier DS-SS : multi-user detection, space-time spreading, synchronisation, networking, and standards*, Chichester :J. Wiley, 2003.
- [66] S. Verdu, "Demodulation in the presence of multiuser interference: progress and misconceptions," in *Intelligent methods in signal processing and communications*, D. Docampo, A. Figueras-Vidal, Eds., pp. 15-44, Birkhauser, Boston: 1997.
- [67] 3GPP, "3rd Generation Partnership Project; Technical Specification Group (TSG) RAN WG4; Deployment Aspects (3G TR 25.943 version 2.0.0)," March 2000.
- [68] M. Chen, Y. Li, S. Cheng, and H. Wang "On the bit estimators of partial parallel interference cancellation for DS-SS," *IEEE International Conf. on Commun., ICC2001*, vol.6, pp.1945-1949, 11-14, June 2001.
- [69] M. Nasiri-Kenari, R. R. Sylvester, and C. K. Rushforth, "An efficient soft-in-soft-out multiuser detector for synchronous CDMA with error-control coding," *IEEE Trans. Veh. Technol.*, vol. 47, no. 3, pp. 947-953, Aug. 1998.
- [70] Z. Guo and K. B. Letaief, "An effective multiuser receiver for DS/SS systems," *IEEE J. Select. Areas Commun.*, vol. 19, no. 6, pp. 1019-1028, June 2001.

- [71] J. Hu and R. S. Blum, "A gradient guided search algorithm for multiuser detection," *IEEE Commun. Letters*, vol. 4. no. 11, pp.340-342, Nov. 2000.

